The work submitted herewith for the degree of Master of Philosophy has been carried out by Hugo Sebastian Shiers

(Director of studies). G. T. Roberts.

(Candidate)... Hugo S. Shiers.

December 1986

DECLARATION

I hereby declare that this work has not been accepted in substance for any degree and is not concurrently submitted in candidature for any degree other than the degree of Master of Philosophy of the Council for National Academic Awards.

December 1986 ..Thos. T. Vivien..

SEALING OF PARTIALLY EVACUATED SOLAR COLLECTORS

by

Hugo Sebastian Shiers, B.Sc.

A thesis submitted during November 1986 in partial fulfilment of the requirements for the award of an M.Phil. degree by the C.N.A.A, describing work carried out in the Department of Science at the sponsoring establishment:
The polytechnic of Wales
The work was done in calibration with
Severn Science Ltd Thornbury, Bristol.

ACKNOWLEDGEMENTS

To Dr. G.T. Roberts for his advice and encouragement, Norman for his lathing, Jeremy for his processing, and to Karen for her typing.

Sealing of partially evacuated solar collectors.

by

Hugo Sebastian Shiers

ABSTRACT

The object of this work is to look into the long term viability of a partially evacuated, high performance, hot water, solar collector proposed by Roberts (1979). The collector involves an absorber plate inside an evacuated domed glass tube, sealed by a polymer seal onto a metal endcap. The proposed collector contains 15 torr of low thermal conductivity gas to suppress conduction losses from spurious gases arising in the collector.

A study was undertaken, and is shown, to predict the loss of vacuum in the polymer sealed collectors; for various vacuum sealing polymers. It is shown that viton is the most suitable polymer, and a design of a suitable seal is shown, with the design of a completed unit. An upper limit of loss of vacuum in the collectors is demonstrated to be 0.5 torr/year. This is due in main to permeation of water vapour, oxygen, and nitrogen through the seals.

An experimental study and theoretical comparison to, find a suitable low thermal conductivity gas, to infill into the collectors and to predict the thermal conductivity of this gas mixed with relevant quantities of the inleaking gases is shown. The thermal conductivity cell and electronic unit to do this study is presented It was found that Halocarbon 11 would be a suitable gas to inflow into the collectors, having a thermal conductivity of

$$8.07 \times 10^{-3}.\ W\ M^{-1} K^{-1}.$$

Theoretical equations for binary, and multi-component gas mixtures are shown compared with our experimental results. These equations do not compare favourably; however it is shown that by using a combination of these equations the thermal conductivity of gases arising in the proposed collectors may be predicted to within 5%. The efficiency test of a completed unit is shown. This shows the efficiency of the partially evacuated collector to be similar to a high vacuum collector. The efficiency of the collector is shown not to deteriorate significantly within a period of ten years.

CONTENTS

Corrigenda.

Page	
iii	Line 5: November 1986, should read December 1986. Line 11: calibration should read colaboration.
1	Line 8: $T_o > T_A$ should read $T_o >> T_A$
2	Line 15: Convections should read Convection.
3	Line 16: ; should be ,
7	Figure 1.1.1: $KW^{-1}M^2$ should read $K\ W^{-1}M^2$.
9	Line 2: phenomena should read phenomenon.
17	Line 1: The rate of outgassing of gas species is due to permeation through a, should read The rate of outgassing of gas species, i, due to permeation through a.
2Ø	Line 17: figure 2.6.1 should read figure 2.1.2.
25	Equation 2.7.4 should read: $Q = (dp/dt)(\text{Volume of chamber})...2.7.4$
3Ø	Line 18/19: The design of the seals are shown in figure 3.1.1 should read The design of the seals is shown in figure 3.1.1.
36	Table 3.3.1: Fifth row first column Ne should read He.
4Ø	Line 15: Fig. 3.4.2 should read Fig. 3.4.1.
46	Figure 4.1.1: Chamber A contains an ion pump.
56	Line 5/6: 2ØØ degrees centigrade should read 2ØØC.
62	Line 19: The resistance should read The resistances.
73	Figure 5.3.3: Monometer should read manometer.
75	Figure 5.4.1: $q/\Delta T\ WK^{-1}$ should read $q/\Delta T \times 1Ø^{-4}WK^{-1}$.
77	Line 21: T_o = Constant should read $(T^2 + T_o^2)(T + T_o)$ = Constant.
79	Line 13: T=T we get should read $T=T_o$ we get.

80 Equation 5.5.2: K should be k.

87 Line 11: dependents should read dependence.
Line 17: which should be erased.
Line 22: than should read for.

91 Equation 5.6.7 should read dx/x = Ø.11

93 Table 5.7.1 standard dev column, Halocarbon 21 row reads Ø.Ø1 should read Ø.1.

101 Equation 6.1.1 should read:

$$K=(E_{trans}\,\mu C_{vtrans})/M + (E_{int}\,\mu C_{vint})/M....6.1.1$$

122 Line 9: tests were to determine t and U_L should read tests were to determine αt and U_L.
Line 17: $T_m - T_u$ should read $T_m - T_a$.

127 Add to references:

J. A. Duffie and W. A. Beckman- Solar Energy Thermal Processes- John Wiley and Sons, 1974.

BS5918: 1980 - Code of practice for solar heating systems for domestic hot water - British Standards Institution.

1 INTRODUCTION

1.1 Current collectors

Solar collectors are primary structures used to heat water or some other fluid by means of radiation energy from the sun. The most simple solar collector is essentially just a dark absorbing surface incorporating some mechanism for the removal of heat. This type of collector is cheap to manufacture and will operate at high efficiencies provided the required output temperature, T_O, is not much greater than the ambient temperature, T_A. This is because the sun plays directly on the absorber surface so the optical efficiency is high, but if $T_O > T_A$. the heat loss will be high as there is no insulation above the absorber.

This type of collector may be ideal for applications such as heating swimming pools where the desired temperatures are of the same order as ambient temperatures. If collectors are to be used in applications where the desired output temperatures are to be greater than ambient temperature then it is necessary to insulate the absorbing surface, to lower the heat loss. Increasing the complexity of the solar collector will, however increase the capital cost of the system, and this must always be balanced against the gain in output of useful heat.

To insulate the absorbing surface from ambient temperatures a glazing system may be used. This will lower the heat loss when the desired temperatures are greater than the ambient temperature but will reduce the optical efficiency as the radiant energy has to be transmitted through the glass cover. This type of flat plate collector has been

available for some years; and is the most common type, production costs for such collectors being of the order of one hundred pounds per square metre. However this type of collector will still lose energy from the absorber by conduction, convection and radiation through the air filled gap; and also by conduction through the insulating slab on the reverse side of the plate. With adequate thickness the heat loss through the insulation can be reduced to a reasonable low level. Radiation losses can be reduced by the use of a suitable selective absorbing black film. Such a film absorbs well the short wavelength visible radiation from the sun, but yet suppress the emission of the long wavelength infrared radiation. Convection losses may be reduced by double glazing, but there is a limit to which heat losses may be suppressed this way. The use of double glazing will, also, reduce the optical efficiency of the system.

Convections losses may be reduced further by either dividing the air space into small cells which are too small for the establishment of natural convection, or to reduce the pressure within the air gap below a level where convection exists. If the pressure is lowered to below 10^{-3}. Torr both convection losses and conduction losses will be suppressed to provide a very low heat loss.

A number of scientists and engineers, within the past ten years, have investigated the possibility of constructing these high efficiency solar collectors, by evacuating the space between the glass cover and the collector.

Due to the large atmospheric forces experienced by the evacuated containers most investigators agree that such collectors should be of the evacuated glass tube type. Some of the various proposed systems being:

1 An evacuated dewar dual glass tube system, for example the system proposed by Owen-Illinois (1966).

2 A collector plate placed inside a single evacuated glass tube, for example the system proposed by Corning, France and Philips. See Bloem, Grigs and de Vaan (1982)

3 A collector plate placed inside a partially evacuated glass tube. See Roberts (1979).

4 A partially evacuated flat plate collector, de-Waal and Simonis (1981)

The designs of 1 and 2 are similar in that they use high vacuum to suppress conduction and convection losses. The system proposed by Corning, France, uses high vacuum to 10^{-6} Torr; which suppress convection and conduction losses. The outer cover tube is made from pyrex, the inlet and outlet tubes for the heat carrying fluid go in and out of the collectors via expensive metal to glass seals.

The system of Owen-Illinois uses an evacuated dewar to insulate an absorber tube, which is coated with a selective absorber. The absorber tube contains two concentric tubes, a delivery tube on the inside, the heat carrying fluid returning on the outside, and inside the absorber tube. The Owen-Illinois system gives high performance, but has the

disadvantage of high cost, due to the complex manifold system and the metal to glass seals. It also has a large heat inertia due to the large amount of fluid that the system contains.

Both the Philips and Corning systems involve a collector plate placed inside an evacuated tube. In the Corning unit heat is removed by a circulating fluid flowing through a pipe which is firmly fixed to the collector plate. This pipe enters and leaves the glass tube by means of graded glass-metal seals; with suitable bellows used to correct for the relative expansion of the metal and glass.

The Philips collector uses a heat pipe to transmit thermal energy from plate to an external manifold. This means that only one graded glass-metal seal is required per tube, and the installation of such a system is simplified.

Both the Philips and Corning systems use expensive sealing methods, but the Philips system has the added disadvantage of resistance to heat flow of the heat pipe and the requirement of a heat exchanger to transmit the heat into a circulating fluid. Since both systems use only glass items, once evacuated their pressures can be kept below 10^{-4} torr by the use of suitable gettering materials.

The system proposed by Roberts (1979) was to use an evacuated glass tube domed at one end, with the other end being sealed onto a metal endcap with a suitable polymer seal. It was presumed that the polymer seal would lead to a decrease of vacuum after some time due to spurious gases, which would appear because of permeation and outgassing of the polymer seal. The thermal conductivity of gases, in a vessel, of the dimensions suggested by Roberts, are independent of pressure above 0.2 torr. Roberts showed that convection losses could be ignored below a

pressure of 20 torr, and therefore proposed that a low thermal conductivity gas be introduced at the production stage at approximately 15 torr to suppress conduction losses from the spurious gases. Commercially it is considered that the main advantage of the partially evacuated collector over other systems will be cost.

The system of de Waal and Simonis (1981) is similar to the system proposed by Roberts, apart from the fact that it does not use glass tube collectors. The basic design consists of a collector plate within a rectangular box, covered by a glass plate in which a vacuum is maintained. Similar to the Roberts design a low thermal conductivity gas is used to suppress conduction losses from inleaking atmospheric gases, which are estimated to be of the order of 1.5 torr per year. Its' main disadvantage is that to support atmospheric pressures toughened glass is needed along with supports every 20 cms.

Table 1.1.1 shows an analysis of the characteristics of the different type of collectors. The table gives efficiencies for the collectors for typical values of$(T_m-T_A)/I$ in the U.K. (T_m being the mean temperature of the collector plate.) Current prices also being shown, this table therefore clearly demonstrates the advantages of the type of partially evacuated collector suggested by Roberts. A plot of efficiencies versus $(T_m-T_A)/I$ is also shown in figure 1.1.1.

Table 1.1.1

Efficiencies and costs of typical collectors

Collector	Efficiency,%			Approx. cost per M^2 in pounds
	Summer $T_m-T_A=.05xI$	Spring/Aut. $T_m-T_A=.12xI$	Winter $T_m-T_A=.18xI$	
Flatplate, neutral absorber	50	0	0	100
Flat plate selective absorber	60	29	3	120
Tubular completely evacuated	68	49	33	250
Tubular partially evacuated	70	47	27	150

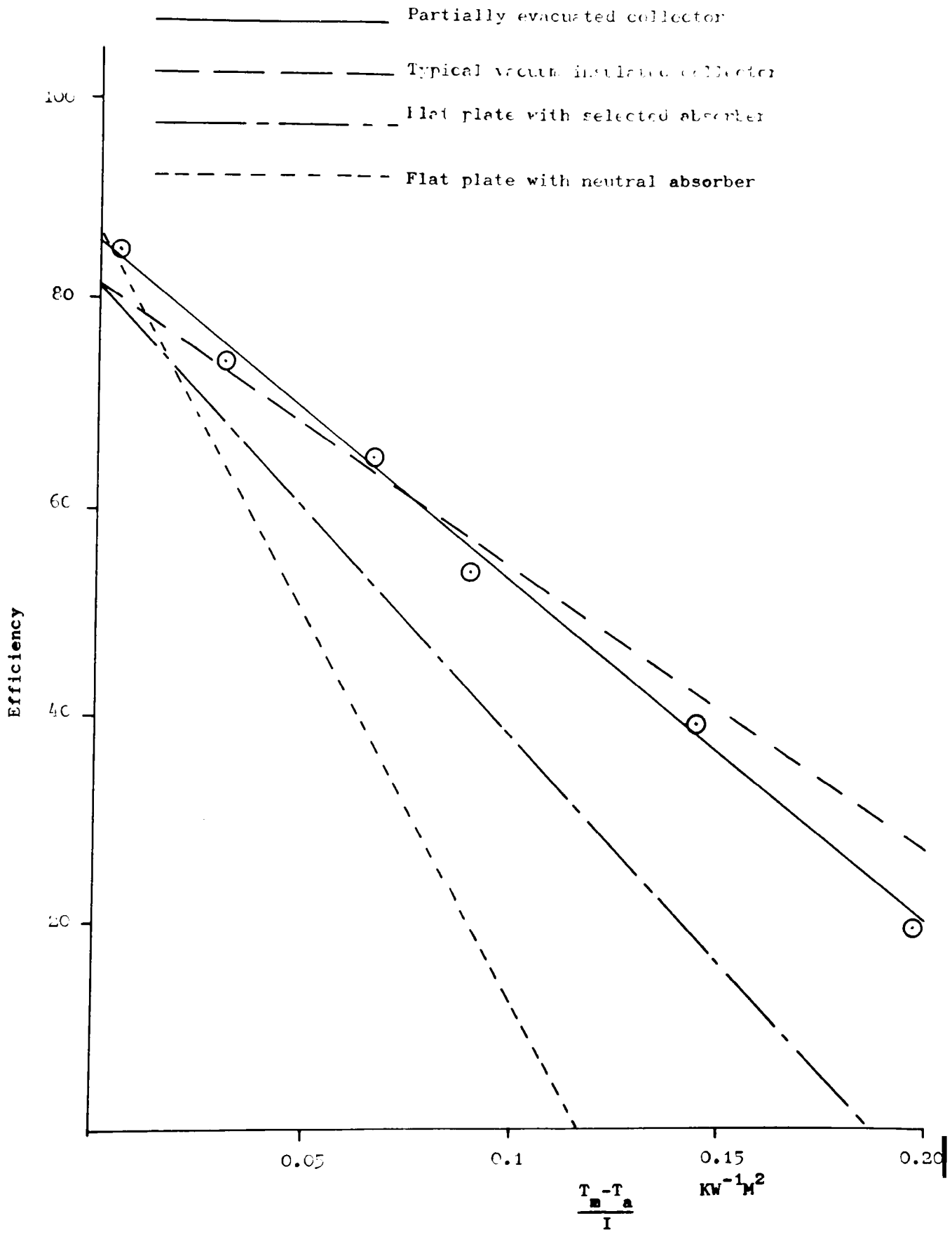

Figure 1.1.1 Plots of instantaneous efficiency versus $(T_m - T_a)/I$

1.2 Aims and summary of thesis

The principal aim of this work has been to determine the long term viability of the partially evacuated collector proposed by Roberts. To do this an evaluation of the expected pressure rise over a period of some ten years, and the determination of the effect of this pressure rise on the collector performance was required. The early chapters of this work describe a literature survey and an experimental investigation into the expected increase in pressure due to outgassing and permeation. Results suggest that over a period of 10 years increases of pressure will be less than 5 torr; exact pressure increases depending on detailed arrangement of seals and volume of glass tubes. An analysis of the actual gases shows that most of the pressure rise is due to water vapour and nitrogen.

Chapters 5 and 6 discuss the properties of the gases and vapours which could be used for infilling the tubes, along with an extensive study of the thermal conductivity of relevant mixtures of gases. Therefore as a result of these two investigations the change in thermal conductivity of the gases within the collectors, with time, is predicted.

Finally a prototype collector is described, which was designed in light of the results of the previous sections. Efficiency tests on the prototype collector described, were undertaken, these tests are described in chapter 7; along with the results of the tests. It is shown that the efficiency of the collectors will not deteriorate more than 10% over a period of ten years.

2 THEORY AND MEASUREMENT OF OUTGASSING

2.1 Introduction

When a material is placed in a vacuum gases will be liberated from its surface. This phenomena is generally known as outgassing. The rate of evolution of a gas from a particular material is normally expressed in terms of an outgassing rate of Torr. Litre/Sec. cm^2. Outgassing may be attributed to four major factors:

1 De-adsorption of gas from the surface of the material. Gas adsorbed onto the surface of the material while exposed to the atmosphere is released slowly when the material is under vacuum. The desorption rate of the gas will depend on its binding energy to the surface of the material, the surface temperature and the surface coverage.

2 De-absorption of gas from the material. Gas which is dissolved in the material will diffuse out and be released into the vacuum. The rate at which a gas diffuses out will depend on the solubility of the gas in the material and its rate of diffusion.

3 Permeation of gas through the material. If the material acts as part of the walls of the vacuum chamber gas on the high pressure side is absorbed into the material and diffuses across the material to be released into the vacuum. The rate at which gas permeates a material will depend on the rate of diffusion

and solubility of gas in the material.

4 The vapour pressure of the material. In this case the gas or vapour evolved will normally be molecules of the material itself.

Experimental observations of outgassing rates, at constant temperature, can be expressed by the empirical formula below: Roth (1976)

$$Q_h = Q_u + Q_1 t_h^{-x} \ldots 2.1.1$$

Where Q_h and Q_1 are the outgassing rates at h hours and one hour respectively after placing the material in a vacuum. Q_u is the limiting value of Q_h and for many materials is negligible unless t_h is very large. x is a number which varies with time in the vacuum. At the commencement of pump down x is relatively large and outgassing rates fall rapidly. This is due mainly to desorption rates of adsorbed gas. After half an hour x becomes smaller and practically constant. At this time x is usually 1.0 for a metal and for non-metals is often between 0.5 and 1.0 Ward and Bunn (1967).

The two main methods commonly used for measuring the outgassing rates of materials are the throughput method and the pressure rate of rise method.

In the throughput method a sample is placed in a vacuum chamber connected by a small aperture of known conductance to a high vacuum pump. The pressure drop across the conductance is noted, at time t, under steady state conditions. This pressure drop multiplied by the conductance of the aperture gives the outgassing rate of the sample and chamber at the time t.

In the pressure rate of rise method a sample is placed in a vacuum chamber and then pumped down. The outgassing rate at any time is obtained by sealing the chamber and noting the instantaneous rate of rise of pressure. The outgassing rate of the sample plus chamber is then the instantaneous rate of rise of pressure with respect to time multiplied by the volume of the chamber.

Experimental results are tabulated giving the outgassing rates of materials after specified pumping times of 1, 10 and 100 hours (Q_1, Q_{10} and Q_{100}) together with the slope of the log - log plot for the same time. Esley (1975). A typical plot of outgassing rate with respect to time is given in Figure 2.1.1.

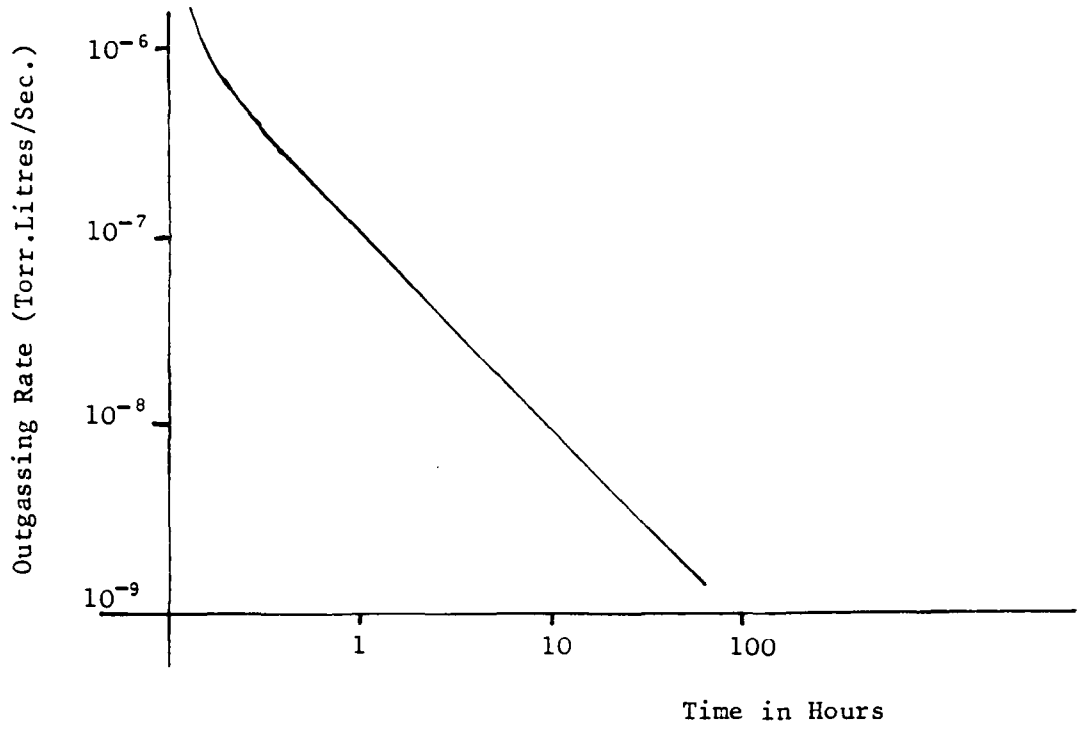

Figure 2.1.1 Typical outgassing rate plot

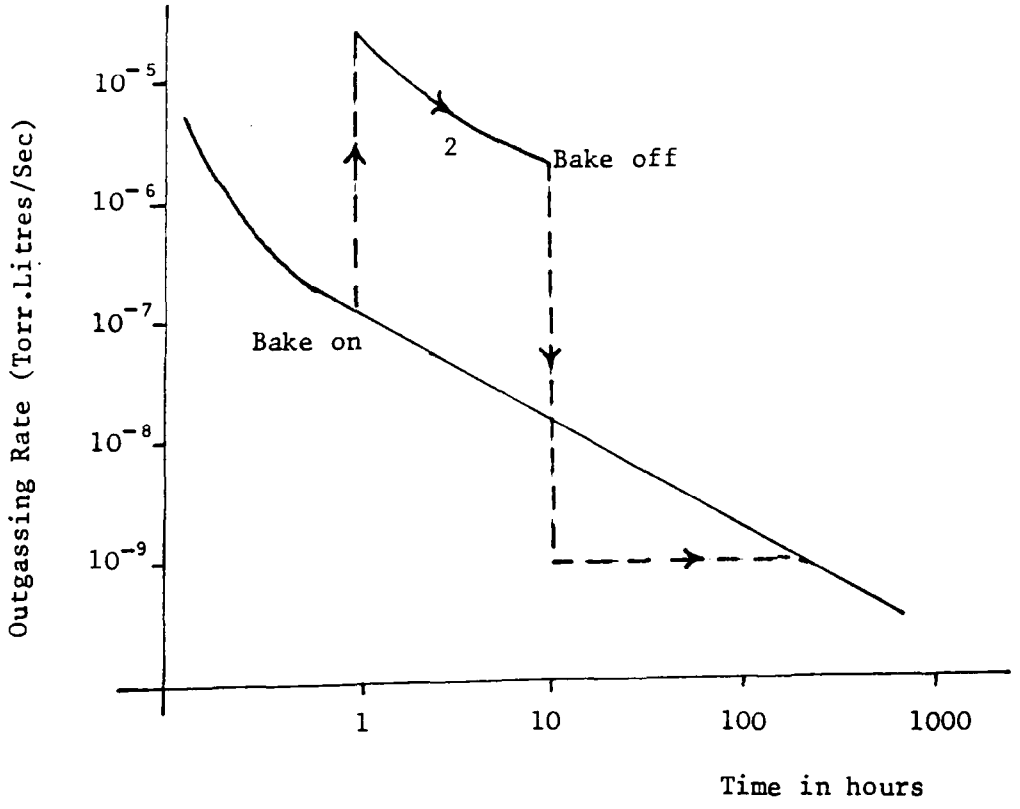

Figure 2.1.2 Typical variation of outgassing rate during baking cycle

2.2 Outgassing by de-adsorption

Adsorption of a gas onto a solid surface may be either physical or chemical. In physical adsorption the gas molecules are attracted by Van der Waal's forces and the heat of adsorption is usually less than 42 $KJmole^{-1}$, while in chemical adsorption a chemical combination occurs and the binding energies are far higher, normally within the range 84-840 $KJ\ mole^{-1}$.

De-adsorption is the reversal of these processes. Assuming that the surface has less than a monolayer coverage (and that the outgassing rate is small) then the outgassing rate at time t due to desorption of adsorbed gas may be given by the equation below, Ward and Bunn (1967).

$$Q_t = (10^{-7}\ T\ C_0 / t_s\ )\ \exp(-t/t_s) \ldots\ldots 2.2.1$$

where

Q_t outgassing rate at time t $(T.L.S^{-1}\ cm^{-2})$

T temperature degrees Kelvin

t_s. sojurn time, the average time to stay on a surface site, s.

C_0 surface coverage at t = 0.

From equation (2.2.1) it can be seen that

1 for small values of t_s, corresponding to physically adsorbed gas, the initial outgassing rate is very high but will fall off rapidly.

2 for large values of t_s, corresponding to chemically adsorbed gas, the initial outgassing rate is low but falls only slowly with time.

Experimental results do not always agree with equation 2.2.1, in particular this theory is unlikely to account for the observed outgassing of water vapour from metals as it assumes a monolayer coverage whereas water vapour may be adsorbed several monolayers thick. Dayton (1962) has suggested that water vapour is held in pores of the layer of oxide which is usually present in most metals. A semi-empirical analysis of the distribution of pore size and layer thickness leads to an expression for the outgassing rate which varies inversely with time.

2.3 Outgassing by de-absorption

Absorption refers to a gas which diffuses into a solid and exists within the solid in a dissolved state; de-absorption is the reverse of this process. The outgassing rate resulting from absorbed gases is based on the laws of diffusion. Roth (1976).

In general the de-absorption of a gas from a wall of thickness h_0 (cm) may be expressed as:

$$Q_h = (Q_1/t_h^x)...2.3.1$$

Where:

$$t_h^x = t_h^{0.5} - 0.57^{0.5}(1 - \exp(t_h/2y)...2.3.2$$

$$y = 3.145\ h_0^2/(5.76 \times 10^4 D).....2.3.4$$

Where D is the diffusion coefficient.

The total outgassing from a material due to de-absorption will then be a summation of equation 2.3.1 over all gases present in the dissolved state.

A molecule de-absorbed from a solid may be held at the surface by adsorption. This would imply that to go into the theory of de-absorption, consideration of the de-adsorption must simultaneously be taken. However, as the rate of de-adsorption is normally so large compared with the rate of diffusion, this is not necessary.

2.4 Outgassing by Permeation through the vacuum chamber

Outgassing by permeation refers to gas which evolves after diffusing through the walls of the vacuum chamber from the high pressure side. There are three main steps in the process

1 The permeant dissolves in the permeable membrane on the side of higher concentration.

2 The gas diffuses through the membrane towards the side of lower concentration.

3 The permeant becomes desorbed on the side of lower concentration.

The permeability constant P, at constant temperature is given by

$$P = D \times S \ldots 2.4.1$$

Where

D = Diffusion coefficient

S = Solubility of material for the gas

The permeability increases with temperature. The temperature dependence of P, D and S may be expressed by the following equations:

$$P = P_0 \, Exp(-E_p/RT) \ldots 2.4.2$$

$$D = D_0 \, Exp(-E_d/RT) \ldots 2.4.3$$

$$S = S_0 \, Exp(-H_s/RT) \ldots 2.4.4$$

Where

E_p = Activation energy for the overall permeation.

E_d = Activation energy for the diffusion process.

H_s = Heat consumed in dissolving a mole of permeant in the membrane.

From equations 2.4.1 to 2.4.4

$$P = D_0 \, S_0 \, \exp [- (E_d + H_s)/RT] \ldots 2.4.5$$

The rate of outgassing of gas species is due to permeation through a slab of material surface area A and thickness d into a vacuum is given by:

$$Q_i = P_i \, A/d \, (P_{1i}^{n} - P_{2i}^{n}) \ldots 2.4.6$$

Where

n is the inverse of the number of atoms (or radicals) into which the gas molecule splits when absorbed into the solid. For gases in non-metals n = 1 for diatomic gases in metals n = 1/2.

P_{i1} and P_{i2} are the partial pressures of the gas permeating on the high and low concentration sides of the slab respectively.

The total permeation outgassing is then given by the sum of equation 2.4.6 over all gases present.

$$Q_{total} = \sum_i Q_i = \sum_i P_i \, (A/d) \, (P_{1i} - P_{2i}) \ldots 2.4.7$$

Outgassing by permeation becomes of major importance in the following cases:

1 Hydrogen from the atmosphere permeating through the walls of a metal in an ultra high vacuum system.

2 Helium from the atmosphere permeating through the walls of a glass in a ultra high vacuum system

3 Atmospheric gases permeating through polymer gaskets.

Equation 2.3.1 may be rewritten to include permeation outgassing

$$Q_h = Q_u + (Q_1 / t_h^x) \ldots 2.4.8$$

Where Q_u is the the permeation outgassing rate.

2.5 The vapour pressure of the material

The saturated vapour pressure P_v, of a pure material increases with the absolute temperature in accordance with equation 2.5.1 below

$$\text{Log } P_v = A - B/T \ldots\ldots 2.5.1$$

Where A and B are constants depending on the material in question. The values for A and B for many materials may be found in Roth (1976).

The vapour pressures of most constructional materials employed in vacuum systems are insignificant at room temperature. The vapour pressure only offers a major contribution to the outgassing rate at room temperature of substances such as liquids and polymers. Consider the vapour pressures of the materials listed in table 2.5.1.

Material	Temp	Vapour Pressure (Torr).
Copper	25C	1×10^{-40}.
Aluminium	25C	2×10^{-45}.
Teflon	25C	9.8×10^{-8}.
Butyl Rubber	25C	9.8×10^{-6}.
Apiezon Vacuum greases	20C	$10^{-7} - 10^{-10}$.
Apiezon Oils	20C	$10^{-5} - 10^{-7}$.

TABLE 2.5.1

When considering the increase of pressure within a sealed system after a number of years the loss of vacuum due to the vapour pressure of most materials, even polymers, will be insignificant in comparison with the outgassing from materials by other factors mentioned previously.

2.6 Temperature variation of outgassing rates

Dayton (1963) has investigated the effect on materials outgassing rates during a baking cycle; assuming that the outgassing is due to de-absorption. He assumes that most of the adsorbed gas is released within the first half hour of pump down. Therefore the outgassing will be primarily de-absorption after this time.

Dayton shows that if the temperature is suddenly raised from T_a to T_b at time t_b after the start of pump down, then the outgassing rate (due to de-absorption) after a total pump time t_h is given by:-

$$Q_h = \frac{[\ D_b/D_a\ ]Q_1}{[\ D_b/D_a\ (t_h - t_b) + t_b\ ]^{.5}} \quad (t_h > t_b) \ldots\ldots\ldots 2.6.1$$

where

Q_1 = Outgassing rate that would have existed after one hour (t_h = 1) if the temperature had not been changed.

D_a = Diffusion rate of the gas through the solid at T_a.

D_b = Diffusion rate of the gas through the solid at T_b.

At the instant the temperature of the material is raised, the rate of outgassing has increased sharply in ratio $(D_b/D_a) >> 1$.

If, now, the temperature is suddenly returned to T_a when $t_h = t_c$ then the subsequent outgassing rate is given by:

$$Q_n = Q_1 /(t_h + (D_a/D_b)\ (t_c - t_b))^{.5} \ldots 2.6.2$$

Which means that at the instant of reducing the temperature the outgassing falls to

$$Q_C = Q_1/((D_b/D_a)\ t_c)^{.5} \ldots 2.6.3$$

If baking had not been carried out then the outgassing rate Q_c would not have been achieved until after a time t_x where

$$Q_c = Q_1/t_x^{0.5} \ldots 2.6.4$$

substituting Q_c from equation 2.6.3 into equation 2.6.4 gives

$$t_x = t_c(D_b/D_a) \ldots 2.6.5$$

A graph of the outgassing from a material versus time during such a baking cycle is shown in figure (2.6.1); superimposed on top of a graph of the material, versus time, if it had not been through such a baking cycle.

It is clear from this that to reduce the outgassing of a material quickly and substantially, it is necessary to bake it. However, baking a system or material will also have the effect of causing activated chemisorption of physically adsorbed gas, which can then be desorbed only by prolonged heating at much higher temperatures. Therefore a

degassing program should begin by pumping for approximately 30 minutes at room temperature to remove the majority of physically adsorbed gas, followed by a prolonged bake.

2.7 Methods of measurement of outgassing

As mentioned in the Introduction the two main methods commonly used for measuring the outgassing rates of materials are

1 The Throughput method

2 Pressure rate of rise method

These methods, along with the results obtained by different workers whilst using them, have been abridged by Esley (1975). The main principles and some of the problems of these procedures are described in brief here. It should be noted that these methods do not take into account the outgassing by permeation.

1 The Throughput Method

The Throughput method has become the more popular method of measuring outgassing rates. It is especially appropriate where a mass spectrometer is used to analyse the outgassed species, Barton and Govier (1964). Essentially a sample is placed in a chamber connected by a small aperture, of known conductance, to a high vacuum pump. Ion gauges are connected to the system on both sides of the aperture and the pressure drop across the conductance is noted with respect to time; see figure 2.7.1. The outgassing rate from the sample and the chamber due to a particular gas, species i , given off by the sample and

THROUGHPUT METHOD APPARATUS

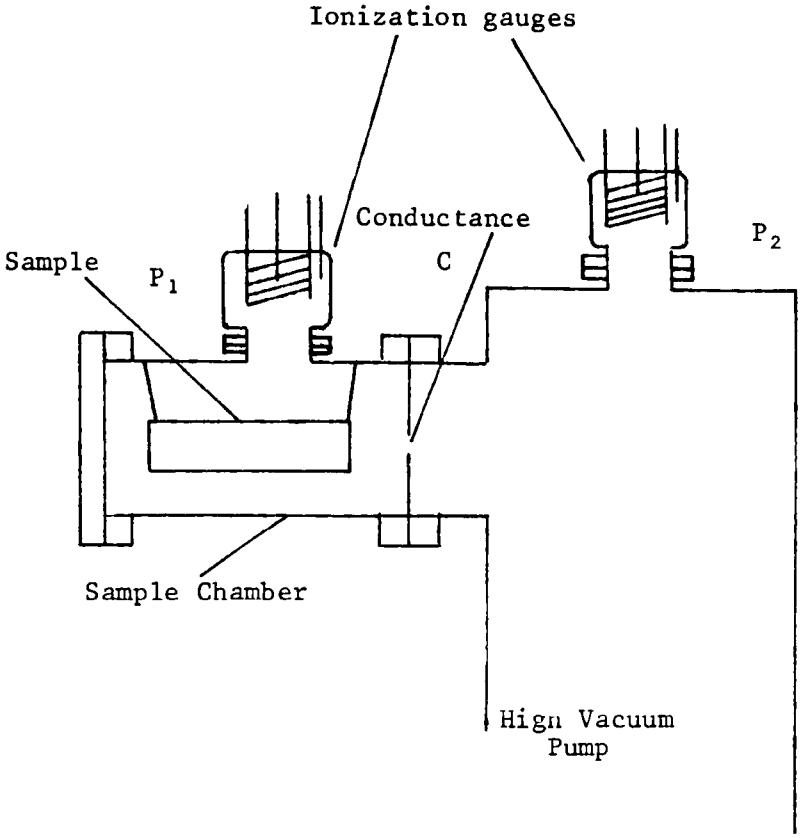

Outgassing of Sample + Chamber = $C (P_1 - P_2)$

Figure 2.7.1 Throughput apparatus

chamber is

$$Q_i = C_i(P_{1i} - P_{2i})...2.7.1$$

Where p_{1i} and p_{2i} are the partial pressures of the gas, species i, before and after the conductance respectively. The conductance C_i of the orifice, for a particular gas, is given in litres per second by the Knudsen formula below

$$C_i = 3.64(T/M)^{.5} A...2.7.2$$

where

A = area of orifice, cm^2.

M = relative molecular mass of the gas.

T = temperature of the gas, degrees Kelvin.

The total outgassing from the sample and chamber is then just the sum, over all gases being outgassed of equation 2.7.1 which is

$$Q = \sum_i C_i (P_{1i} - P_{2i})...2.7.3$$

A mass spectrometer has to be connected to the apparatus to find the relative abundance of each species of gas in the vacuum system. Using this and equations 2.7.1 and 2.7.2 it is possible to obtain the relative outgassing rates of each species of gas outgassed.

To obtain the outgassing rates of the sample only a blank run is needed.

It is difficult to make a quantitative study of outgassing rates without the aid of a mass spectrometer, because not only is the conductance of the orifice different for the different gases but also the sensitivity of the ionization gauges varies between the gases. Workers who do not incorporate a mass spectrometer in their apparatus express their results in nitrogen equivalents Esley (1975). This is not as inconvenient as may first appear since the throughput method parallels the process that occurs when a vacuum system is being pumped down.

Errors may be incorporated in the results by the inherent differences in sensitivities and working conditions of the two gauges. Ways to overcome this problem have been studied by Ben-hui et al (1978). With a relatively low conductance orifice this problem may be minimised. However, if the conductance is too small in relation to the surface area of the sample, problems may arise due to re-adsorption, Dayton (1959). Dayton states that in general, re-adsorption becomes negligible if the conductance is greater than a few tenths of a litre per second for several square centimetres of sample area.

Another source of error may arise due to pumping by the pressure transducer gauge heads, Moraw (1974).

2 The Pressure Rate of Rise Method

Basically the sample to be studied is placed in a vacuum chamber and then the chamber pumped down. The chamber is then sealed off from the pumps,at a time t, after the commencement of pump down, and the instantaneous rate of rise of pressure noted.

The outgassing rate of the chamber and sample, at time t, is given by equation 2.7.4 below:

$$Q = (dP/dT)\ (\text{volume of chamber}) \quad ...2.7.4$$

In order to minimise the effects of re-adsorption of outgassed species as the pressure in the chamber rises, the chamber is evacuated between measurements. Outgassing rate measurements are made at suitable intervals so that a plot of outgassing rate versus time may be achieved.

As in the throughput method it is necessary to carry out a blank run to obtain the outgassing of the chamber alone.

It is important to use a gauge with a very low pumping speed. If looking at outgassed rates of material at elevated temperatures it is important to make sure there are no temperature changes during measurements.

This method does not lend itself well to mass spectrometeric observations due to

1 The high pressures attained.

2 The difficulty of making a quantitative analysis in the presence of a rising pressure.

3 The tendency for constituents of low saturation pressure to be re-adsorbed and so be obscured by more volatile components.

2.8 Discussion

The theoretical and experimental basis of outgassing has been reviewed. However, in the experimental techniques for the measurement of outgassing, no consideration has been made of permeation,

It will become evident in chapter 3 that the data currently available on permeation through the various relevant materials is considered, to be adequate for the present study. However, available data for other outgassing phenomena from polymers are not adequate for the study of collector characteristics, therefore a review of various measurement techniques has been included. Further, as indicated in section 2.4, it is reasonable to treat outgassing by permeation separately from other forms of outgassing.

3 THEORETICAL PREDICATION OF LOSS OF VACUUM WITHIN THE COLLECTOR UNIT

3.1 Introduction

The initial design of the partially evacuated tubular collector has been described by Roberts (1979). A diagram of such a collector tube is shown in figure 3.1.1. This design uses glass tubes, domed at one end and sealed at the other by a metal end-plate. The end-plate comprises a suitable polymer seal together with a means of allowing the fluid-carrying tubes to enter and leave the glass tube. Such an arrangement becomes rather involved when a number of tubes are to be used in each collector unit, therefore it is proposed to inter-connect a series of such tubes with a manifold as shown in figure 3.1.2. [Manifold design is also described in detail by Roberts (1985)]. Inter-connecting the tubes in this way leads to two major advantages.

1 When manufacturing the collectors a series of tubes are evacuated and degassed together as opposed to evacuating and degassing each tube individually.

2 The hot fluid tube does not leave the vacuum as it goes from one tube to another. This greatly reduces heat loss at tube inlet and exit. (More details on the proposed design for the solar collector system will be given in chapter 7).

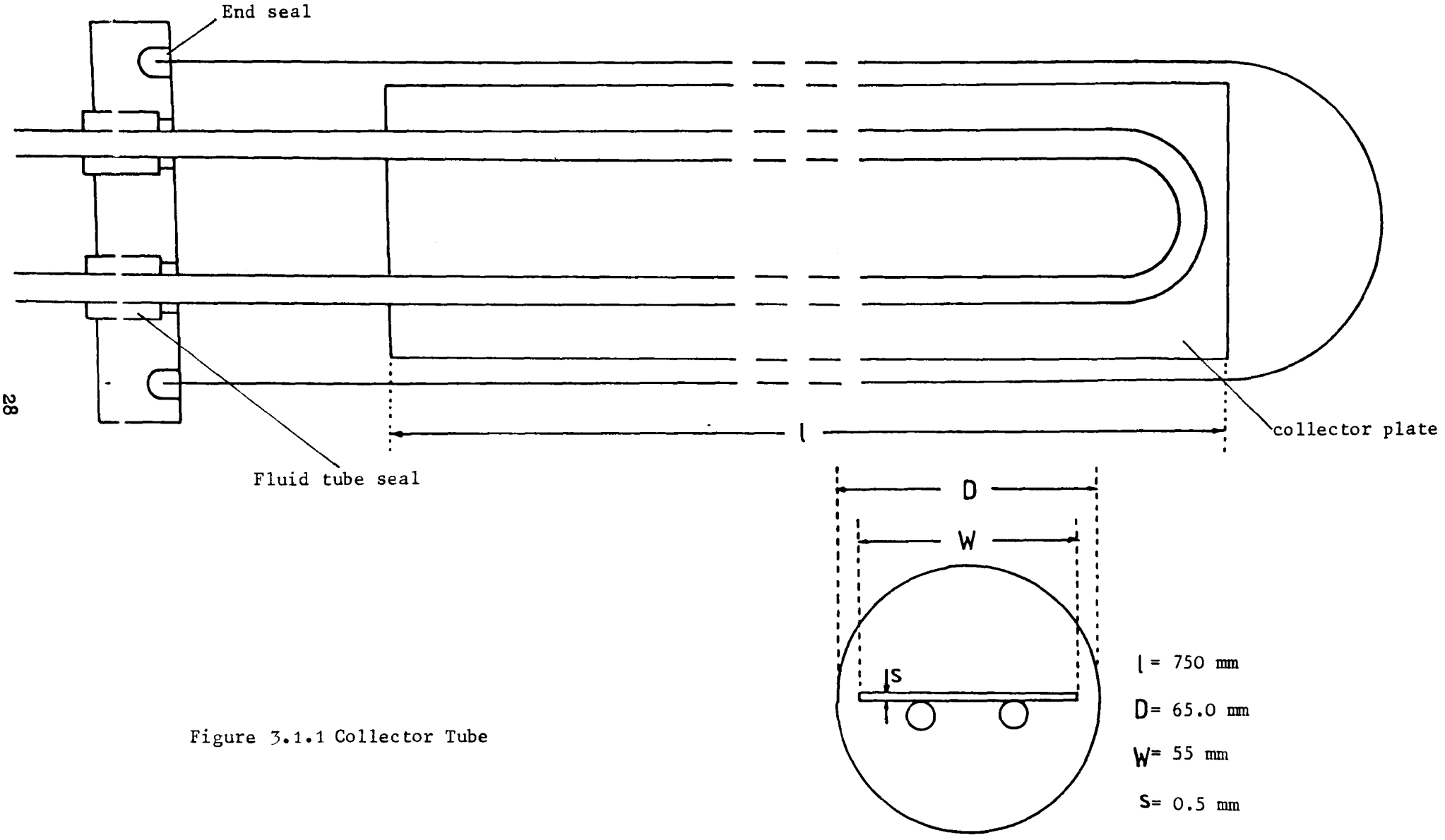

Figure 3.1.1 Collector Tube

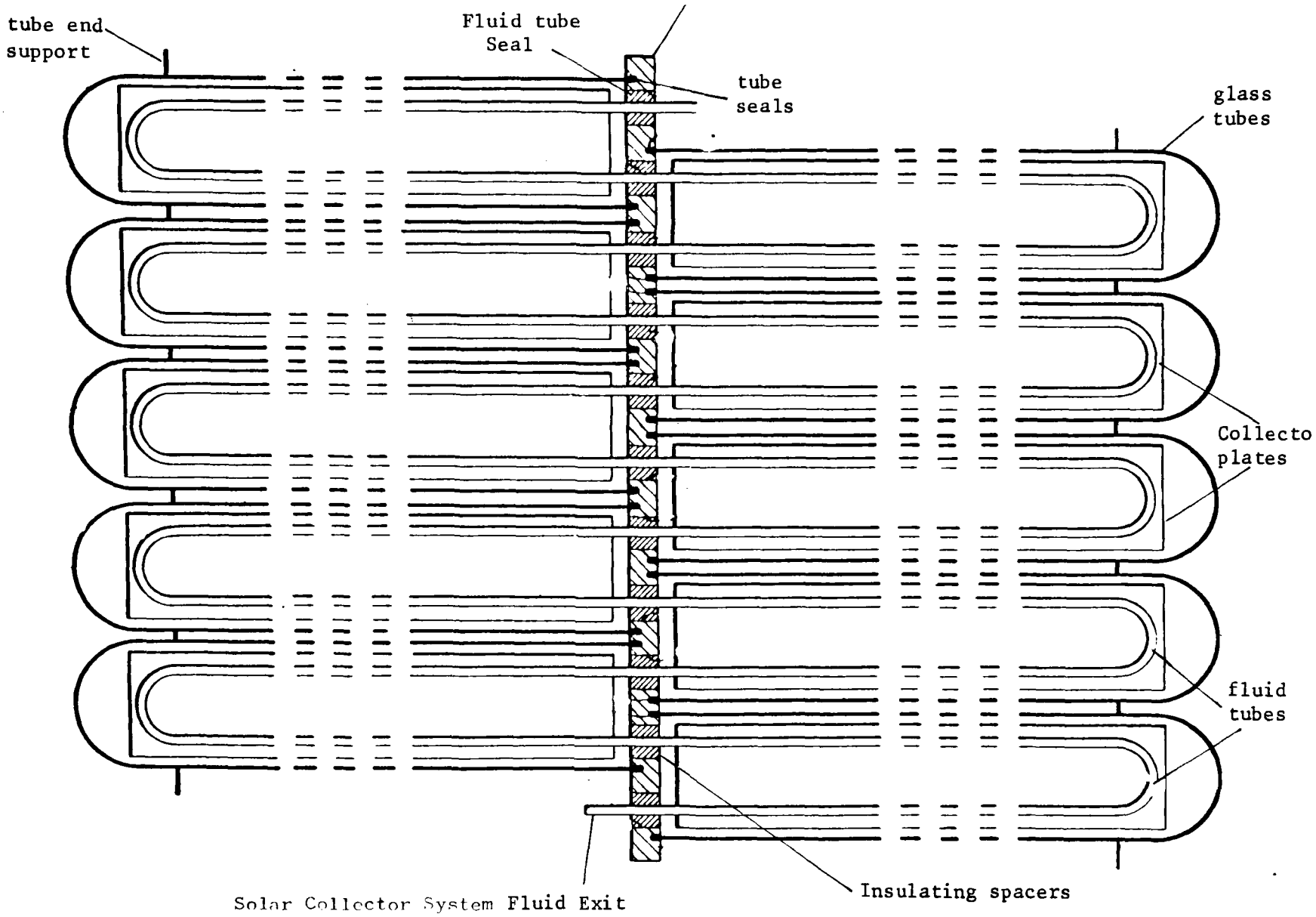

Figure 3.1.2 Solar Collector System

Polymer seals are needed between the aluminium manifold and the glass tubes. The Polymer seals must not only seal the glass tubes, but also be elastic enough to take up excess strain caused by the different expansion coefficients of the glass and aluminium. The polymer also needs to have low outgassing and permeation rates. The polymer chosen as the most suitable for this seal was Viton. This has good vacuum properties and at the same time is elastic enough to take up any excess strains at the metal-polymer - glass junction. An initial design of the Viton seal is shown in figure 3.1.3.

The single fluid pipe that threads the glass tubes and manifold must be thermally insulated from the manifold. This is done by thermally insulating the fluid pipe, as it goes through the manifold, with a polymer spacer. This polymer must have a low outgassing rate and a low thermal conductivity. PTFE was chosen for this job as having one of the lowest outgassing rates for polymers and also a very low thermal conductivity.

The hot fluid pipe however, must enter and leave the collector system. PTFE O-rings are again used for this job. The design of the seals are shown in figure 3.1.1

It is well known that glass tubes evacuated and sealed will keep high vacuum for many years in spite of outgassing. Evacuated tubular solar collectors have been produced, with a high cost glass to metal seals, which will keep ultra high vacuum for a number of years; H Bloem, J C de Grigs, and R L C de Vaan, (1982).

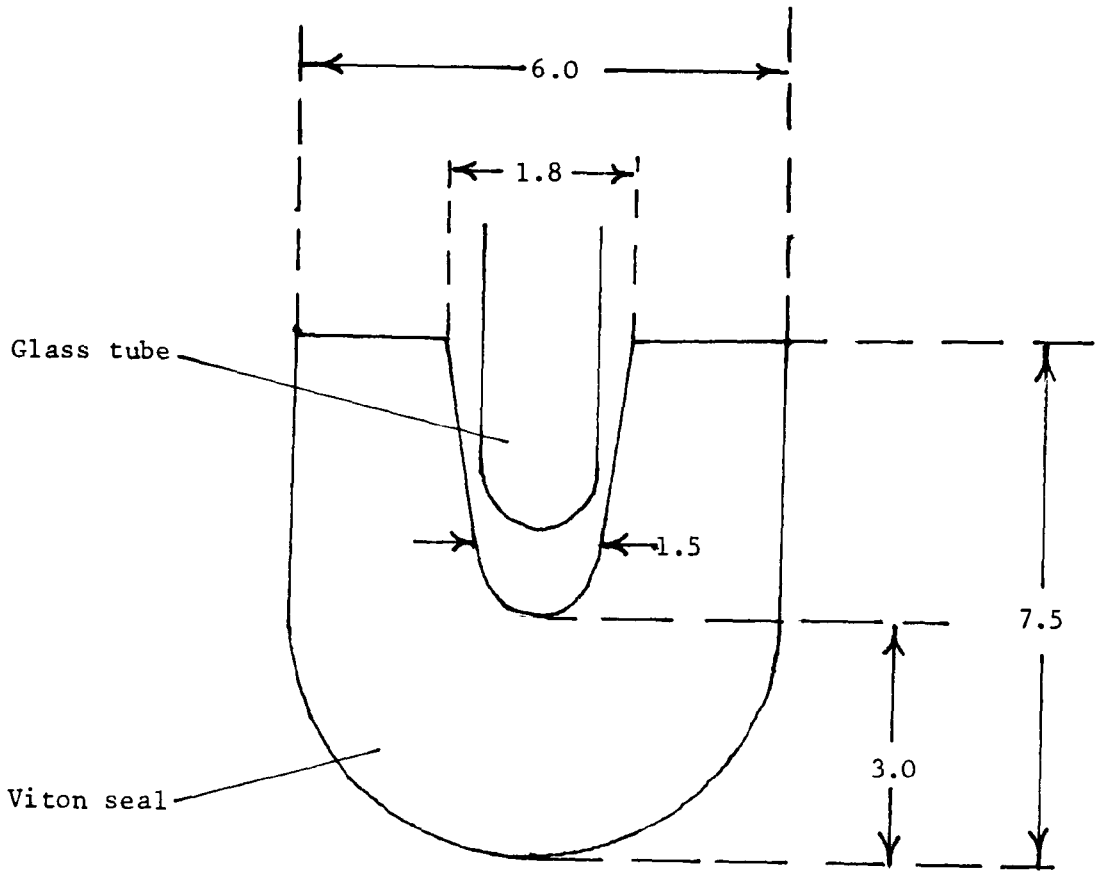

All measurements given in mm

Figure 3.1.3 Cross-section of Viton end seal

The unknown quantity in the loss of vacuum for the new type of collector being considered here, is the outgassing from the polymer seals.

The proposed collectors must keep a reasonable vacuum (<5 Torr) for at least ten years if they are to be commercially viable. Therefore, currently available data on the outgassing and permeation rates of materials which are to be used in the collectors, are presented. An analysis is carried out of the rate of increase in pressure in the tubes, based on previously published data on outgassing. As a guide, estimated pressure increase after 10 years is calculated. The treatment includes the effects of permeation of atmospheric gases through the various wall components, together with the outgassing from the various components within the evacuated space. It is assumed however, that the loss of vacuum will be due solely to outgassing and permeation effects. Loss of vacuum due to chemical reactions, dissociation of gases etc, are assumed to be negligible.

3.2 Loss of vacuum due to outgassing

Outgassing rates, at ambient temperature, for the proposed collector materials, may be found in the literature.

Consider the outgassing rates of the materials tabulated in Table 3.2.1, units of $T.L.S^{-1}.cm^{-2}$., from Esley (1975).

MATERIAL	Q(1)	Q(10)	x
ALUMINIUM	$6.3\ 10^{-9}$	$6.0\ 10^{-10}$	1.0
COPPER	$4.0\ 10^{-8}$	$4.2\ 10^{-9}$	1.0
GLASS	$7.3\ 10^{-7}$	$5.5\ 10^{-10}$	1.7
VITON	$1.1\ 10^{-6}$	$1.8\ 10^{-7}$	0.8
TEFLON	$6.5\ 10^{-8}$	$2.5\ 10^{-8}$	0.5

Q(1) and Q(10) being the outgassing rates, after one and ten hours respectively in the vacuum in $T.L.S^{-1}.cm^{-2}$. x is the slope of the log(outgassing) versus log(time) plot; the main outgassed species being water vapour.

The outgassing rates for the polymers quoted are some five hundred times greater than the outgassing rates for glass and metals after ten hours. Therefore although the surface area of the polymers within the tubes is some hundred times smaller than the surface area of the metal and glass, the contribution to the total outgassing from the polymers will be of major importance in considering the loss of vacuum within the tubes.

The data provided in table 3.2.1, together with the expression 2.3.1 can be used to estimate the pressure in the tubes after a suitable period of time. As mentioned in the introduction it is estimated that the life span of collectors should be at least ten years. Therefore, the pressure rise due to the various parts of the collector after a period of ten years is calculated by applying equation 2.3.1 to each type of material within the collector.

Equation 2.3.1 reads

$$Q_h = (Q_1/t_h^x.) \ldots . 2.3.1$$

Then by changing the units to seconds

$$Q_t = (Q_{3600})\ (3{,}600)^x\ t_s^{-x} \ldots 3.2.1$$

Then intergrating with respect to time,

$$Q = \Delta PV/A = \int_0^t Q_t\ dt = Q_{(3600)}\ (3600)^x \int_0^t t_s^{-x} dt \ldots 3.2.2$$

ΔP is the increase in pressure due to the material

A is the surface area of the material

V is the volume of the evacuated region

Assuming x is constant with respect to time, then from equation (3.2.2) the pressure rise in the collectors may be calculated after any period of time due to the outgassing from any one component.

Assuming an initial pump down time of ten hours, at ambient temperatures, before the collectors are sealed, the pressure rise in each tube due to each component after ten years, is given in table 3.2.2 below:

Component Material	Pressure rise after ten yrs in Torr
Glass envelope	5×10^{-3}.
Aluminium manifold and collector plate	5×10^{-2}.
PTFE O-rings & spacers	1×10^{-1}.
Viton Seal	5×10^{-1}.

TABLE 3.2.2. Pressure in collectors after 10 yrs due to outgassing; excluding permeation.

The assumption that x is constant is probably incorrect. In fact x has been reported in the literature to decrease with time. This would lead to a slightly higher pressure rise in the tubes than is indicated in Table 3.2.2. However, in contrast to this, much of the outgassed species from the unbaked materials will be water, which tends to be re-adsorbed. This will lead to lower values of pressure rise in the tubes.

Even though Table 3.2.2 is not very accurate, it is estimated on the basis of the data used, that it is correct to within 30%. However, it clearly shows that the main contribution of outgassing is due to the viton seals.

3.3 Loss of vacuum due to permeation from the atmosphere

Permeation from the atmosphere, through glass, at room temperature, has been examined thoroughly Norton (1962). Norton shows that one of the glasses with the highest permeability is vitreous silica. He considered the flow of atmospheric gases through a vitreous silica bulb at 25C with walls of 1mm thick, surface area 100 cm^2. These results are shown tabulated in Table 3.3.1.

Gas Species	Atmospheric Abundance C cm Hg	Permeation Rate, P CC(STP)mm cm2 sec. Cm Hg	Inflow CxP	Order of Inflow	Pressure Increase in bulb/Yr, Torr
N_2	$5.95 \times 10^{+1}$	2.0×10^{-29}	1.2×10^{-27}	5	-
O_2	$1.59 \times 10^{+1}$	1.0×10^{-28}	1.6×10^{-27}	4	-
Ar	7.05×10^{-1}	2.0×10^{-29}	1.4×10^{-29}	6	-
Ne	1.8×10^{-1}	2.0×10^{-15}	3.6×10^{-17}	2	10^{-7}
Ne	4.0×10^{-4}	5.0×10^{-11}	2.0×10^{-14}	1	10^{-4}
H_2	3.8×10^{-5}	2.8×10^{-14}	1.0×10^{-18}	3	10^{-8}

Table 3.3.1 - Pressure increase in Vitreous Silica bulb due to permeation.

Norton states that for the same size bulb made from soda lime the pressure increase in one year for helium is 10^{-8} Torr. This gas having by far the highest inflow rate from the atmosphere.

Therefore it may be assumed that the permeation of atmospheric gases through the glass tubes into the collector system will be negligible compared with the outgassing of the various components and (as will be shown later) the permeation through the polymer seals.

Due to the thickness of the manifold and the very low permeation values for aluminium, permeation through the manifold can be neglected.

Permeation through polymers is discussed in detail by Lebovits (1966). The overall permeation rate for the polymers, from the atmosphere is some 10^8 times greater than that for soda lime glass.

Tables 3.3.2 and 3.3.3 give the inflow of various gases through viton and PTFE when atmospheric conditions exist on the high pressure side of the sample. Using the data in tables 3.3.2 and 3.3.3 the loss of vacuum due to permeation through polymers may be calculated.

The PTFE O-rings, used to seal the fluid tubes at inlet and exit positions, are shown in Figure 3.1.1. There are only two such seals in each unit, hence since each unit will contain at least ten tubes, the resulting pressure increase has been adjusted accordingly.

The resistance to permeation is equal to the distance the permeant has to travel in the polymer divided by the cross-sectional area, in accordance with the units of Table 3.3.2 in mm/cm^2.

The resistance to flow (by a PTFE O-ring) = 6.03 mm/cm^2

The conductance of the PTFE O-ring = 0.17 cm^2/mm

The pressure within a unit of ten tubes after ten years due to permeation through the PTFE seals is given by Table 3.3.4

Gas Species	Atmospheric abundance C, Cm.Hg	Permeation Rate, P $\frac{CC(STP)mm}{cm^2 sec.Cm\ Hg}$	C x P (initial inflow)
N_2	5.95×10^{1}	1.0×10^{-10}	5.95×10^{-9}
O_2	1.59×10^{1}	4.0×10^{-10}	6.36×10^{-9}
H_2O	1.19×10^{0}	3.6×10^{-8}	4.3×10^{-8}
He	4.0×10^{-4}	3.0×10^{-9}	1.2×10^{-12}
H_2	3.8×10^{-5}	1.0×10^{-9}	3.8×10^{-14}
Co_2	2.5×10^{-2}	1.2×10^{-9}	3.0×10^{-11}

Table 3.3.2 Order of flow of atmosphere through PTFE for 1 mm thick 1 cm^2 area.

Gas Species	Atmospheric abundance C,	Permeation rate, P $\frac{CC(STP)mm}{cm^2 sec.Cm\ Hg}$	C x P (initial inflow)
N_2	5.95×10^{1}	4.4×10^{-10}	2.62×10^{-8}
O_2	1.59×10^{1}	1.5×10^{-9}	2.39×10^{-8}
H_2O	1.19×10^{0}	5.2×10^{-8}	6.19×10^{-8}
CO_2	2.5×10^{-2}	7.8×10^{-9}	1.95×10^{-10}
He	4.0×10^{-4}	9.87×10^{-9}	3.95×10^{-12}
H_2	3.8×10^{-5}	4.61×10^{-9}	1.75×10^{-13}

Table 3.3.3 Order of flow of atmosphere through Viton for 1 mm thick 1 cm^2 area.

Gas	Pressure rise in tube after 10 yrs in Torr
N_2	0.02
O_2	0.02
H_2O	0.12
$\sum$other gases	<2 x 10-4

Table 3.3.4 Pressure rise in tubes due to permeation through PTFE seals.

An analysis of the seal between endcap and glass tubes, used by Roberts (1979), assumes that the glass only makes an effective seal at the bottom of the groove within the Viton, see Fig. 3.1.3; this is where the thickness of the glass tube equals the width of the groove.

The resistance to permeation within the viton seal, on the basis of the assumption above = 1.2 mm/cm^2. The pressure rise in the tubes due to permeation through the seals using the above resistance, and the data given in Table 3.3.3 was calculated and is shown in Table 3.3.5 below:-

Gas	Pressure rise in tube after 10 yrs in Torr
H_2O	4.8
N_2	2.0
O_2	1.8
$\sum$other gases	$<0.2 \times 10^{-2}$

Table 3.3.5 Pressure rise in tubes due to permeation through Viton seals.

The values calculated for pressure rises in the tubes due to permeation through the end seals, were felt to be very high. The seals also had the tendency to be pushed out by the glass tubes from the grooves in the manifold when being evacuated. For these reasons a new Viton end seal was designed.

3.4 A new design for the end seal

A new end seal was designed to increase the path that permeating gas has to take. The cross-section of this seal is shown in Fig. 3.4.1

The lip on the groove is to ensure a continuous and tight seal between the glass and the Viton all the way down the groove. The lip is placed on the outside of the groove to ensure that at all times the manifold applies an inward force on the glass tube.

The resistance to permeation of gas by the seal may be easily calculated. Consider the seal in three sections - A, B, and C - as shown in Fig. 3.4.2 The resistance to permeation of A is the distance for the permeant to travel, 3.25mm divided by the cross-sectional area through which the permeant travels - $3.1cm^2$.

The resistance for Section A $=3.25/3.1 = 1.05\ mm/cm^2$

Similarly for Section C, the resistance $=0.48\ mm/cm^2$

The resistance to Section B is calculated
by intergrating d/A (as the cross-sectional area is not constant)

Resistance $=0.59\ mm/cm^2$

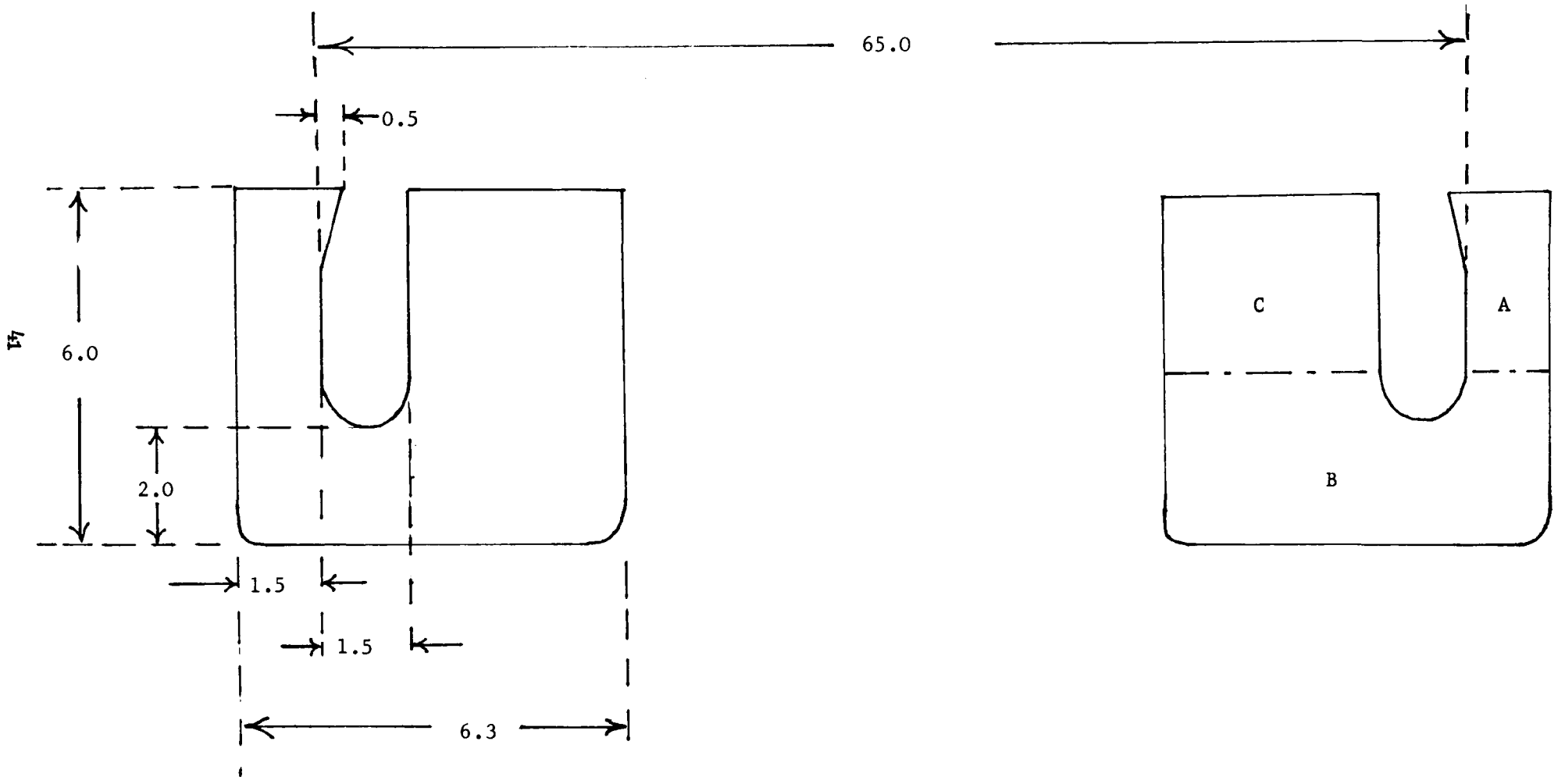

Figure 3.4.1 Section of new Viton end seal; all dimensions in mm.

Thus, the total resistance for the seal $=2.12\ mm/cm^2$

Using this result and the data in Table 3.3.3, the pressure increase in the proposed collectors may be calculated. Table 3.4.1 shows the pressure increase in the tubes after ten years due to permeation through the end seals.

Gas	Pressure rise in tube after 10 yrs Torr
N_2	1.09
O_2	1.00
H_2O	2.58
$\sum$Other gases	$<1 \times 10^{-2}$.

Table 3.4.1 Pressure increases in tubes due to permeation of Viton seals.

It is probable that the actual permeation rates will be lower than quoted in Table 3.4.1, because the Viton end seals will be compressed when the system is under vacuum, thus making the resistance in section B of the seal much larger.

3.5 Discussion

The analysis of the loss of vacuum in the proposed solar collector system in this chapter, gives an indication of the viability of the collector system. The analysis also shows that the main cause of loss of vacuum is due to the polymer sealing technique. According to the analysis the pressure rise in the collectors after a period of ten years - due to outgassing and permeation - is equal to 5.49 Torr. The

composition of gases is shown in Table 3.5.1 below:

Gas	Pressure rise in tube after 10 yrs in Torr
H_2O	3.36
N_2	1.11
O_2	1.02

Table 3.5.1 Gas pressures in collectors after ten years due to outgassing and permeation.

The main phenomena which leads to this pressure rise will be permeation of gas through the Viton end seals. As mentioned previously, the rise in pressure due to this is expected to be lower owing to the compression of the seals when under vacuum.

The pressure increases in Tables 3.2.2, 3.3.4, 3.3.5, 3.4.1, and 3.5.1, all assume collector tubes to be approximately 80cm long. These are the tubes used in the testing of the complete collector unit. However, according to present design, the full-scale collector units will have tubes 120cm long. This will have the effect of reducing all the pressure rise data in the Tables to approximately 67% of the values quoted.

Currently available data on relevant permeation rates of various gases through viton and PTFE are considered to be good enough for an accurate analysis of the loss of vacuum in the collector system.

The data currently available on the outgassing by desorption from viton and PTFE are, however, not adequate for an accurate prediction of the loss of vacuum in the collectors, by this method, for the reasons listed below:

1 The polymer spacers around the hot fluid pipe will become hot, therefore it is necessary to know the outgassing rates of polymers at high temperatures, with particular interest in the species of gas being desorbed. This data was not available in the literature.

2 The analysis of the outgassing by desorption, as carried out in section 3.2., assumed that the values of x were constant and that a baking cycle had not been used. Data on the values for x after many years, and also on suitable baking cycles, were not readily available from the literature.

For the above reasons a series of experiments have been carried out on the outgassing from Viton and PTFE These are described in detail in chapter 4. The results of these experiments will allow more accurate evaluation of long term outgassing by desorption to be carried out, and make it possible to suggest suitable baking cycles for the production of collector units.

4 MEASUREMENT & RESULTS OF OUTGASSING BY DESORPTION

4.1 Introduction

A study of the outgassing rates of Viton, PTFE and Fluorel at elevated temperatures was undertaken, with particular interest in the analysis of the species of gases being desorbed.

A throughput method was used; the apparatus is indicated in Fig. 4.1.1

Results from this study are presented. These results are used for the prediction of the loss of vacuum within the collectors due to desorption from the PTFE spacers.

An experimental study was also undertaken into the desorption rates of Viton after baking. A suitable baking cycle will produce much lower values for the desorption rates. This experimental study was done using the pressure rate of rise method. From these results an upper limit to the pressure rise in the system due to desorption from the seals was found.

A suitable degassing program is suggested for the production of the collectors.

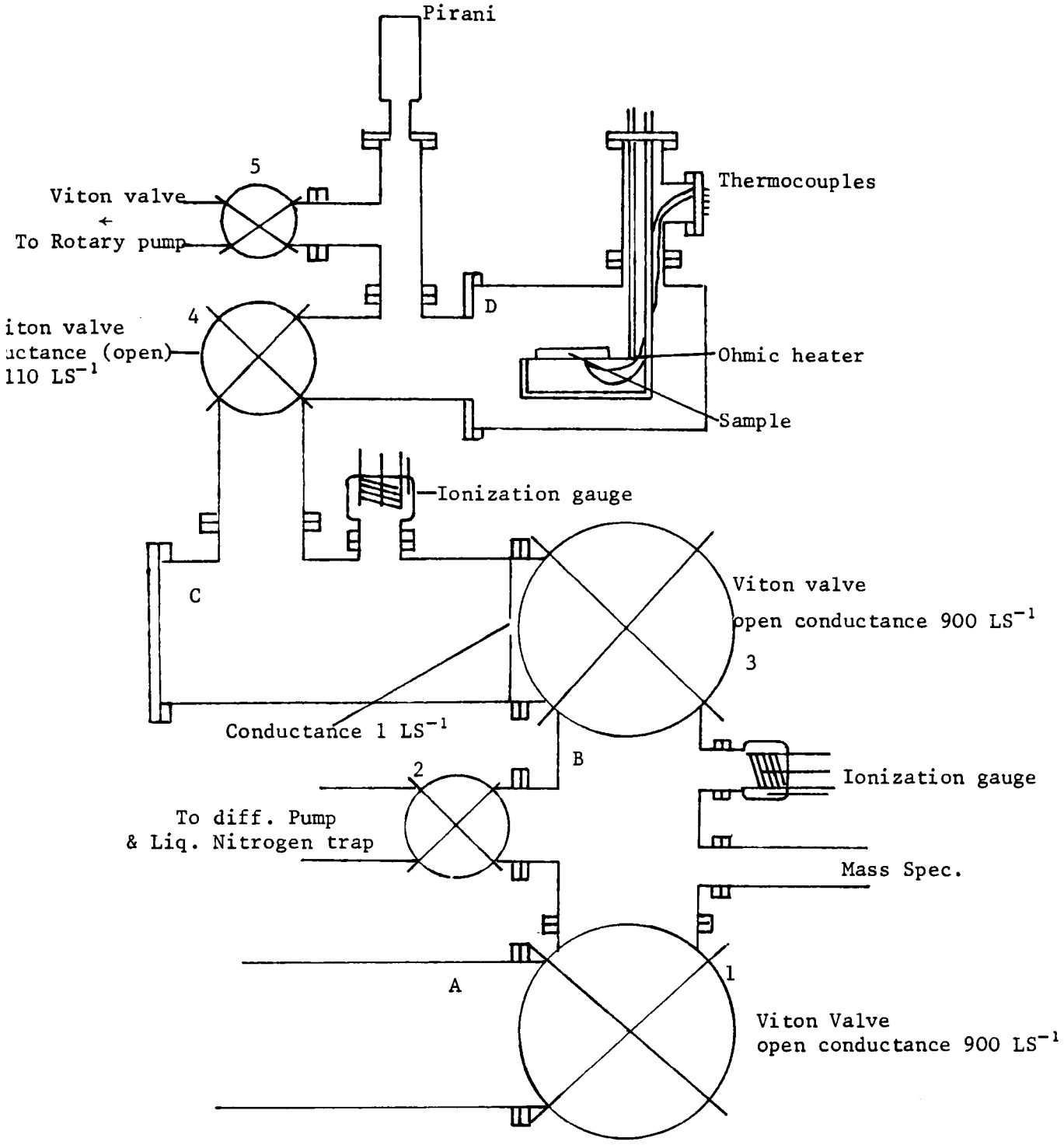

Figure 4.1.1 Experimental apparatus for throughput method

4.2 Experimental procedure

Before any outgassing experiments were undertaken, all the system was evacuated and degassed by baking at 80C for at least two days. Between experiments, the conductance between chambers C, and B was removed (without destroying the vacuum) and the whole system kept at a pressure less than 10^{-6} Torr by the aid of the ion pump, see Fig. 4.1.1

A sample which was to be studied was fixed onto a thin sheet of stainless steel, approximately 0.05 mm thick. This was then connected to the two electrodes in chamber D. The stainless steel acted as an ohmic heater, therefore making it possible to elevate the temperature of the sample. The sample was fixed onto the stainless steel by means of a thin layer of araldite. The argument for a negligible effect on the outgassing rates measured, due to the araldite, being that outgassing is primarily a surface effect and that the surface of the araldite open to the vacuum was less than 0.1% of the surface area of the sample material; the outgassing rate of araldite being of the same order as that for Viton at room temperature; Esley (1975).

Following the introduction of a sample into the chamber D (the chamber was let up to atmosphere for a short a period as possible, always less than 1 hour) the chamber is pumped with the rotary pump via valve 5. After pump down, valve 4 is opened, allowing gas outgassed in chamber D to flow through chambers C, B, and A into the pumps. During actual experiments valve 1, is kept closed and the diffusion pump used to evacuate chamber B.

The outgassing rate of chambers C, D and the sample, is then determined by noting the pressure difference across the conductance. In all cases blank runs were carried out to determine the effective outgassing from the various chambers of the system.

The conductance of valve 2 is comparatively small, namely, approximately 70 ls^{-1}. Between experiments the ion pump is kept continuously on, to attain pressure less than 10^{-6} Torr as already indicated. The use of the diffusion pump instead of the ion pump during actual experiments was due to the relatively high flow rates through the system, and the large variation in pumping speed of the ion pump to different gases.

The analysis of the gas desorbed was carried out in chamber B, with the SupVac mass spectrometer. Due to the two conductances, the partial pressures of gases in chamber B will be in the same ratio as the partial pressures in chambers C and D, if the base pressure of the pump is sufficiently low.

Consider the representation of the apparatus as below and a species of gas i emitted from the sample:

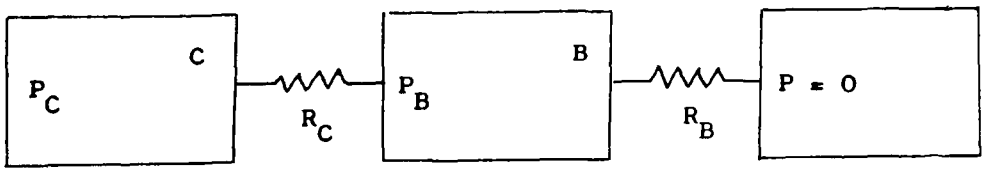

Then,

$$P_{Bi} = P_{Ci}\ (R_{Bi}/(R_{Ci} + R_{Bi}))...4.2.1$$

Where $I/R = C = 3.64\ (T/M)^{\cdot 5}\ A.....4.2.2$

and P_{Ci}, P_{Bi} are the partial pressures of gas i in chambers C and B respectively. Equation 4.2.2 may be re-written as

$$R_{Ci} = Y_C\ M_i^{\cdot 5}$$

and $R_{Bi} = Y_B\ M_i^{\cdot 5}$.

where Y is a function of conductance and temperature only.

Therefore,

$$P_{Bi} = P_{Ci}[Y_B/(Y_C + Y_B)]...4.2.3$$

A similar expression may be written for a gas of species j, then

$$\frac{P_{Bi}}{P_{Ci}} = \frac{P_{Bj}}{P_{Cj}} = \frac{P_B}{P_C} \quad ....4.2.4$$

where P_B and P_C are the total pressures in the two chambers. Therefore the ratio of partial pressures of gases in chambers B, and C are the same. Knowing the total pressures in chambers B, and C, and the partial pressures in chamber B, it is possible to determine the outgassing rate of different species of gas from the sample. The outgassing rate of species i is then given by:

$$Q_i = 3.64(T/M)^{1/2}\ A(P_C - P_B)\ (P_{Bi}/P_B).....4.2.5$$

4.3 Results

Experiments were carried out on samples of PTFE, Viton A, and Fluorel suppled by Du Pont and 3M. Each sample used was approximately 3mm thick. Note that Fluorel is 3M's approximate equivalent polymer to Viton.

Some of the experimental data obtained is given in Tables 4.3.1 and 4.3.2, in the form described in section 2.1.

A typical outgassing graph of a sample and chamber, superimposed on an outgassing graph of just the chamber, is shown in Figure 4.3.1.

It was found with all the samples tested that water vapour was the major species desorbed and amounted to at least 90% of the gases outgassed. Figure 4.3.3 shows a mass spectrum of gases found in the apparatus when no sample was being tested. Figure 4.3.2 shows a typical mass spectrum of the gases found in chamber B, when a sample was under test.

The experimental values of outgassing, found for samples at room temperature, are in good agreement with other workers.

There is little experimental data available for outgassing of samples at elevated temperatures. However, it is worth noting that Santhanam and Vijendram (1982) have reported that for polyesters there is no appreciable change in the slopes of the outgassing graphs with temperature. This was not the case in the present investigation.

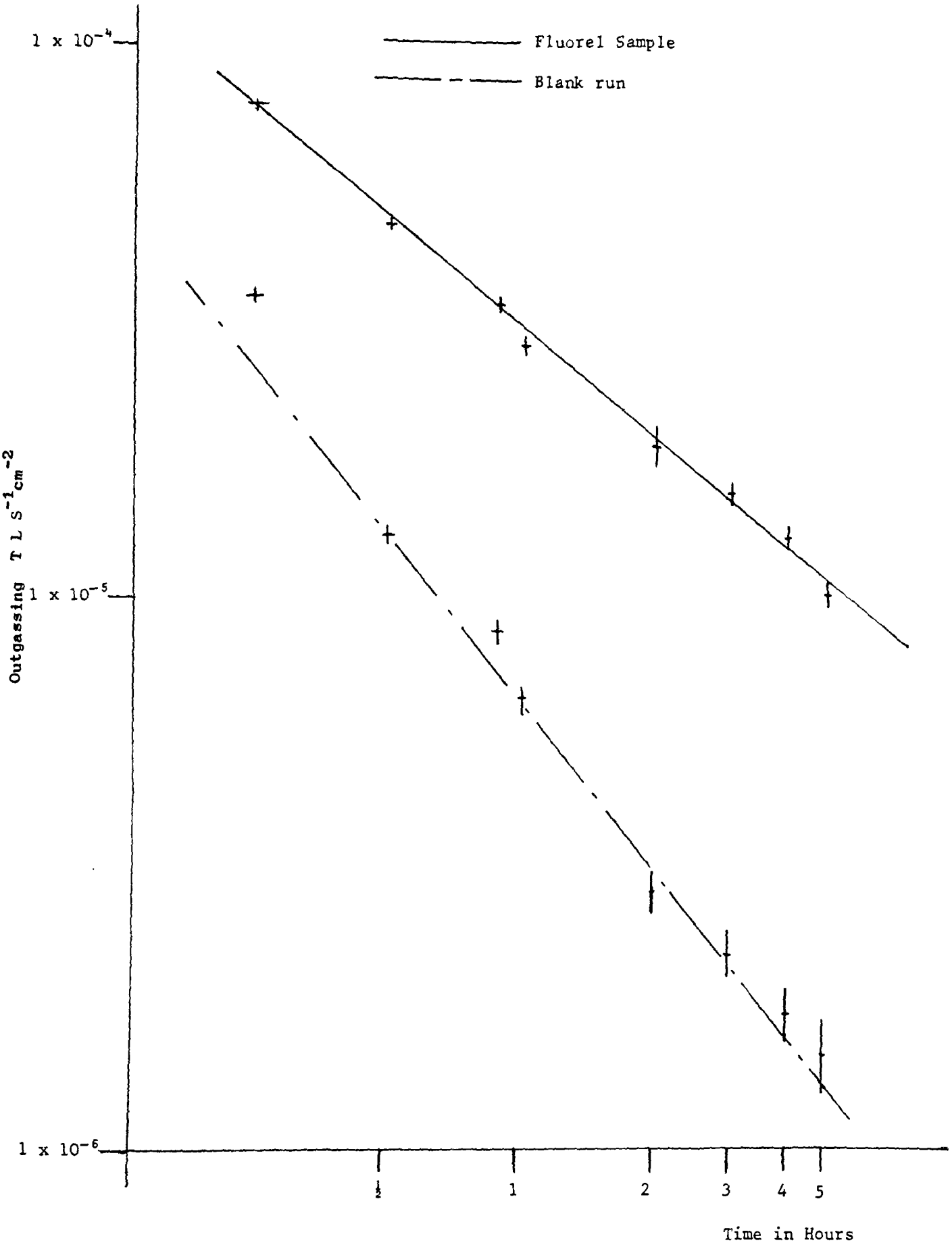

Figure4.3.1 Outgassing rate plot of Fluorel and chambers

Figure 4.3.2 Mass spectrum of outgassed species from Fluorel

Total Pressure = 1 x 10^{-5} Torr

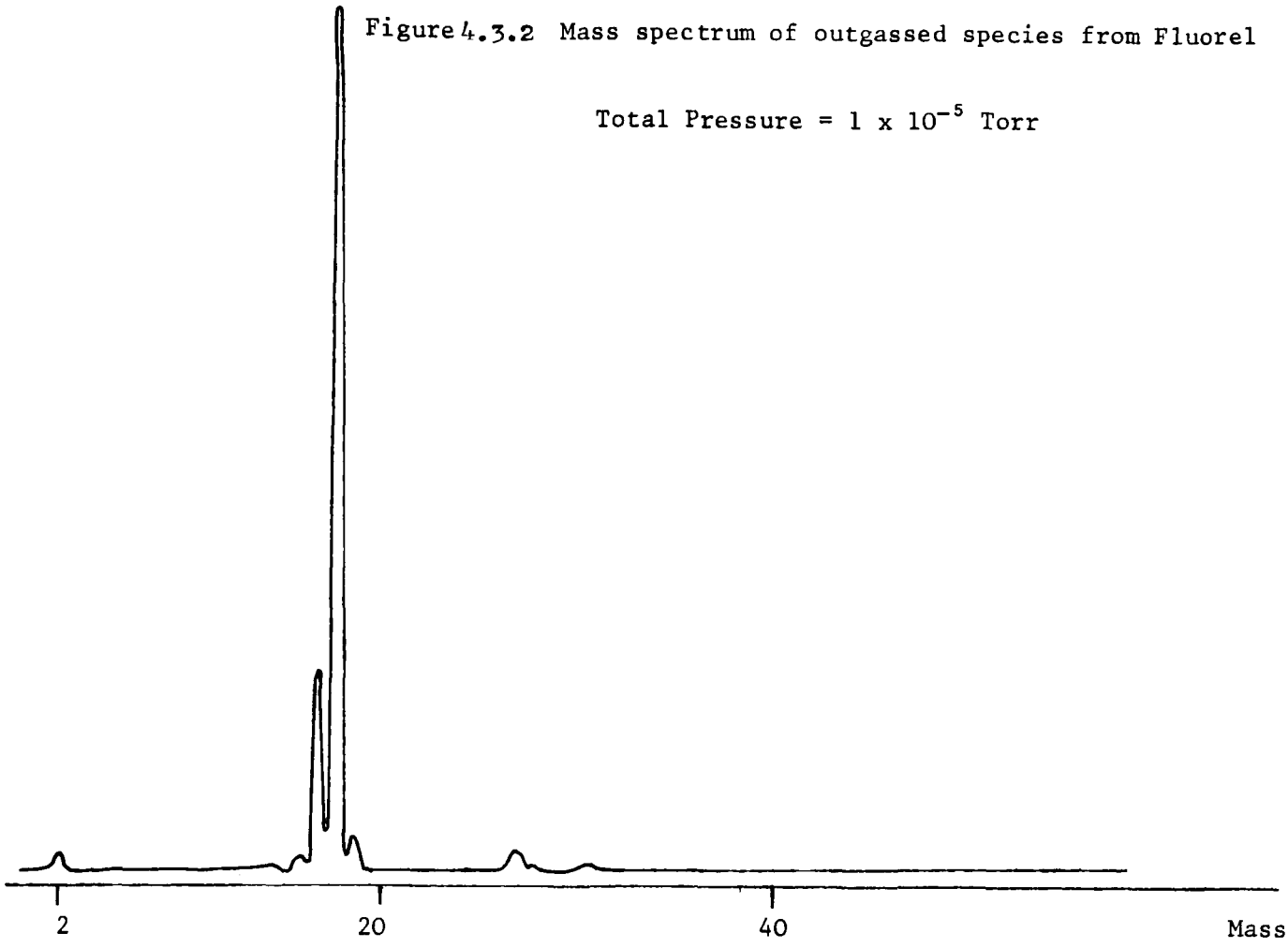

Figure 4.3.3 Mass spectrum of outgassed species from Chambers

Total Pressure = 5 x 10^{-7} Torr

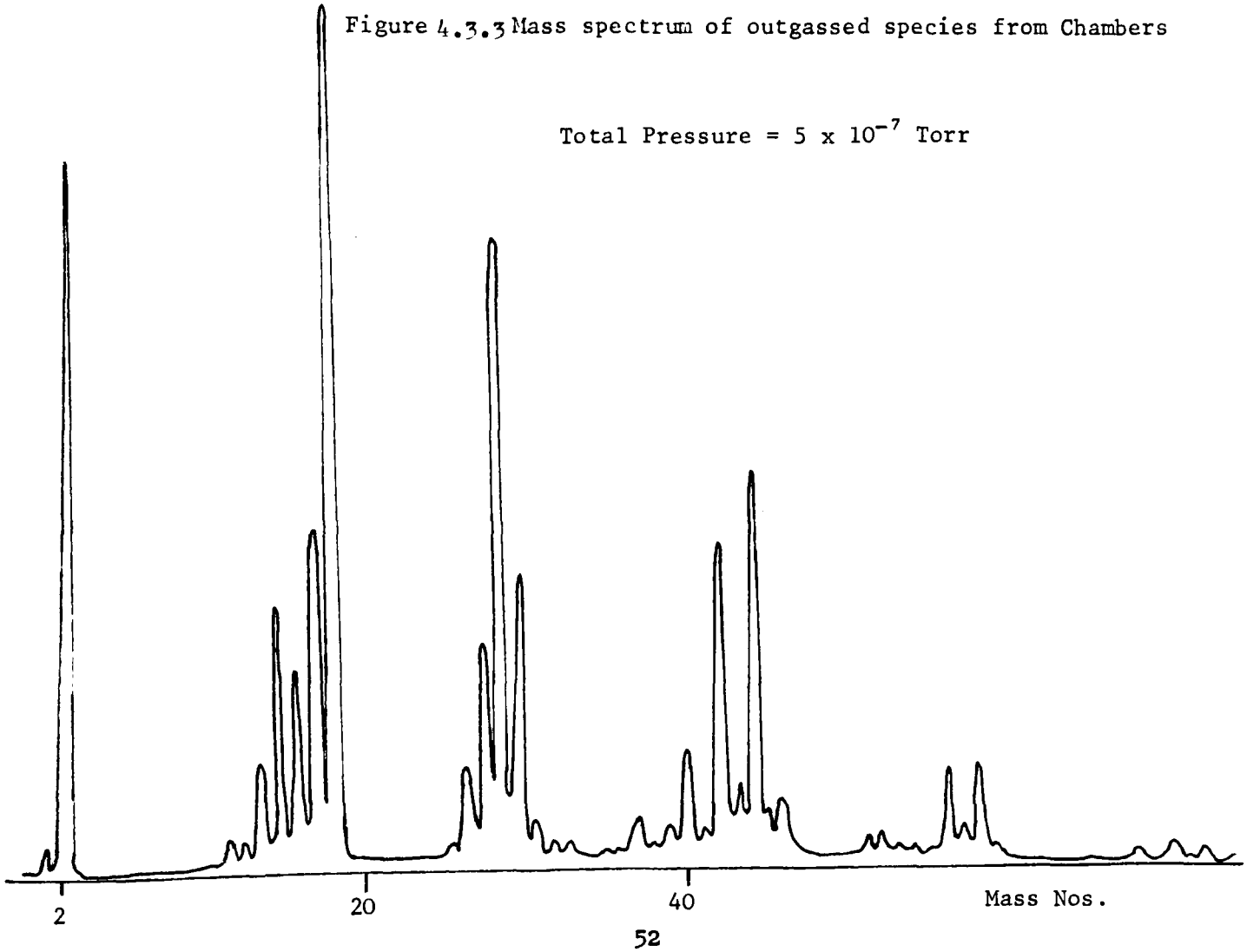

TABLE 4.3.1
Outgassing rates at 20C.

Material	x	Q_1 T.L.S^{-1}.cm^{-2}.	Q_5 T.L.S^{-1}.cm^{-2}.
Fluorel	-0.58 +/-0.08	1.02×10^{-6}.	4.61×10^{-7}.
Viton	-0.62 +/-0.10	1.02×10^{-6}.	3.85×10^{-7}.
PTFE	-0.44 +/-0.10	1.51×10^{-7}.	6.67×10^{-8}.

TABLE 4.3.2
Outgassing rates at 120C +/-5C.

Material	x	Q_1 T.L.S^{-1}.cm^{-2}.	Q_5 T.L.S^{-1}.cm^{-2}.
Fluorel	-1.39 +/-0.08	5.56×10^{-5}.	4.60×10^{-6}.
Viton	-1.43 +/-0.18	2.12×10^{-5}.	1.94×10^{-7}.
PTFE	-1.01 +/-0.20	8.24×10^{-6}.	5.32×10^{-7}.

Data was also required on the polymers subsequent to various degassing procedures. It was found that the outgassing rate from such polymers was so low that meaningful results could not be obtained with the throughput method as described, since it was found that it was not possible to distinguish between the outgassing rate of the sample and the apparatus.

To determine these very low outgassing rates, a stainless steel chamber was constructed which could fit into an oven. The chamber was connected to a diaphragm gauge and measurements were made by the pressure rate of rise method. Samples (approximate area 200 cm^2) were rolled up and placed in the chamber. The chamber was then pumped down for half an hour before commencement of baking, The chamber and sample was then baked at 160C, 140C and 120C for six hours. In each case after baking the chamber was then sealed for two weeks. Blank runs were also carried out.

It was found that in each case the pressure rise after two weeks was very small. It was not possible to distinguish between the sample tests and the blank runs. If the blank runs were ignored then an upper limit for the outgassing rates of the samples in each case was found to be of the order of:-

$$Q = 2.10^{-10} \ (T.L.s^{-1} \ cm^{-2})$$

This value is far lower than any other value found in the literature. It was concluded that the outgassed water was being re-adsorbed on the surface of the chamber and the sample.

4.4 Discussion

Initially in the throughput experiments the diffusion pump was not connected to the apparatus shown in figure 4.1.1. All experiments at that time were conducted using the ion pump. However, problems arose during the analysis of the gases due to;

1 Regurgitation effects of the ion pump

2 Far larger differences in pumping speeds, for different gases, than expected.

Because of this interference to gas analysis from the ion pump, a diffusion pump was connected to the apparatus and used in all experiments.

The results presented for the throughput experiments may be used to calculate the expected outgassing rates of the PTFE spacers at collector operating temperatures of between 20C and 120C. These results also show that even at high temperatures the main species desorbed is water vapour.

A degassing program by baking of a collector system is limited by the temperature that;

1 The polymers may be baked

2 The glass may be baked

3 Any selective adsorbing surface used is still stable.

The evolution from the soda glass has a maximum value of approximately 140 - 150C; at higher temperatures physically adsorbed gas tends to become chemically adsorbed; See Roth (1976).

The maximum temperature at which Viton should be baked is 200 degrees centigrade as suggested by Du Pont.

For these reasons a degassing program by baking should not exceed a temperature of approximately 150C.

Results show that after Viton has been through one of the baking cycles, as described in section 3.3, the desorption rate has an upper limit of 2×10^{-10} T.L.S^{-1} cm^{-2}.

Using this result, the rate of rise of pressure in the collectors, neglecting permeation, is calculated as follows:

Surface area of Viton per collector tube	= 6 cm^2
Volume of experimental tubes	= 2.70 litre
Increase in pressure per year	= 1.4×10^{-2} Torr

This gives an upper limit to the rate of rise of pressure in the tubes due to desorbed gas, which is far superior to the analysis given in section 3.2., as this relied on the fact that x from equation 2.2.1 was constant.

As discussed in chapter 3, the pressure rise in the collectors due to permeation is thought to be approximately 0.5 Torr/yr, which is greater than the rate of rise in pressure due to desorption from the Viton seals.

The following degassing programme for the production of the collector units from the results is therefore suggested:

1 Evacuate the system for half an hour before commencement of baking.

2 While the system is still being evacuated, bake at 140C for six hours.

3 Allow the system to cool to room temperature whilst still being pumped.

4 Introduce the low thermal conductivity gas (details will be given in later chapters).

5 Seal the collector system.

It is predicted that the pressure rise in the tubes after such a baking cycle will be due, in the main, to permeation effects. The predicted rate of rise of the partial pressure in the tubes with respect to time is shown in Fig. 4.4.1.

To predict the theoretical performance of the collectors after many years, the thermal conductivity of the low thermal conductivity gas introduced, mixed with the spurious gas, which will arise due to permeation, must be known.

Figure 4.4.1 Rate of rise of pressure in Solar collector unit

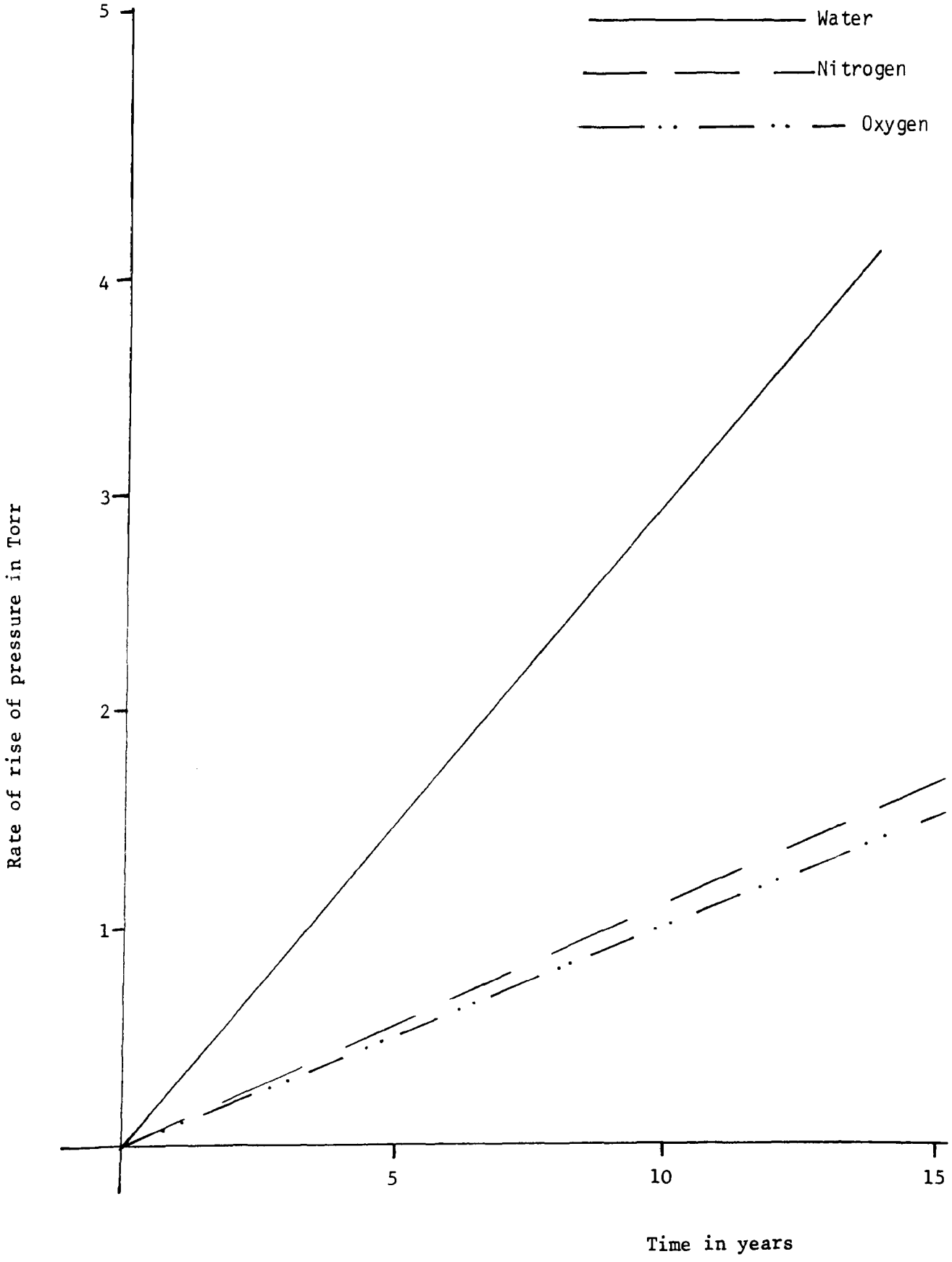

There is very limited data available on the conductivity of gas mixtures involving such gas as the Halocarbons, methyl iodide, mixed with water, oxygen and nitrogen.

In the following chapters an experimental and theoretical analysis is shown of the thermal conductivity of the gas mixtures arising in the collectors. From these analyses a choice of a suitable low thermal conductivity gas to inflow into the system, at the production stage, will be made.

5 EXPERIMENTAL WORK ON THE THERMAL CONDUCTIVITY OF GAS MIXTURES

5.1 Introduction

The predicted maximum rise in pressure, within the solar collectors, after one year is 0.5 Torr. The mean free paths of the predicted spurious gases at this pressure is approximately 0.1 mm. As the minimum distance between the collector plate and the glass tube is approximately 10 mm the so called gas to wall collisions within the collector will be negligible in comparison to the gas to gas collisions. Kinetic theory and experimental results show that the thermal conductivity of gases in these conditions is independent of pressure. This pressure independence may be easily explained since at high pressures there will be more carriers of energy, but each carrier transports less heat because it moves a shorter distance between collisions. This phenomena obviously breaks down when the pressure of the gas is so low that the mean free path of the gas molecules is of the same order or less than the dimensions of the vessel holding the gas.

After one year, the heat loss due to conduction will reach an approximately constant value which depends on the composition of the gas. The heat loss may however be considerably reduced by the introduction of a suitable low thermal conductivity gas at the collector fabrication stage. Introducing a low thermal conductivity gas within the collectors will have the effect of reducing the thermal conductivity of the gas mixture, as it will

1 bring in molecules which will not transfer energy so readily.

2 will shorten the average mean free path of the gas molecules at any one pressure.

Convection losses are effectively zero, in the tubular collectors, at pressures below 20 Torr, Roberts (1979). Therefore, it has been proposed to introduce into the collector system a low thermal conductivity gas to suppress conduction losses through the spurious gases. The total gas pressure being still low enough to suppress convection losses.

As mentioned in section 4.4, data is required on the thermal conductivity of relevant gas mixtures. As a result of a study of thermal conductivity, cost, stability, and compatibility with components of the collector system, the gases and vapours of most interest are listed below :-

Halocarbon 11, Halocarbon 12, Halocarbon 13, Halocarbon 21, Halocarbon 113,

Methyl Iodide, Sulphur Hexafluoride, and Krypton.

The thermal conductivity of these gases mixed with the spurious gases, namely, water, nitrogen, and oxygen is of vital importance to the project. Long term efficiency of the collectors can only be estimated if such data is available. As this data was not available a thermal conductivity cell was designed, built, and tested to undertake these measurements.

5.2 The construction of the thermal conductivity cell

A conventional thermal conductivity cell with a horizontal test layer heated from above was constructed as shown in figure 5.2.1. At one time this type of cell had become unpopular with workers due to the difficulty in controlling the guard. The regulation of the guard temperature increases the time needed to reach steady state conditions where readings are usually taken. However, it was felt that with the advancement of modern electronics, this problem could easily be overcome. A control unit was designed, and constructed, figure 5.2.2, to :-

1 Keep the temperature of the guard the same as that of the plate.

2 Display the temperature of the guard, plate, and sink at any time.

The operation of the unit relies on the use of platinum film temperature sensors (RS 158-238) to measure the temperature of the guard plate and sink, together with ohmic heaters in the guard and plate. Heat was removed from the sink by circulating water between the sink and a suitable constant temperature bath.

The resistance of the platinum sensors were measured with bridges as shown in figure 5.2.2 The voltages from the bridges are fed, via a 3x3 way switch to a D.P.M. (RS 258-827). The voltages from any one bridge may be selected at any one time via the 3x3 way switch. The

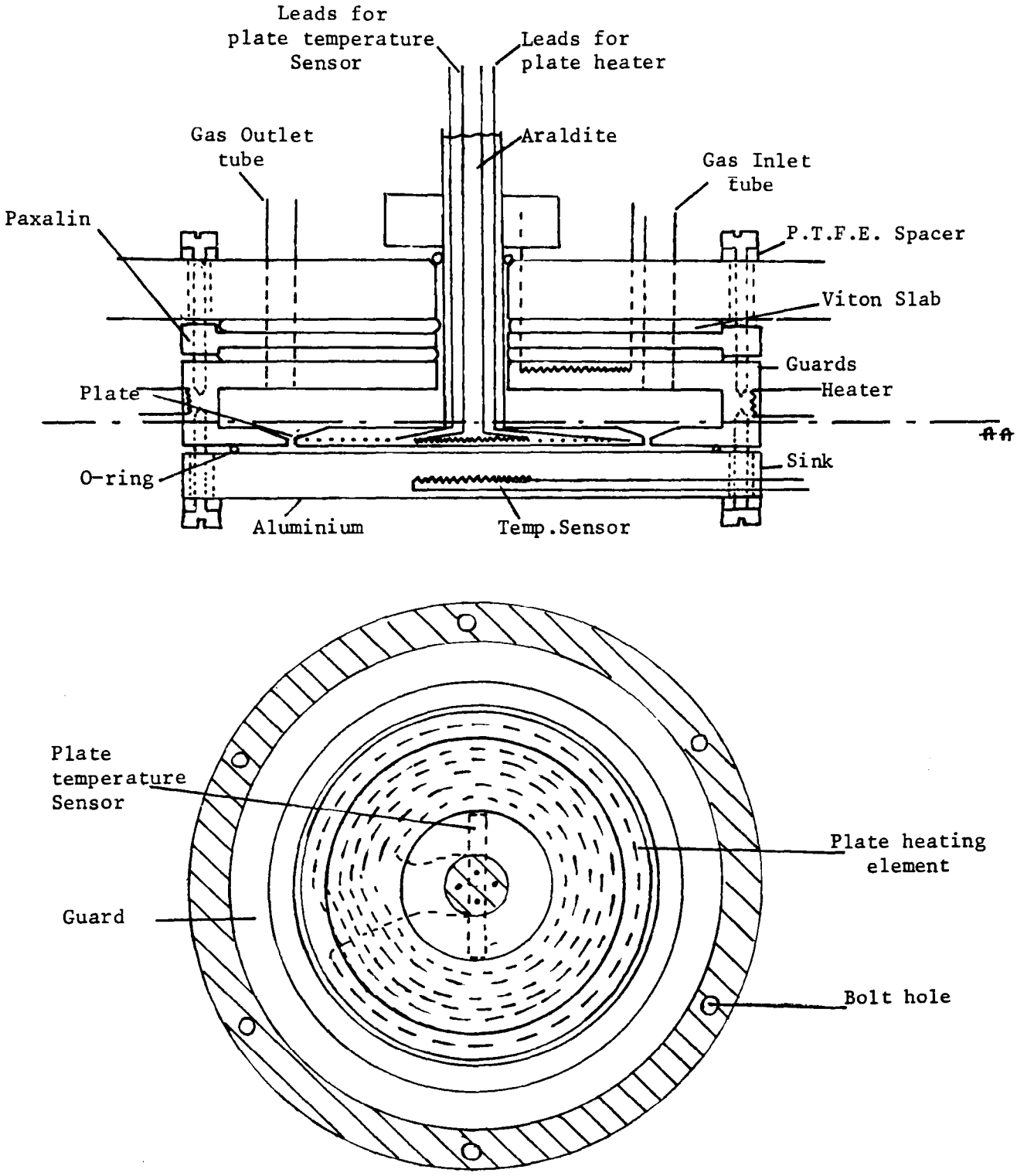

Section AA

Figure 5.2.1 Thermal Conductivity Cell

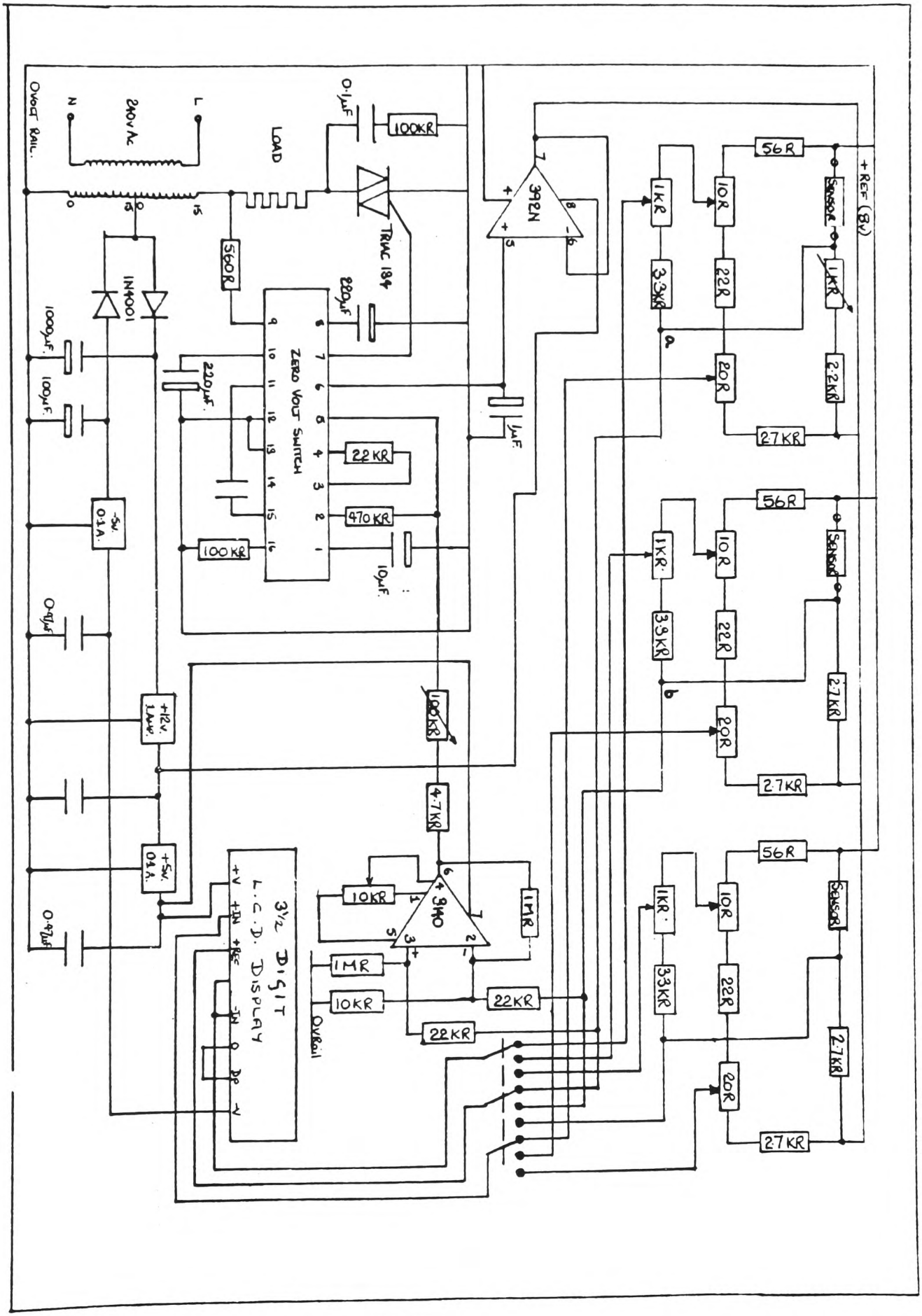

Figure 5.2.2 Electronic Control Unit

differential voltage across a particular bridge is measured, one side of which is at a constant voltage. The constant voltage may be adjusted by the zero voltage pot. The other voltage, which is the unknown, may be multiplied by a constant via the span pot. The linearity pot voltage is used by the D.P.M. as a reference voltage with which the differential voltage is compared. The comparison methods used in measuring the output of the bridges, ensure that any fluctuation in supply voltage will not alter the detected resistance of the sensors. The calibration of the bridges is described in the RS data sheet R/3914. The bridges were also calibrated for the particular sensors before the cell was constructed, since there is a tolerance on their absolute resistance of 0.1% which corresponds to 0.25C, and on their coefficient of resistance with temperature. Also there is a small resistance (0.02 ohms) in the input leads to the sensors which has to be accounted for. The sensors were emerged in a water bath the temperature of which was read by a standard mercury thermometer, reading to 0.05C. The linearity, span and zero potentiometers in the bridges were varied so that the readings displayed on the D.P.M. corresponded to the temperatures in the water bath to within the resolution of the display, namely 0.1 degrees. The temperature of the water bath was varied from 4C to 60C. The sensors where then calibrated to within +/-0.05C.

The sensors and heaters were then embedded in their respective parts of the cell with araldite.

The amount of energy introduced into the guard is controlled by comparing the temperature of the plate and guard. This is done by feeding the appropriate voltages obtained from the plate and the guard bridges (points (a) and (b) in figure 5.2.2 respectively) to a

differential operational amplifier. The signal thus obtained is fed to a zero voltage switch (RS 305-800). The zero voltage switch compares this signal with a ramp voltage signal. When the voltage of the ramp is greater than the voltage from the differential amplifier, power is supplied to the guard heaters by turning on a triac. The ramp is from 0 to 6 volts once every second. Power to the bridges is supplied via a reference voltage from the zero voltage switch. This means that any fluctuations in the reference voltage of the zero voltage switch will appear on the bridges.

Electrical energy is introduced to the heater element of the plate using a Farnell d.c. supply unit. The power is measured using volt and ampere meters to an accuracy of 0.5%.

The resistance of the plate heater is approximately 48 ohms. The resistance of the input leads for the plate heater are less than 0.02 ohms. Therefore, the amount of energy lost in these leads is less than 0.1% of the total input energy.

To ensure that there were no temperature gradients across the glass rod, holding the plate in position and carrying the copper input leads to the plates' heater and temperature sensor, a collar was fixed on to the guard, see fig. 5.2.3. The collar had good thermal contact with the guard and at all times was within 0.5C of the temperature of the guard. The glass rod passed through the collar, which was filled with mercury to ensure good thermal contact with the glass rod and input leads.

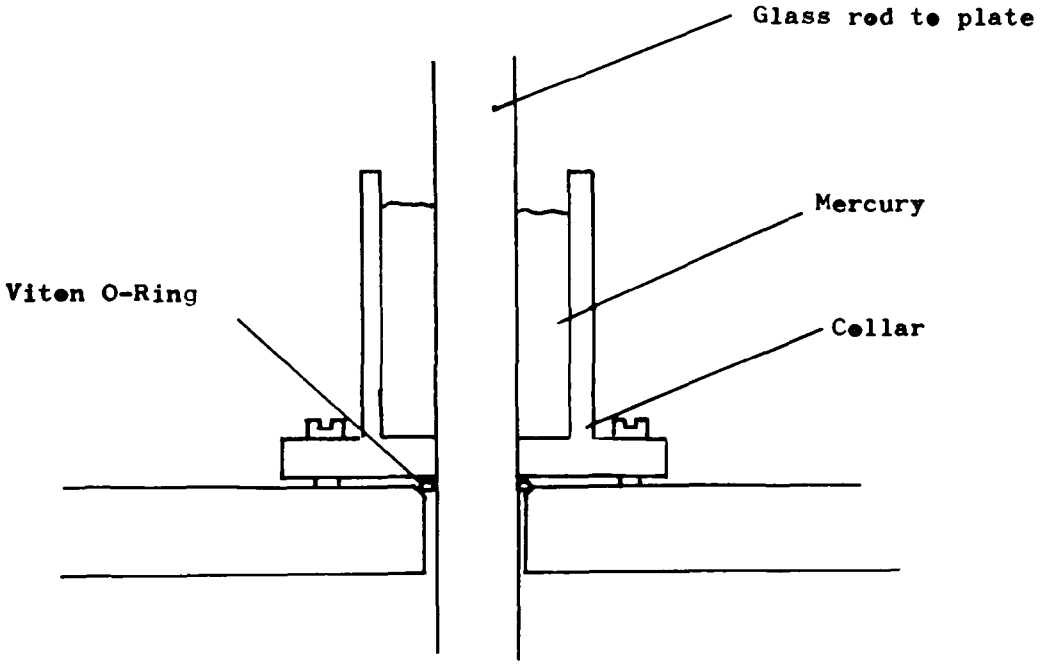

Figure 5.2.3

The plate was made from brass with the sensor and heater embeded in it with araldite. To ensure that the plates' surface had a constant low emissivity, throughout the experiments, the plate was sputter coated with gold.

The thermal conductivity cell was well insulated from the atmosphere, with foam rubber. This was to ensure that no large temperature gradients appeared across the guard and collar.

5.3 OPERATION OF THE THERMAL CONDUCTIVITY CELL

In the steady state condition the energy balance equation for the plate is

$$q = K A \Delta T/d + R\Delta T \quad \text{.....5.3.1}$$

Where:-

q, is the energy injected into the plate per second.

k, is the thermal conductivity of the gas in the cell

A/d=B, is the area of the plate/distance between the plate and the sink.

ΔT, is the temperature difference between the plate and sink.

$R\Delta T$, is used to represent heat loss from the plate due to radiation, this term may also take into account any spurious energy losses through the input leads etc to the plate.

The cells' operating conditions where chosen such that the plate would be at approximately 40C and the sink at 20C The thermal conductivity of the gases was then measured at a temperature of 30C. It was found however, that it was only practical to get the mean temperature to within 2C of 30C. So corrections were made to the results. Table 5.3.1 shows that the percentage increase per degree centigrade of thermal conductivities of various gases at 30C. Corrections were made, assuming thermal conductivity to vary linearly with temperature, So that all measurements would correspond to 30C. the total maximum error due to these corrections will only be 0.2% of the thermal conductivity measured.

It should also be noted that the increase in thermal conductivity of gases with temperature is not an exact linear function with respect to temperature. However, from the data given by Touloukian et al (1970), it was estimated that the error caused to the results due to this effect would be less than 0.5% of the thermal conductivity measured in all cases.

The temperature of plate, guard and sink could be measured to within +/-0.05C. The difference in temperature between plate and guard, 5 minutes after the cell had reached steady state conditions was found to be less than 0.1C. During the transient part of the experiments the temperature of the guard was at all times within 2C to the temperature of the plate. Experiment and theory showed that the cells' time constant for all the gases used was less than 15 minutes hence the maximum time (for the lowest thermal conductivity gas) required for the cell to be within 1% of the steady state condition was 1 hour.

TABLE: 5.3.1

GAS	% INCREASE PER DEGREE AT 30C
H11	0.5
H12	0.5
H13	0.5
H21	0.5
H22	0.5
H113	0.5
H114	0.5
WATER VAPOUR	0.4
KRYPTON	0.3
NITROGEN	0.3
OXYGEN	0.3
ARGON	0.3

Following cell fabrication and subsequently at intervals of two months the cell was pumped down to a pressure less than 10^{-4} Torr for at least one hour, with tests then undertaken to determine leaks and outgassing. This was essential since the introduction of spurious gases into the cell could greatly effect the results. Leak testing was carried out by coupling the cell to a mass spectrometer and probing the cell with a helium jet. At all times the cell was found to be leak tight. The effect of outgassing was determined by operating the cell at normal test temperatures (sink at 20C and the plate and guard at 40C), and evaluating the rate of rise of pressure rise, with the cell sealed from

the pumps. For this test cell pressure was determined by a high quality diaphragm gauge, namely the MKS Baratron with a resolution of 10^{-3} torr. Typical results for the rate of pressure rise are shown in figure 5.3.1.

The total rise in pressure after 1 hour was only 0.013 Torr. This indicates that by using a test gas in the cell at a pressure of 10 Torr, the contamination of the test gas due to outgassing will be only 0.1%. During operation, test gas was supplied to the cell via a 3 litre glass bulb; see figure 5.3.2. A suitably low flow rate through the cell could easily be achieved with the leak valve connected through to the diffusion pump; So that contaminated gas could be pumped away through out the test. If the test being carried out took longer than one hour then the above procedure was used to insure that the test gas did not become contaminated.

Figure 5.3.3 shows the apparatus used to introduce gases into the glass flasks. The flask was always pumped for at least 1 hour before being filled. The outgassing from the flasks was negligible. Mixtures of gases were made by a freezing-out method. For example the following procedure would have been used to make a mixture of 50% Hll. and 50% N_2:- The flask and manifold shown in figure 5.3.3 would be pumped out for at least one hour. Valves 2 and 7 (see diagram) would then be shut, halocarbon 11 then would be let into the system. via one of the gas inlets, to a value of 10 torr. Valve 1 would then be shut valve 2 opened and liquid nitrogen applied to the arm to freeze the halocarbon out. Valve 2 would then be shut and valve 7 and 1 opened, after the manifold had been pumped out again valve 7 would be shut and N_2. let into the system to 10 torr. Valve 1 then being shut and valve 2 opened. Thus giving 50% Hll and 50% N_2. Usually the gases were flushed

Figure 5.3.1 Rise in pressure with respect to time in thermal conductivity cell.

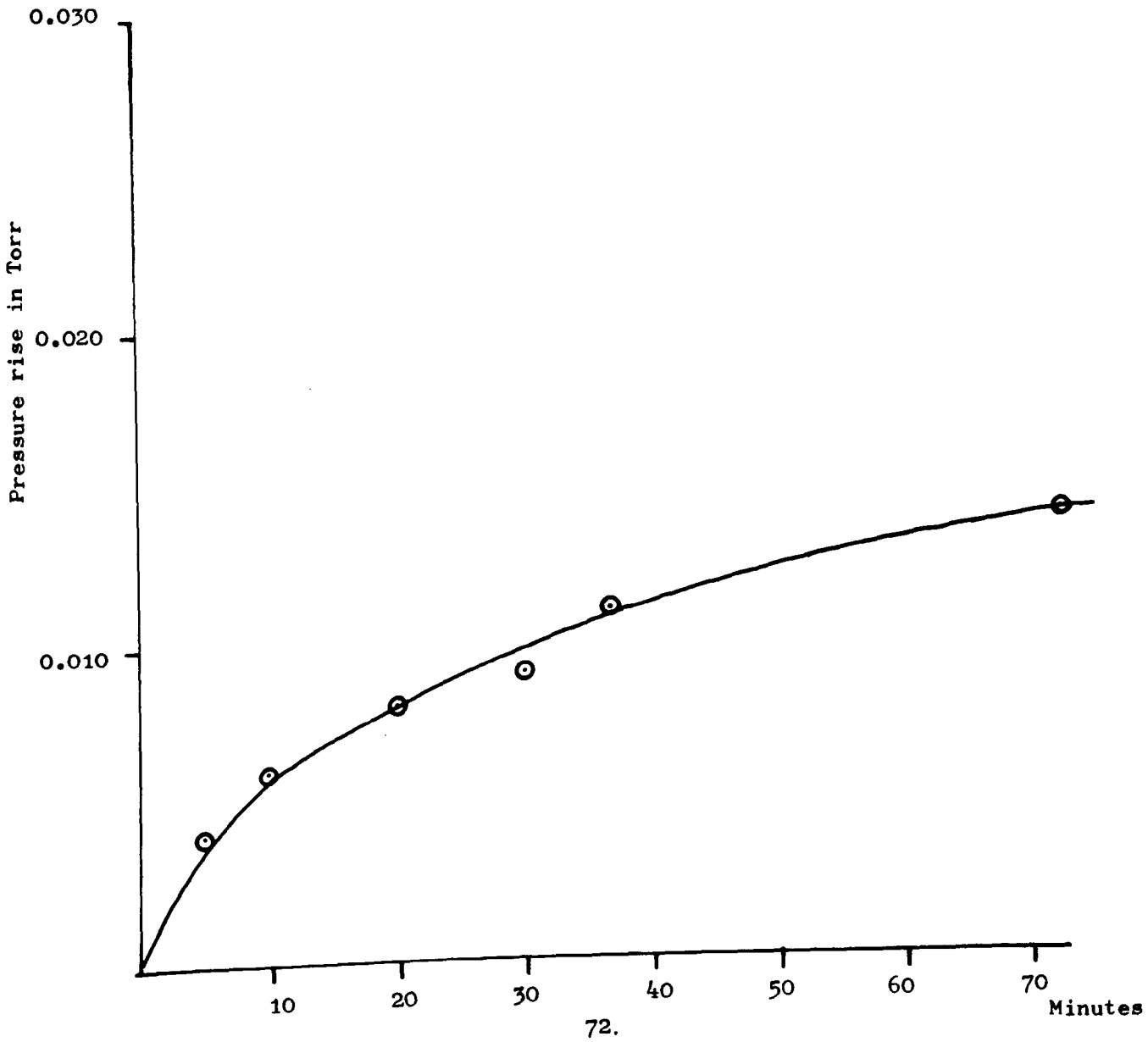

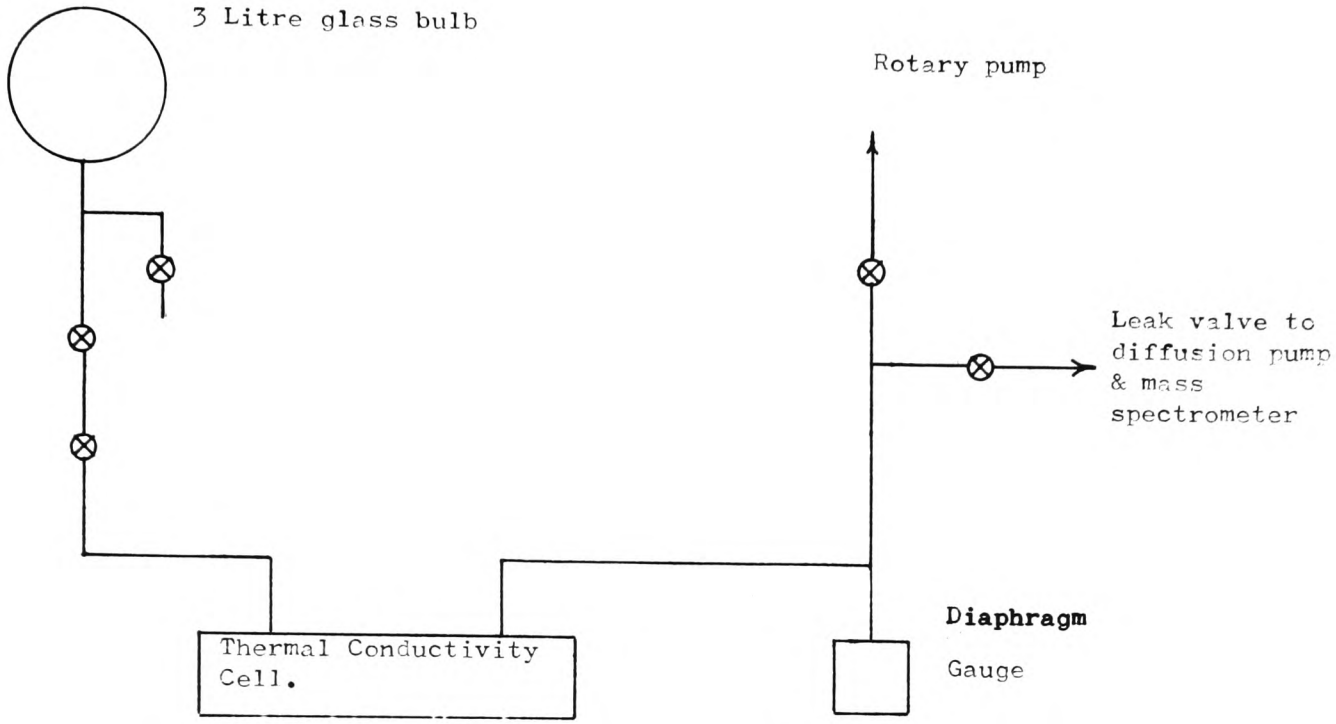

Figure 5.3.2

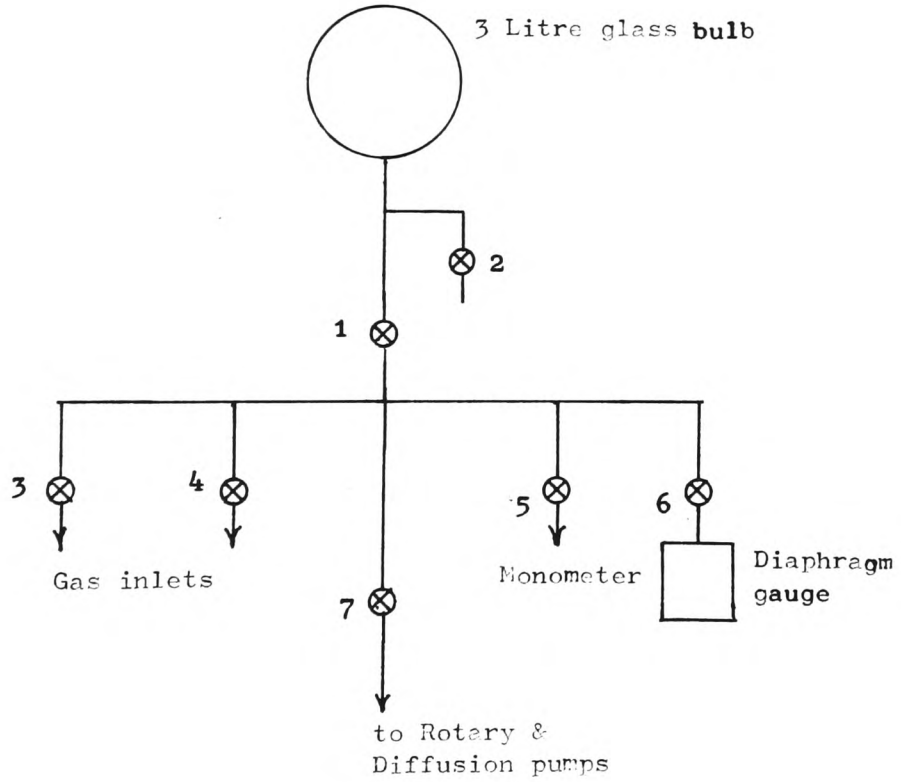

Figure 5.3.3

through the system once, before closing the pumps off from the manifold and flask, to ensure no contamination. It was estimated that the total error in making up binary mixtures of gases was less than 1%.

5.4 CALIBRATION OF THE THERMAL CONDUCTIVITY CELL

The geometric constant of the plate B=A/d (see equation 5.3.1) could be determined by actual measurements. However, due to the difficulty in setting the plate and sink exactly parallel, the value for B was only estimated this way.

The initial accurate determination of B was done using the accurately known thermal conductivity values of Nitrogen, Krypton, and Argon; Touloukian et al, (1970).

As the value for R, from equation 5.3.1. was unknown, a plot of the power divided by the difference in temperature between plate and sink versus the known values for the thermal conductivity of the gases was made. This gave a straight line graph the slope of which is equal to B, and the intercept on the $Q/\Delta T$ axis equal to R, the amount of energy lost by radiation and also heat conduction along the input leads etc. per degree of difference between plate and sink, see figure 5.4.1.

Plots of the temperature difference between the plate and the sink, for the calibration gases, versus time are shown in figure 5.4.2. The thermal conductivities were measured at a pressure of approximately 100 Torr in each case.

Figure 5.4.1 Calibration graph.

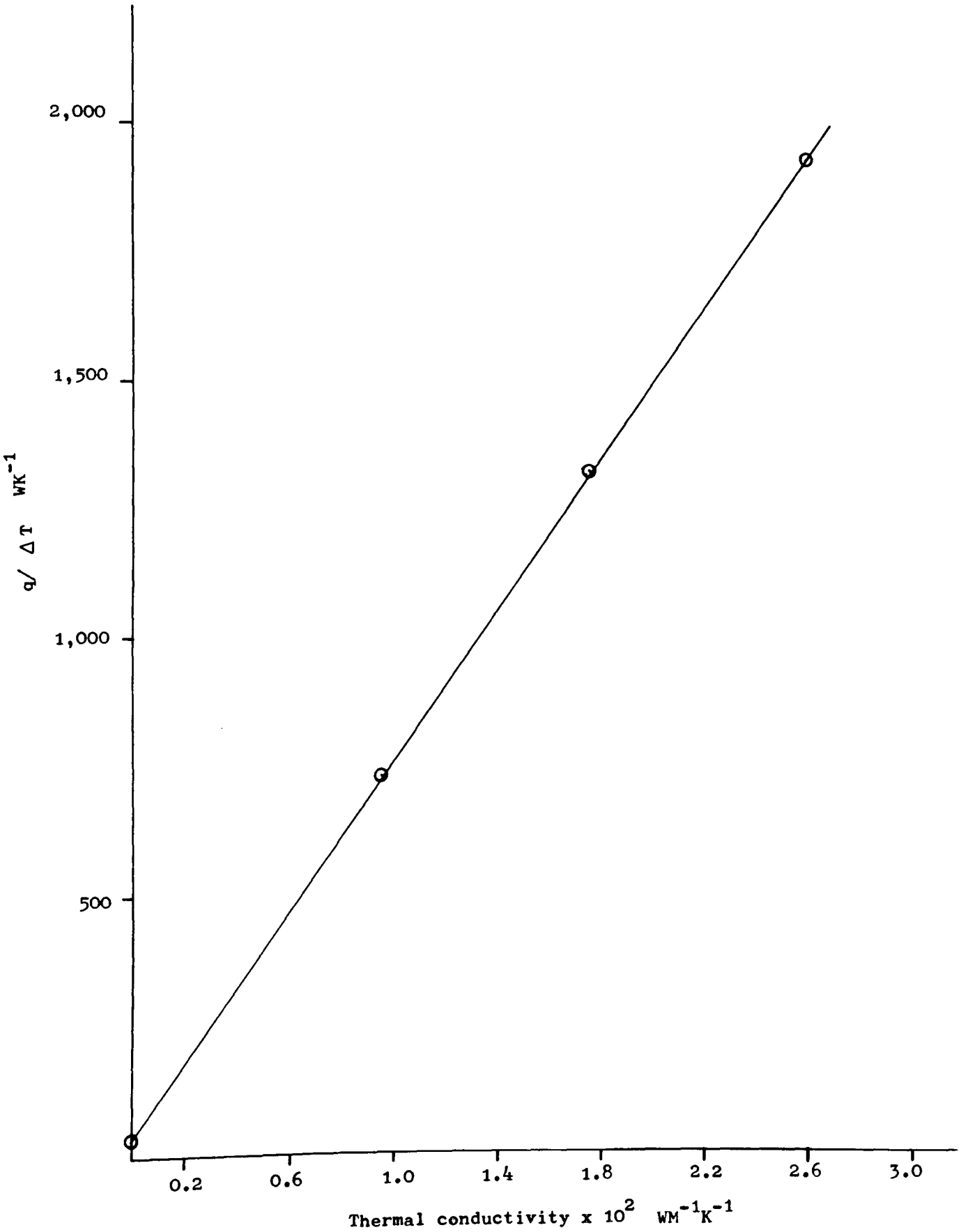

Figure 5.4.2 Plots of increase of ΔT with time.

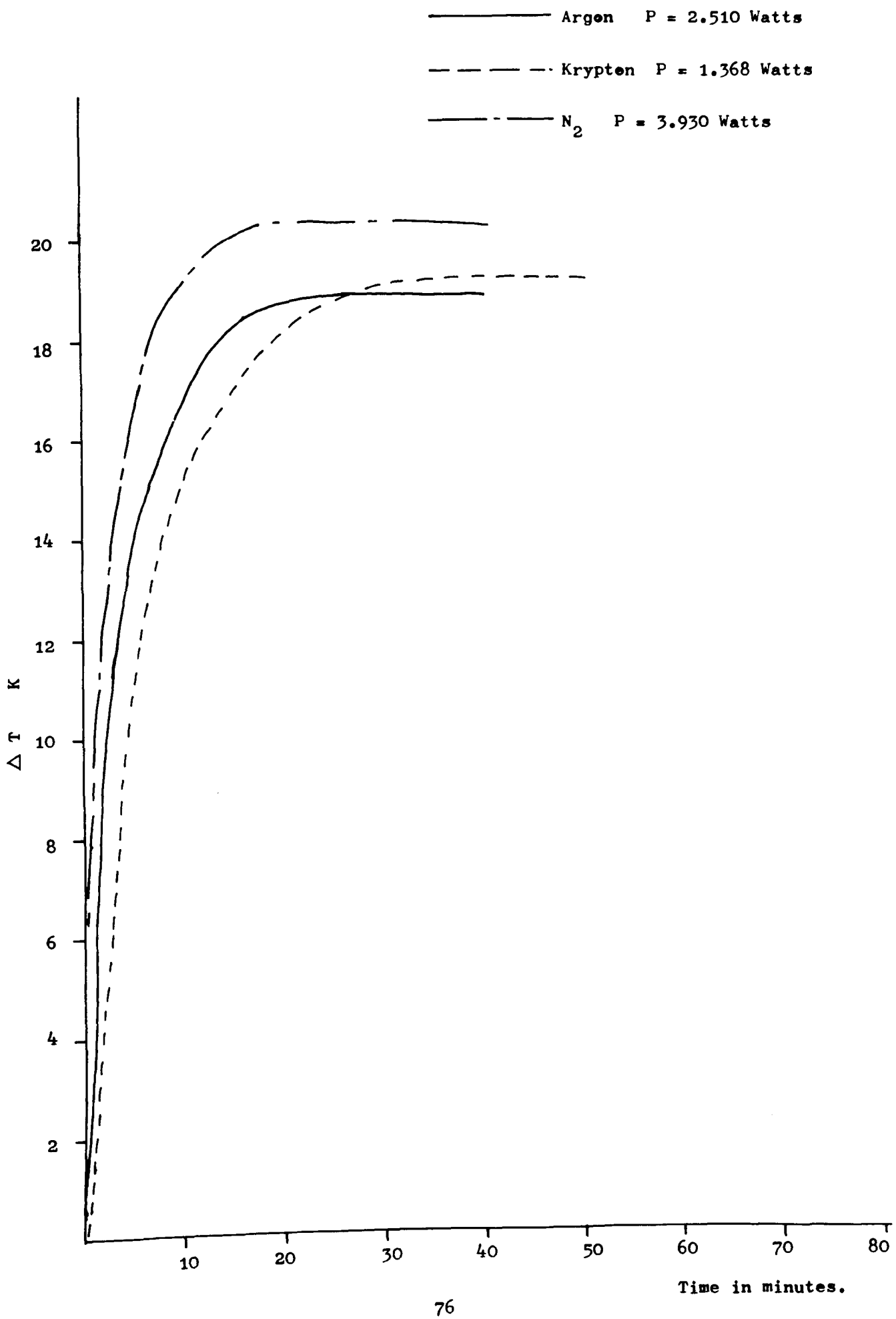

The mean temperature between the sink and the plate being 30C +/- 0.5C. From the results shown in figure 5.4.1 :-

$B = 7.16 +/- 0.04$ M

$R = 45 +/- 5 \times 10^{-4}$. W K^{-1}.

A blank run was undertaken to obtain an approximate check on the value of R. The blank run consisted of operating the cell while the cell was being evacuated. The pressure in the cell during this blank test was less than 10^{-3} Torr, hence plate-sink separation is << than the mean free path, and consequently heat transfer due to conduction is almost zero. Experiments showed that the rate of increase of ΔT was effectively linear for 3 hours, and that a minimum of 10 hours would be required before the system would be within 1% of the steady state condition. However, it was possible to give an upper limit for R from these results. Consider the results shown in figure 5.4.3

The heat loss due to radiation from the plate

$$E = A\sigma (T^4 - T_o^4)/(1/\mathcal{E}_1 + 1/\mathcal{E}_2 - 1)$$

Which may be approximated to

$$E = h_R \Delta T \quad \ldots\ldots 5.4.1$$

Where h_R is a given by:

$$h_R = A\ \sigma\ (T^2 + T_o^2\ )(T+T_o)/(1/\mathcal{E}_1 + 1/\mathcal{E}_2 - 1) \ldots 5.4.2$$

h_R may then be regarded as a constant since T_0 = a constant at T approximately equal to T_0.

The heat loss due to conduction may be given by:-

$$E = h_C\ (T - T_o) \ldots\ldots 5.4.3$$

Figure 5.4.3 Blank run of thermal conductivity cell.

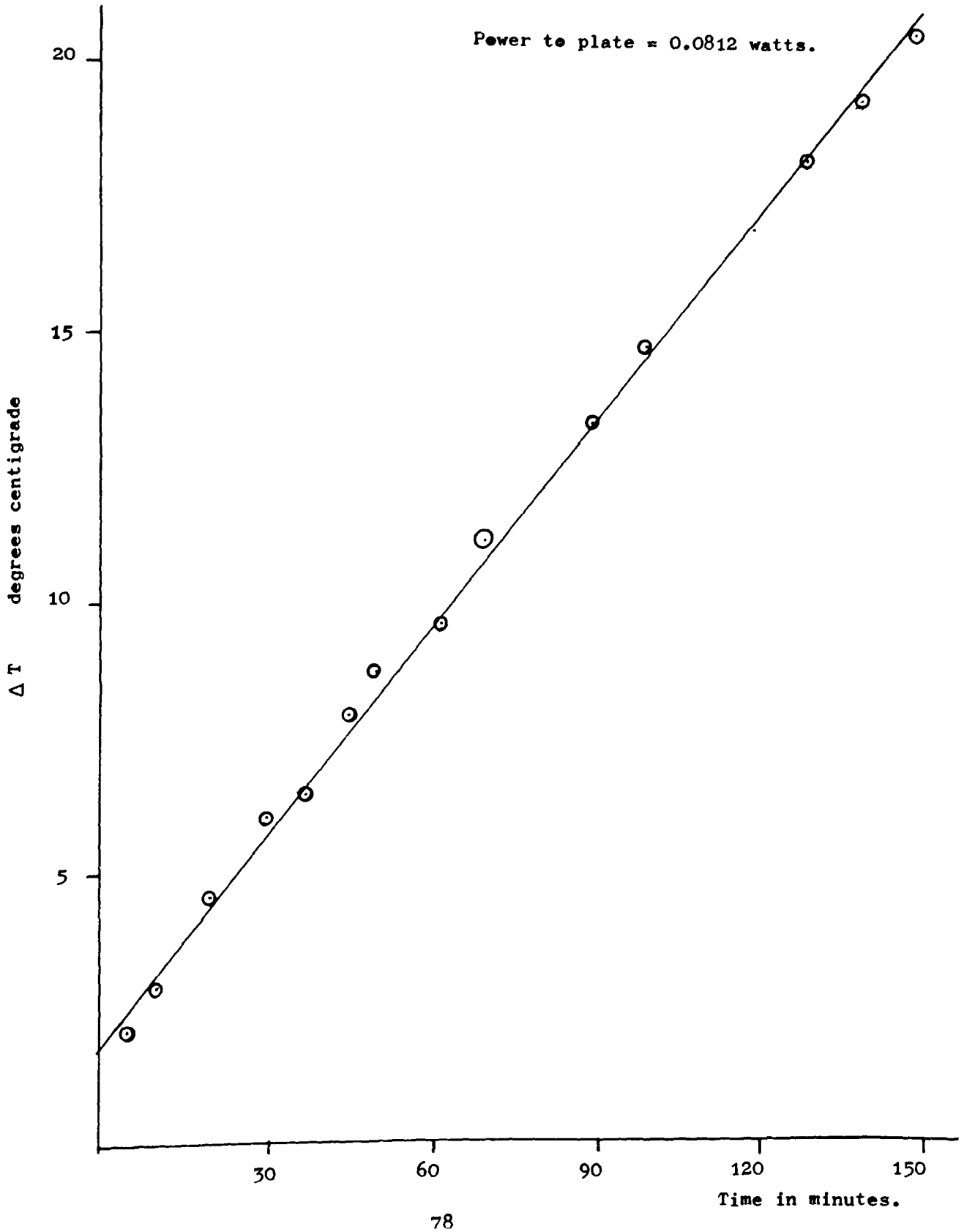

Where the room temperature is near to T (i.e. = 20C)

Therefore, the total spurious loss is:

$$E = R\,\Delta T \text{.....5.4.4}$$

Where $R = h_C + h_R$.

Under blank operation the energy balance equation for the plate may be given by:-

$$Q = \int q\,dt = \int \Delta T\,R\,dt + \Delta T\,C \text{.....5.4.5}$$

Where C, is the heat capacity of the plate, and Q is the total input energy to the plate in a time t.

Differentiating:-

$$dQ/dt = q = R\,(T-T_0) + dT/dt\,C \text{.....5.4.6}$$

Solving this differential equation and using the boundary condition when t = 0, T = T we get

$$\Delta T = q/R\,(1-\exp(-Rt/C)) \text{.....5.4.7}$$

$$dT/dt = q/C\ \exp(-Rt/C)$$

For small values of Rt/C

$$dT/dt = q/C\,(1-Rt/C) \text{.....5.4.8}$$

C may be obtained from the linear part of the graph, see fig. 5.4.3

As dT/dt = q/C

$$C = 40\ JKS^{-1}.$$

dT/dt is still linear after 140 minutes, which implies that from equation 5.4.8 that

R is less than 48×10^{-4}. $W K^{-1}$.

which agrees with the calibration graph, fig. 5.4.1

5.5 Pressure variation & temperature jump effects

When considering energy transfer in the homogeneous gas, it is usual to assume that the gas is dilute enough so that, only binary collisions between gas molecules occur, but, dense enough so that the gas to wall collisions are negligible compared to the gas to gas collisions. Simple kinetic theory predicts that (Kennard 1938)

$$K = 5/2\ \mu C_v \quad \ldots\ldots\ldots \quad 5.5.1$$

Where K is the thermal conductivity of the gas.

C_v is the molar heat capacity of the gas.

μ is the viscosity of the gas.

The viscosity being given by equation 5.5.2 below

$$\mu = (0.998/\pi\sigma^2)[mKT/\pi\ ]^{.5} \ldots\ldots\ldots 5.5.2$$

Where σ is the molecular diameter

k is the Boltzmann constant

m is the mass of the gas molecules in grammes

Combining 5.5.1 and 5.5.2 gives:-

$$K = 5/2 \times (0.998/\pi\sigma^2)[mkT/\pi\ ]^{.5} C_v \ldots\ldots 5.5.3$$

From equation 5.5.3 it is clear that K is independent of pressure as long as the gas is in such a state as to satisfy the initial assumptions. This theory has been proven experimentally many times by various workers, as explained in section 5.1. The gas heat transfer will become linearly dependent on pressure only when the mean free path is much greater than the effective distance, d between plate and tube.

In the region between $\lambda = 50 \times d$ and $\lambda = d/50$ an intermediate region exists explained, by the temperature jump effect. This discontinuity of temperature may be expressed by the mathematical formulae below, Kennard (1938):-

$$T_k - T_w = g\, dT/dn \ldots\ldots 5.5.4$$

Where T_w is the wall temperature

T_k is the temperature that would exist if the temperature gradient along the outward drawn normal to the wall, dT/dn, continued without change right up to the wall.

This effect will cause a slight pressure dependence on the observed thermal conductivity of a gas. For as the pressure decreases the temperature jump distance increases. The temperature jump effect may be explained qualitatively by understanding that a wall will cause a discontinuity in the gas. So that gas molecules which would have travelled on further than the position of the wall can only travel up to the wall. So the amount of heat conducted by such molecules per distance will be reduced. As the pressure is reduced the average mean free path of the gas molecules is increased, and therefore there will be more wall to gas collisions, and less gas molecule to gas molecule collisions. Therefore, more gas molecules will be held up short so to speak, and therefore, the observed thermal conductivity of the gas will

be reduced.

It should also be noted that gas molecules will not transfer energy between the wall and themselves at the same rate as between themselves. With decreasing pressure gas to wall collisions will become a larger percentage of total collisions, and therefore, any effect from the gas to wall collisions will become more important. This particular phenomena has been studied in detail by Knudsen 1911. Whereupon, he introduced a constant called the accommodation coefficient, noted by a, which can be defined as standing for the fractional extent to which those molecules that fall on the surface and are reflected or re-emitted from it have their mean energy adjusted to what it would have been if the returning molecules issuing as a stream out of a mass of gas at the temperature of the wall.

The pressure dependents of thermal conductivity of a gas was measured using the thermal conductivity cell, the distance between the plate and sink being approximately 0.5 mm. It can be shown, Kennard (1938), that the heat conducted through a gas of conductivity K, per unit area, between parallel plates, per degree distance in temperature between them is :-

$$q = K/(d+g_1+g_2) \quad \ldots\ldots\ldots 5.5.5$$

g_1 and g_2 being the temperature jump distance at the two plates, g_1/d and g_2/d being assumed to be much less than 1. The temperature jump distance is given by :-

$$g = (2 - a)\, 2K\lambda / a(\gamma + 1)\mu C_v \quad \ldots\ldots\ldots 5.5.6$$

Where $\gamma = C_p / C_v$.

Assuming an accommodation coefficient of 1, a plot of predicted

variation and of observed thermal conductivity from the thermal conductivity cell versus pressure may be plotted.

Fig. 5.5.1 and 5.5.2 show the predicted and the experimentally found plots of the thermal conductivity of Nitrogen, and Water with pressure respectively. From these results it is clear that the theory describes within experimental error the effect of temperature jump.

The thermal conductivity variation with pressure of a mixture of 50% Nitrogen and 50% Halocarbon 11 was also studied, see figure 5.5.3.

A simple empirical formula for correcting the observed thermal conductivity of a gas mixture was developed. Assume that the K for binary gas mixture may be given by:-

$$K(mix) = K(1)\,X(1) + K(2)\,X(2) \quad \text{.....5.5.7}$$

Where X(1) is the concentration of gas 1
and X(2) is the concentration of gas 2

If K(1P) is the measured thermal conductivity of gas 1 at pressure P, and similarly for K(2P), then the following correction may be used on the measured thermal conductivity of the gas mixture at pressure P.

$$K(mix) = K(measured)\,(K(1)\,X(1)/K(1P) + K(2)\,X(2)/K(2P)) \quad \text{.....5.5.8}$$

Where K(mix) is the thermal conductivity of the gas mixture, and K(measured) is the measured thermal conductivity of the gas mixture. A plot of the theoretically found thermal conductivity of 50% Halocarbon 11, and 50% Nitrogen is shown superimposed on figure 5.5.3. It is clear from this figure that the above equation is correct to within less than 0.25% of the total value of the thermal conductivity.

Figure 5.5.1 Pressure dependance of thermal conductivity of Nitrogen.

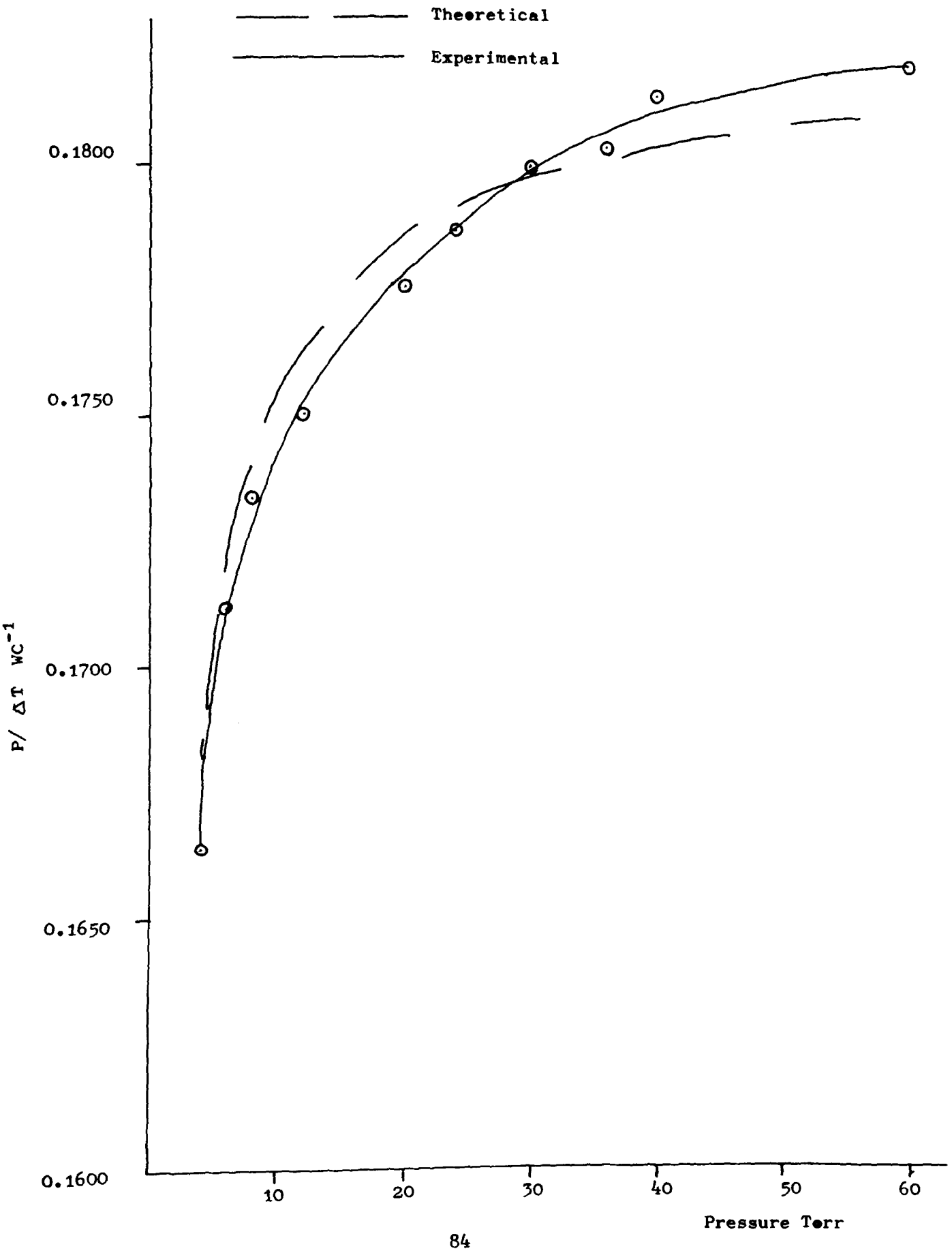

Figure 5.5.2 Variation of thermal conductivity of water vapour with pressure.

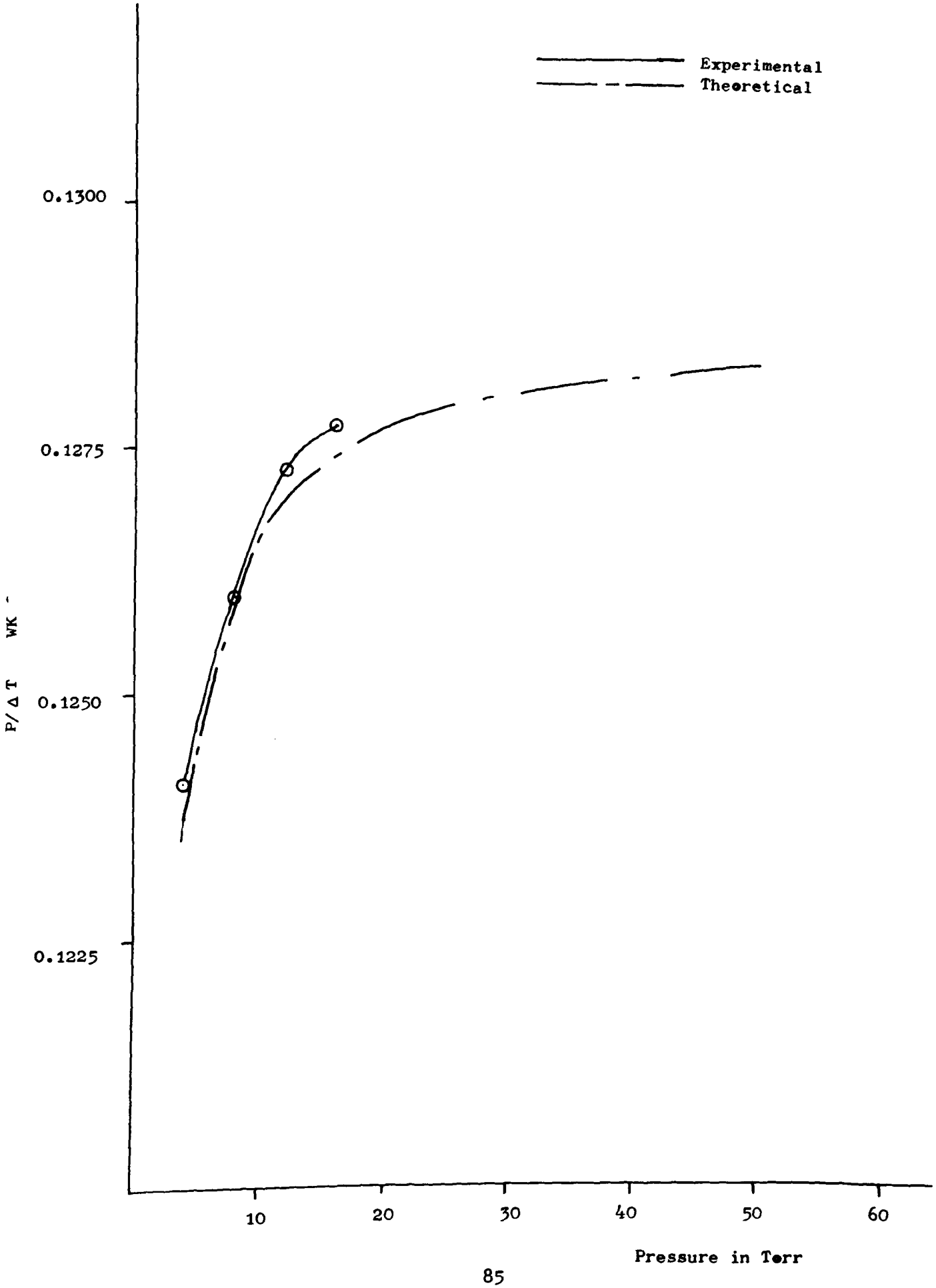

Figure 5.5.3 Pressure dependance of thermal conductivity of mixture of 50% Nitrogen and 50% Halocarbon 11.

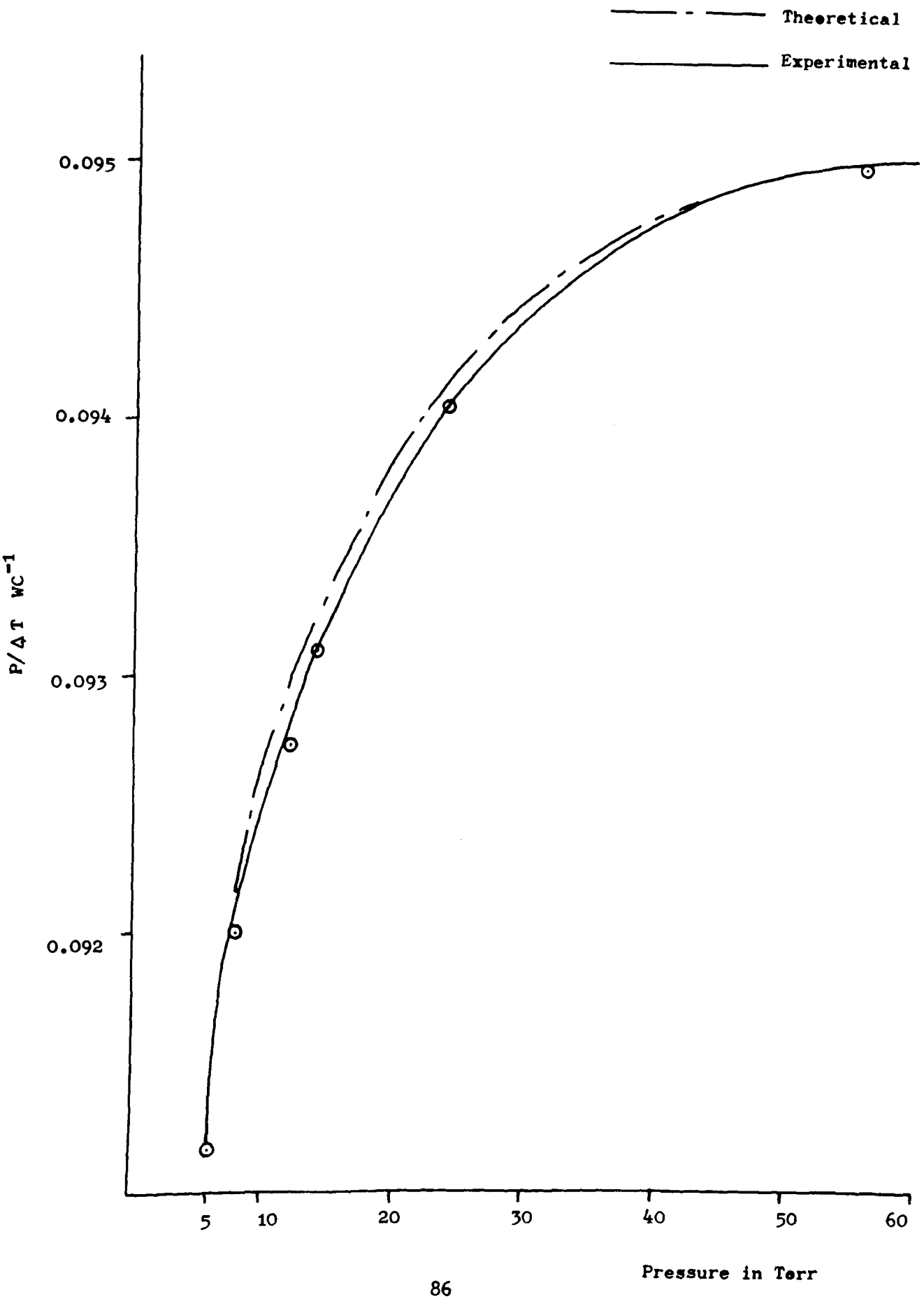

Because the total vapour pressure for water at 20C is only 18 Torr, it is not possible to carry out thermal conductivity measurements on water vapour mixtures at high enough pressures for the temperature jump effect to be negligible. Therefore, the appropriate corrections were made to the results of all experiments involving water vapour. On the basis of the results of this section, it is argued that the maximum error introduced due to the need for this correction is 0.25%.

The temperature jump effect will not be noticeable in the solar collectors because of the dimensions of the collectors. Considering the collectors to consist of parallel plates separated by 10 mm the pressure dependents on the thermal conductivity of a gas may be calculated using equation 5.5.5. This was done for Nitrogen, as Nitrogen shows the largest temperature jump distances for all the main spurious gases which will arise in the collectors. Fig. 5.5.4 shows the thermal conductivities versus pressure dependence. After one year of operation of the tubular collectors, it is predicted that the spurious gases which will rise to a pressure of approximately 0.5 Torr. If this gas was all nitrogen, the thermal conductivity would be approximately 3% lower than if the pressure was at 760 Torr. However, Nitrogen will be the worst main component of the spurious gases for temperature jump distances. Therefore, this effect will be even less than the thermal conductivity of the spurious gases themselves.

Thermal conductivity variation with pressure in collectors, of Nitrogen

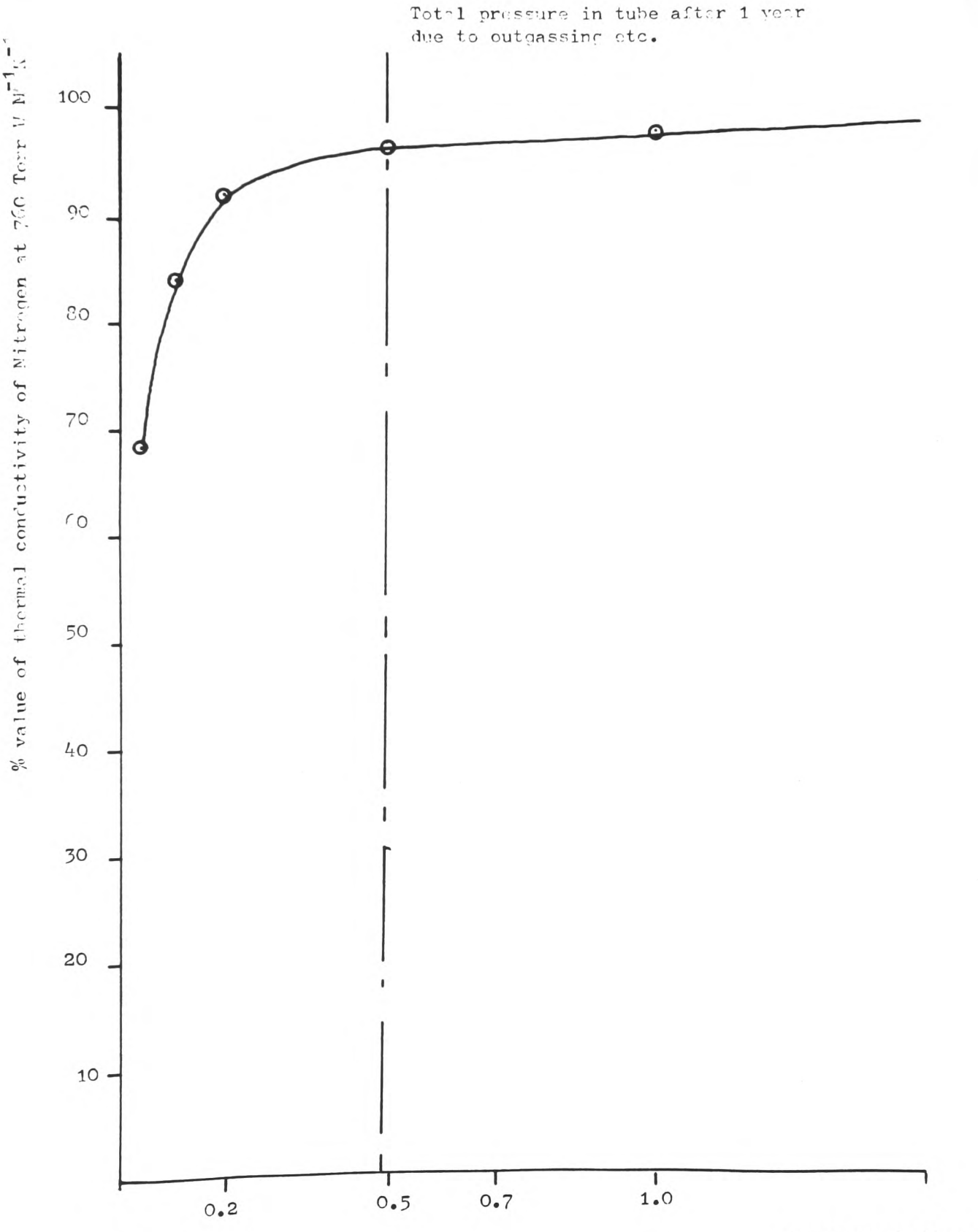

Figure 5.5.4

TABLE: 5.5.1

P = pressures in torr.

SAMPLE	λ, Mean free path x 10^{+3}.M.	g/λ assuming a=1
NITROGEN	5.06/P	1.59
OXYGEN	5.55/P	1.63
WATER	3.44/P	1.07
HALOCARBON 11	1.37/P	1.39
HALOCARBON 12	1.75/P	1.42
HALOCARBON 13	2.14/P	1.33
HALOCARBON 21	1.72/P	1.26
HALOCARBON 113	1.13/P	1.30
KRYPTON	4.18/P	1.86
SULPHUR-HEXAFLUORIDE	1.97/P	1.29

5.6 ERRORS

As mentioned in section 5.3 in the steady state condition, the energy balance equation for the plate is :-

$$q = K B\Delta T + R\Delta T \ldots\ldots 5.3.1$$

Which implies

$$K = [q - R\Delta T]/B\Delta T \ldots\ldots 5.6.1$$

The errors in B and R maybe obtained from the cells calibration graph (see section 5.3)

$$B = 7.16 +/- 0.04 \quad M$$

$$R = [46 +/- 5] \times 10^{-4}. W K^{-1}$$

The temperature of the plate could be read to within +/-0.05C. and similarly for the sink, which gives a statistical error T of +/-0.07C. The error in measuring q, the energy supplied to the sink comes in measuring V and I, these combine to give a +/-0.5% error in q. The amount of energy dispersed in the input leads to the plates heater is less than 0.04%. These errors may be combined to give the uncertainty in K. From equation 5.6.1:-

$$K = (q/[B\Delta T]) - R/B \ldots\ldots 5.6.2$$

Let $y = (q/B)\Delta T$ AND $x = R/B$

Then $K = y-x$

and $dK = ((dy)^2 + (dx)^2)^{0.5}$ 5.6.3

Considering the error in y

$$y = (q/B)\Delta T$$

Taking natural logs and differentiating

$$dy/y = (dq/q) +/- (dB/B) +/- (d\Delta T/\Delta T)....5.6.4$$

Combining the uncertainties

$$dy/y = ((dq/q)^2 + (dB/B)^2 + (d\Delta T/\Delta T)^2)^{0.5}..5.6.5$$

Substituting in the errors gives

$$dy/y = 8.27 \times 10^{-3}.....5.6.6$$

Similarly for x

$$dx/x = ((dR/R)^2 + (dB/B)^2)^{0.5}.$$

$$dx/x = 1.09.....5.6.7$$

Combining 5.6.6 and 5.6.7 using equation 5.6.3 gives

$$dK=[\ (8.27 \times 10^{-3} \times K\ )^2 + (7.00 \times 10^{-5})^2\ ]^{0.5}.....5.6.8$$

It is clear from equation 5.6.8 that the percentage error for K will increase for decreasing values of K.

For Nitrogen $K = 2.62 \times 10^{-2}\ WM^{-1}K^{-1}$.

The percentage error in K = +/-0.87%

For Halocarbon 11, $K = 8.07 \times 10^{-3}\ WM^{-1}K^{-1}$.

The percentage error in K =+/-1.2%

As mentioned in section 5.5, errors in the measurement of the thermal conductivity of gas mixtures with water vapour as one of the constituent will arise due to the temperature jump effects. However, after correction the percentage error due to this effect will only be 0.25%.

As mentioned in section 5.3 the thermal conductivities were not always measured exactly at 30C. Due to correcting for this an error of 0.1% will arise. Due also to the fact that the thermal conductivity does not increase exactly linearly with temperature an estimated error of 0.5% will arise.

Adding all the uncertainties together it can be seen that after corrections the thermal conductivity measurements were maded to within 2%.

5.7 Results of thermal conductivity measurements

Table 5.7.1 show the results of the thermal conductivity of the pure gases/vapours measured at 30 degrees C. after corrections were made for the 1. Temperature jump effect

2. Bringing the mean temperature to 30 degrees (as discussed in 5.6)

As discussed in 5.6 an upper limit on the errors of these measurements is set at 2%. Along with these results are printed values from Touloukian et al (1970) and Peters Breunese, & Hermans (1982). with estimated errors for this data.

TABLE 5.7.1. Results of thermal conductivity measurements of pure gases x 10^3 in $WM^{-1}K^{-1}$ at 30C.

Sample	Exp. Results	Standard dev.	Values from Touloukian,1970
HALOCARBON 11	8.07	0.12	8.03
HALOCARBON 12	9.94	0.10	10.00
HALOCARBON 13			12.37
HALOCARBON 21	8.54	0.01	8.74
HALOCARBON 113	8.92	0.12	7.78
SULPHUR-HEXAFLOURIDE	12.8	0.30	
KRYPTON	9.50	0.15	9.51
NITROGN	26.2	0.17	26.23
WATER VAPOUR	18.4	0.21	18.33
METHYL IODIDE	5.30	0.20	
OXYGEN			27.00
ARGON	17.9	0.19	17.90

The results of Nitrogen, Argon, and Krypton are somewhat fictitious, in that these gases were used in the calibration of the cell. However, they do show the repeatability of the thermal conductivity cell. Of these results only Halocarbon 13, and Halocarbon 113 show distinct variation from other workers results. For the purpose of the solar collectors Halocarbon 11 looked the most promising.

The results of the gas mixtures are tabulated in tables 5.7.2 to 5.7.4 These results have been adjusted for corrections 1 and 2. Results of halocarbon 11/water vapour, halocarbon 11/nitrogen, and water vapour/nitrogen are displayed graphically in figures 5.7.1, 5.7.2, and 5.7.3 respectively. Of special interest in these results are those of Nitrogen with water vapour. A mixture of 20% water and 80% Nitrogen showing a higher thermal conductivity than Nitrogen on its own. These results compare favourable with the work of Dijkema, Stouthart, & de Vries, who observed similar effects.

Results for halocarbon mixtures are not readily available in the literature for comparison with this work. However of interest Peters, Breunese, and Hermans (1982) produced some results of halocarbon-11/nitrogen and halocarbon-12/nitrogen. After adjusting their results to 30C for comparison it was found that the results fitted to within 2%; the accuracy of our experiments.

TABLE 5.7.2. Results of thermal conductivity measurements of binary gas mixtures at 30C in $W M^{-1}K^{-1}$.

Halocarbon 11 / Water Vapour

Conc of water vapour	0	20	40	60	80	100
Thermal conductivity x 10^3	8.07	9.24	11.3	13.4	15.8	18.4

Halocarbon 12 / Water Vapour

Conc of water vapour	0	20	40	60	80	100
Thermal conductivity x 10^3	9.94	11.3	13.2	14.6	16.6	18.4

Halocarbon 21 / Water Vapour

Conc of water vapour	0	20	40	60	80	100
Thermal conductivity x 10^3	8.54	9.97	11.6	13.4	15.4	18.4

Halocarbon 113 / Water Vapour

Conc of water vapour	0	20	40	60	80	100
Thermal conductivity x 10^3	8.92	9.78	11.6	13.8	16.3	18.4

Methyl Iodide / Water Vapour

Conc of water vapour	0	20	40	60	80	100
Thermal conductivity x 10^3	5.35	6.65	8.66	11.0	14.0	18.4

TABLE 5.7.3. Results of thermal conductivity measurements of binary gas mixtures at 30C in $W M^{-1}K^{-1}$.

Krypton / Water Vapour

Conc of water vapour	0	20	40	60	80	100
Thermal conductivity x 10^3	9.50	11.8	14.0	15.5	17.5	18.4

Sulphur Hexafloride / Water Vapour

Conc of water vapour	0	20	40	60	80	100
Thermal conductivity x 10^3	8.07	9.24	11.3	13.4	15.8	18.4

Nitrogen / Water Vapour

Conc of water vapour	0	20	40	60	80	100
Thermal conductivity x 10^3	26.2	26.8	26.1	24.1	21.5	18.4

TABLE 5.7.4. Results of thermal conductivity measurements of binary gas mixtures at 30C in $W M^{-1}K^{-1}$.

Halocarbon 11 / Nitrogen

Conc of Nitrogen	0	20	40	60	80	100
Thermal conductivity x 10^3	8.07	9.70	11.8	14.8	19.4	26.2

Halocarbon 13 / Nitrogen

Conc of water vapour	0	20	40	60	80	100
Thermal conductivity x 10^3	8.92	9.80	11.9	15.0	19.4	26.2

Methyl Iodide / Nitrogen

Conc of water vapour	0	20	40	60	80	100
Thermal conductivity x 10^3	5.35	8.02	11.6	15.3	20.5	26.2

Sulphur Hexafluoride / Nitrogen

Conc of water vapour	0	20	40	60	80	100
Thermal conductivity x 10^3	12.8	14.5	16.8	19.0	21.8	26.2

Figure 5.7.1 Thermal conductivity for mixtures of water vapour with with Halocarbon 11, at 30C.

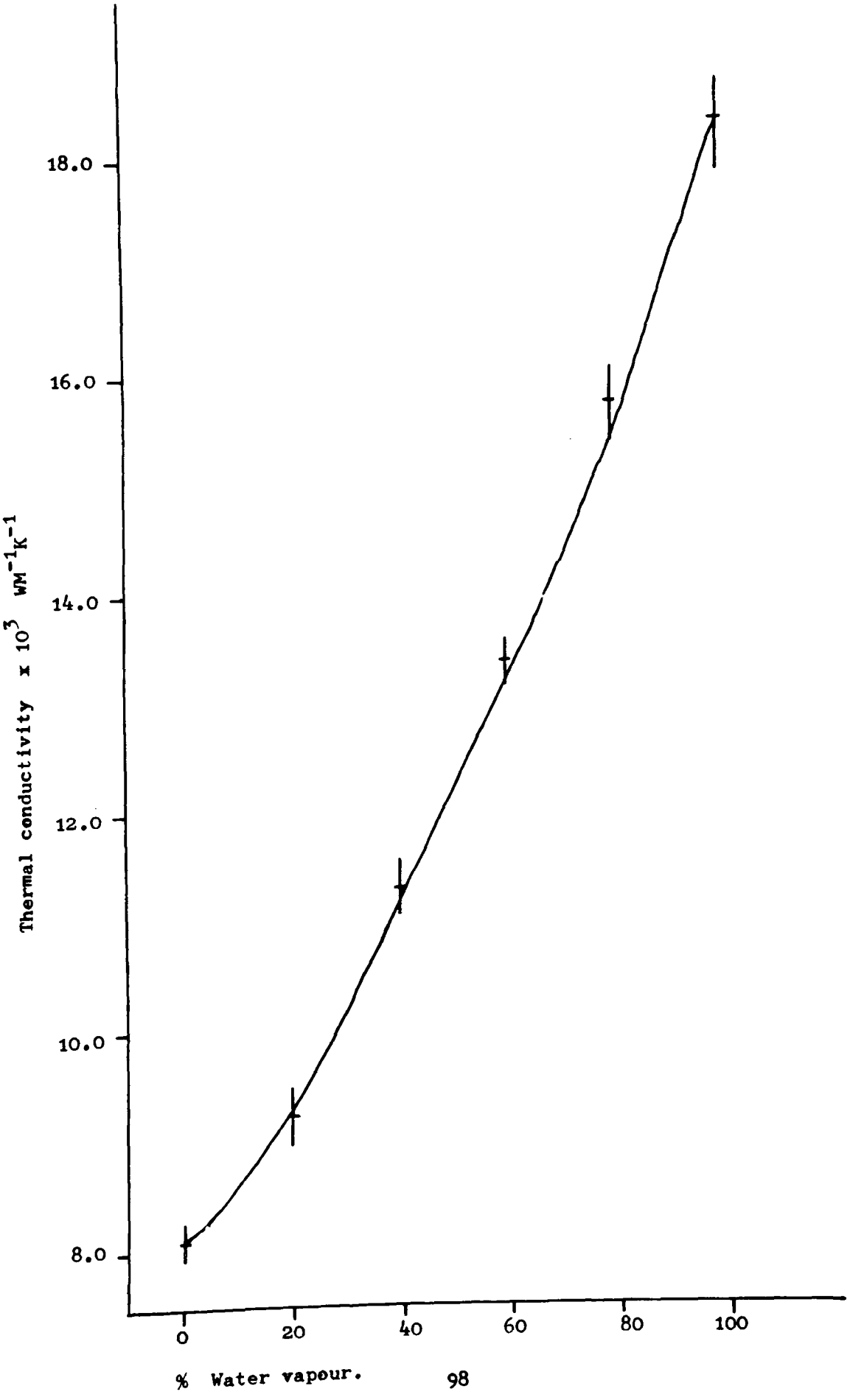

Figure 5.7.2 Thermal conductivity results for mixtures of Nitrogen with Halocarbon 11, at 30C.

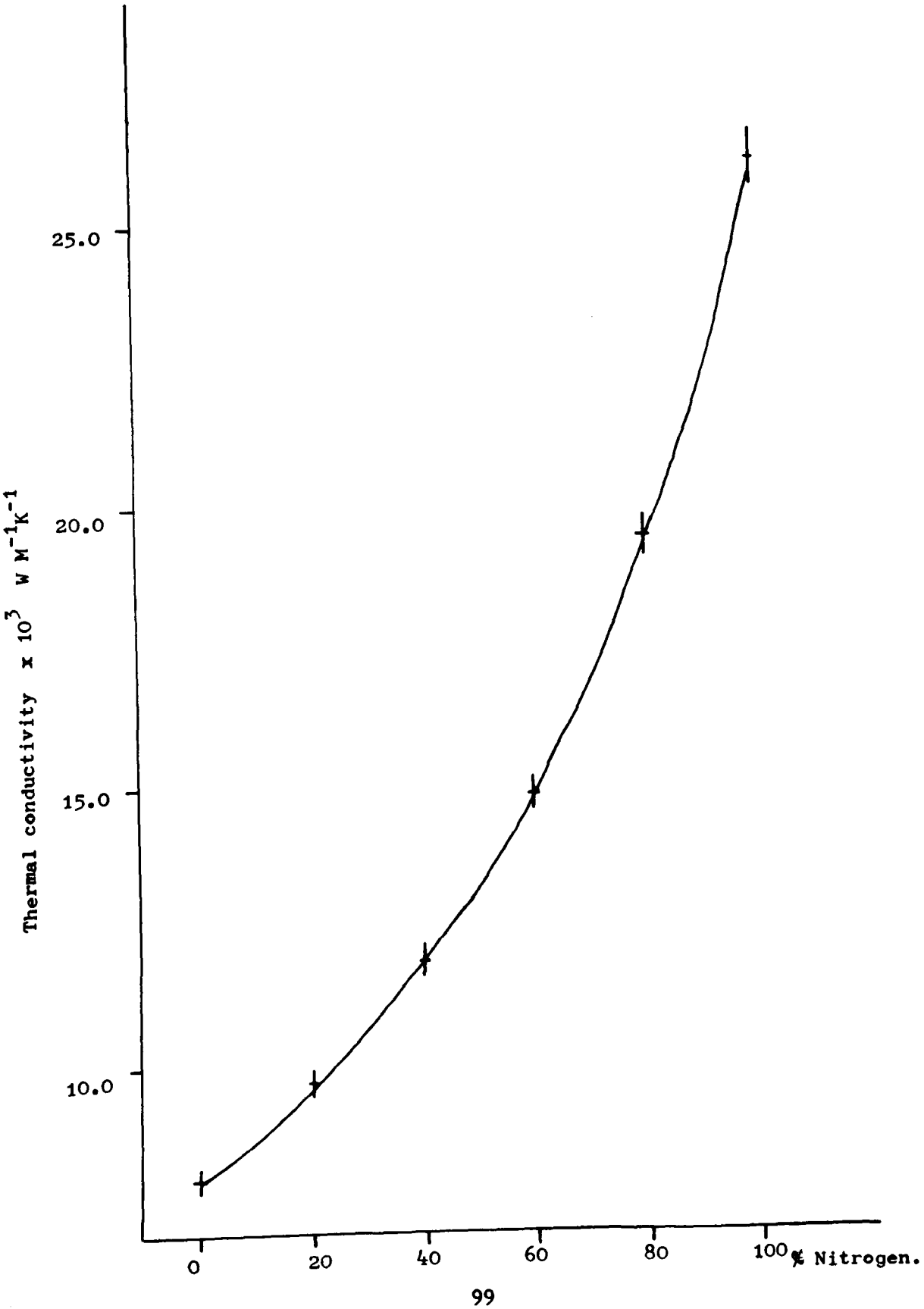

Figure 5.7.3 Thermal conductivity results for mixtures of Nitrogen with water vapour, at 30C.

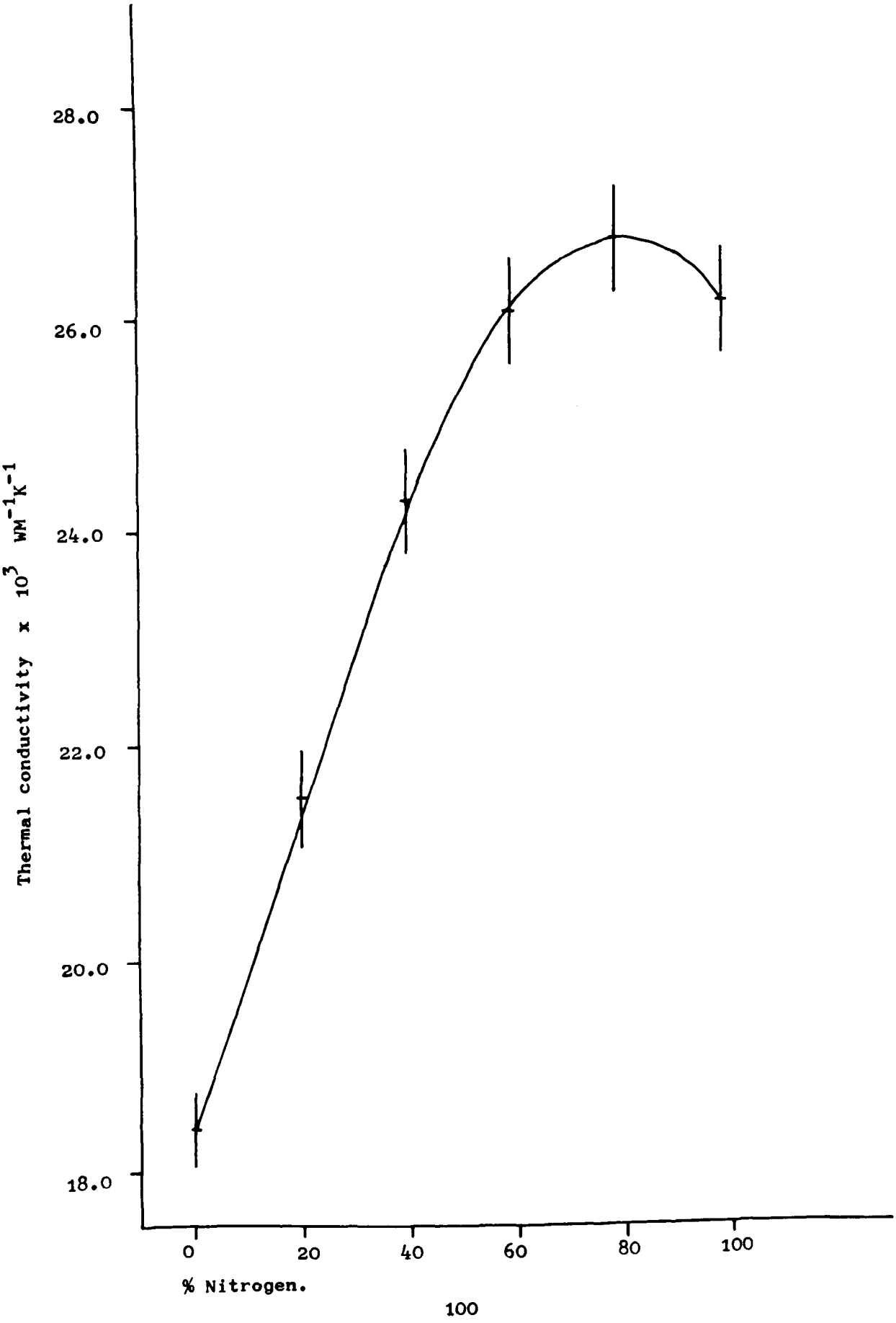

6 THEORETICAL WORK ON THERMAL CONDUCTIVITY OF GASES

6.1 Introduction

Modern theories of transport properties of gases were developed from the hard sphere theory. The basis of modern theories, which deal with the shortcomings of the hard sphere theory, were laid down by Maxwell in 1866, when he considered the distribution function for a gas. However, it was not until 1917 that two theoreticians, Chapman and Enskog, came up with the practical solutions of being able to relate the transport properties of gases to the forces acting between the molecules of the gases. This led to much improved theoretical values for the transport properties of gases.

There was also a basic refinement needed in the theory of heat conduction through polyatomic gases. It had been assumed that the efficiency of transfer of translational thermal energy is the same as that of transfer of internal energy of the molecules. Eucken, in 1913, reasoned that one should consider the two terms separately. He proposed a semi-empirical equation of the form:-

$$K = (E_{trans}\ \mu\ C_{vtrans})/M + (E_{int}\ C_{vint})/M \ldots 6.1.1$$

Where C_{vtrans} and C_{vint} are the contributions of translational energy and internal energy to the molar heat capacity. E_{trans} and E_{int} are the appropriate numerical factors, and u is the viscosity of the gas.

Exact theory gives $E_{trans} = 5/2$. A value of $E_{int} = 1$ was suggested by Eucken. This is believed to be wrong as the efficiency with which vibrational energy is transferred in collisions is poor and in any case, varies between different gases.

Euckens' Theory led to improvements between theory and experiment for diatomic molecules but not so much for polyatomic gas molecules; for reasons discussed earlier.

From modern theory, workers have produced various formulae for calculating the coefficient of thermal conductivity for mixtures of gases. In the case of monatomic gas mixtures, the formulae have achieved a certain amount of success. However, in the case of polyatomic gas mixtures, a rigorous equation is hard to produce which correctly takes into account the transfer of internal energy between molecules. A common semi-empirical method of overcoming this Hirschfelder (1954) is:-

> To calculate the thermal conductivity of the gas mixture, assuming the gases to be monatomic; this result is denoted by K_{mon}.
>
> To compute a correction term for each component Ei where
>
> $$E_i = (K_i)_{exp}/(K_i)_{mon} \text{.....6.1.2}$$

An empirical expression for the coefficient of the thermal conductivity for the mixture is then;

$$K_{mix} = \sum K_{mon}(X_i\ E_i) \text{.....6.1.3}$$

Where x_i is the molar concentration of gas species i.

A more general equation suggested by Lindsay and Bromley (1950) for the thermal conductivity coefficient of a mixture of gases based on an equation by Wassiljewa (1904), is of the form:-

$$K_{mix} = \sum_{i=1}^{n} \frac{K_i}{\frac{1}{X_i} \sum_{j=1}^{n} A_{ij} X_j} \qquad \text{.....6.1.4}$$

$$\text{Where } A_{ij} = \frac{1}{4}\left[1 + \left[\frac{\mu_i}{\mu_j}\left(\frac{M_j}{M_i}\right)^{\frac{3}{4}} \frac{(1 + S_{i/T})}{(1 + S_{j/T})}\right]^{\frac{1}{2}}\right]^2 \frac{(1 + S_{ij/T})}{(1 + S_{i/T})} \qquad \text{...6.1.5}$$

Where μ_i is the viscosity coefficient, M_i the mass, and S_i the sutherland constant approximated by $S_i = 1.5\ T_{bi}$, where T_{bi} is the normal boiling point of the i component, while S_{ij} is the geometric mean of S_i and S_j. Thus $S_{ij} = (S_1 S_2)^{.5}$.

If one of the constituents is strongly polar then $S_{ij} = 0.733(S_1 x S_2)^{.5}$.

Mason and Saxena (1958) approximated A_{ij} to 6.1.6 below:

$$A_{ij} = \frac{1}{2\sqrt{2}}\left(1 + \frac{M_i}{M_j}\right)^{-\frac{1}{2}} \left[1 + \left(\frac{K_i^{mon}}{K_j^{mon}}\right)^{\frac{1}{2}} \left(\frac{M_i}{M_j}\right)^{\frac{1}{4}}\right]^2 \qquad \text{....6.1.6}$$

Where $K_{mon} = 2.5\ C_v$ and $C_v = 1.5\ R/M$ (R is the gas constant.

Equations 6.1.5 and 6.1.6 were computed for relevant gas mixtures, using data as shown in table 6.1.1 these computations being shown in table 6.1.2.

6.2 Comparison of theoretical and experimental results.

To compare the experimental results with the Lindsay and Bromley equation, and the Mason and Saxena equation

data as shown in table 6.1.2, was used to compute equation 6.1.4. These theoretical results were then compared with our experimental results as given in tables 5.7.2-5.7.4. The comparisons are shown in tables 6.2.1-6.2.3.

It can be seen from these comparisons that in the majority of cases the Mason and Saxena expression provides values that differ by less than than 5 percent from the experimental results. The Lindsay and Bromley equation, on the other hand, does not even fit the results to 10 percent in many cases. However in the case of Nitrogen versus Water the Lindsay and Bromley equation fits the results to 5 percent whilst the Mason and Saxena equation only fits to within 10 percent.

This is similar for the experimental results of Dijkema et al for nitrogen/water vapour, see table 6.2.4. Also from the experimental data of Dijkema et al it can be seen that the Lindsay and Bromley equation fits the best for oxygen and water; see table 6.2.4. Therefore, for calculations, it is proposed to use the Mason and Saxena equation for the A_{ij} terms for the Halocarbon mixtures and the Lindsay and Bromley A_{ij} terms for the nitrogen/water and oxygen/water terms, to

TABLE 6.1.1

Gas	Temperature Centigrade	Viscosity $\times 10^{5}$ N.S.M^{-2}	Boiling Pt. in Klevin	Mass AMU
Hal. 11	30	1.07	296.97	137.35
Hal. 12	30	1.288	243.36	120.9
Hal. 13	30	1.460	191.75	104.45
Hal. 21	30	1.164	282.07	102.9
Hal. 113	30	1.038	320.72	187.35
Sulphur Hex.	30	1.588	-	146
Krypton	30	2.56	119.80	83.80
Water	30	0.977	373.15	18
Nitrogen	30	1.793	77.35	28
Oxygen	30	2.067	90.33	32

TABLE 6.1.2

A(i,j)	Lindsay & Bromley	Lindsay & Bromley one species pol.	Mason & Saxena
$A(H_2O,Hll)$	2.378	1.983	2.227
$A(Hll,H_2O)$	0.5673	0.473	.3197
$A(H_2O,N_2)$	.8192	.7193	.9189
$A(N_2,H_2O)$	1.077	.9461	1.082
$A(H_2O,O_2)$	.8019	.7000	.9041
$A(O_2,H_2O)$	1.119	.9768	1.093
$A(N_2,Hll)$	2.405	2.123	2.757
$A(Hll,N_2)$	.4361	.3863	.3360
$A(N_2,O_2)$	.9709	.8951	.9868
$A(O_2,N_2)$	1.030	.9496	1.013
$A(O_2,Hll)$	2.543	2.239	2.897
$A(Hll,O_2)$	.4347	.3827	.3440

TABLE 6.2.1

THERMAL CONDUCTIVITY OF WATER MIXTURES x 10^3 in $WM^{-1}K^{-1}$ at 30C.

% Conc. of gas vs water	Exp. Results	Lindsay & Bromley	Lindsay & Bromley one species pol.	Mason & Saxena
Conc. Nitrogn	Greatest % diff. v Exp.	-10%	-4.5%	-12%
20	21.5	20.2	21.1	19.9
40	24.3	21.9	23.3	21.4
60	26.1	23.5	23.9	23.0
80	26.8	24.9	25.9	24.6
Conc. Krypton	Greatest % diff. v Exp.	-8%	-1.7%	-5%
20	17.46	16.5	17.2	16.9
40	15.5	14.7	15.7	15.1
60	14.0	12.9	13.8	13.3
80	11.8	11.2	11.8	11.4
Conc.Sulphur Hexafluoride	Greatest % diff. v Exp.	-17%	-11%	-6.6%
20	19.2	16.0	17.1	17.9
40	17.6	14.5	15.8	16.7
60	16.0	13.7	14.7	15.3
80	14.7	13.2	13.7	14.0
Conc. H11.	Greatest % diff. v Exp.	-14%	-5.7%	-4%
20	15.8	14.0	15.1	15.4
40	13.4	11.5	12.6	12.9
60	11.3	9.9	10.8	10.9
80	9.24	8.82	9.28	9.33
Conc. H12	Greatest % diff. v Exp.	-12%	-4%	-3%
20	16.6	15.1	16.2	16.5
40	14.6	13.0	14.2	14.5
60	13.2	11.6	12.6	12.7
80	11.3	10.6	11.2	11.2

TABLE 6.2.2

THERMAL CONDUCTIVITY OF WATER MIXTURES $x10^3$ in $WM^{-1}K^{-1}$ at 30C.

% Conc. of gas vs water	Exp. Results	Lindsay & Bromley	Lindsay & Bromley one species pol.	Mason & Saxena
Conc. Nitrogn	Greatest % dif. v Exp.	-10%	-4.5%	-12%
20	21.5	20.2	21.1	19.9
40	24.3	21.9	23.3	21.4
60	26.1	23.5	24.9	23.0
80	26.8	24.9	25.9	24.6
Conc. H21	Greatest % diff. v Exp.	-8%	+3%	+2%
20	15.4	14.8	15.8	15.8
40	13.44	12.4	13.6	13.5
60	11.6	10.7	11.7	11.5
80	9.97	9.4	10.0	9.90
Conc. H113	Greatest % diff. v Exp.	-18%	-9.2%	-4%
20	16.3	13.7	14.9	15.6
40	13.8	11.4	12.6	13.3
60	11.6	10.1	11.0	11.4
80	9.78	9.39	9.82	10.0

TABLE 6.2.3

THERMAL CONDUCTIVITY OF NITROGEN MIXTURES $\times 10^3$ in $WM^{-1}K^{-1}$ at 30C.

% conc. of gas vs N_2.	Exp Results	Lindsay & Bromley	Lindsay & Bromly one species pol.	Mason & saxena
Conc. Hll	Greatest % diff. v Exp.	+1%	+7.6%	-2.3%
20	19.4	19.3	20.3	19.0
40	14.8	14.9	15.9	14.6
60	11.8	11.9	12.7	11.7
80	9.70	9.74	10.1	9.62
Conc. Hl13	Greatest % diff. v Exp.	+1%	+7.6%	-2.3%
20	19.4	18.9	19.9	18.8
40	15.0	14.7	15.7	14.7
60	11.9	12.1	12.8	12.1
80	9.80	10.3	10.6	10.2
Conc Sulphur Hexafluoride	Greatest % diff. v Exp	-4.9%	-3.0%	-2.6%
20	21.8	21.5	22.5	22.0
40	19.0	18.3	19.4	18.8
60	16.8	16.0	16.8	16.4
80	14.5	14.2	14.6	14.4

TABLE 6.2.4

THERMAL CONDUCTIVITY x 10^3 in $WM^{-1}K^{-1}$
RESULTS FROM DIJKEMA ET AL.

	WATER	VS	NITROGEN	
% Conc. of water	Exp. Results Bromley	Lindsay & Bromley one	Lindsay & Saxena species pol.	Mason &
	Greatest % diff v Exp.	-6.7%	-3%	-7.9%
20	26.7	24.9	25.9	24.6
40	25.9	23.5	24.9	23.0
60	23.9	21.9	23.3	21.4
80	21.3	20.2	21.1	19.9
	WATER	VS	OXYGEN	
% Conc. of water	Exp. Results	Lindsay & Bromley	Lindsay & Bromley one species pol.	Mason & Saxena
	Greatest % diff v Exp.	-6%	-2%	-7%
20	27.1	25.5	26.5	25.2
40	26.3	23.8	25.3	23.4
60	24.2	22.1	23.5	21.7
80	21.7	20.3	21.2	20.0

predict the thermal conductivity of the gases arising in the solar collectors.

6.3 Multi-component mixtures

Thermal conductivity measurements of a few multi component mixtures were made. The results of these are shown in table 6.3.1. Using the A_{ij} terms as listed in table 6.1.2, in the way described in section 6.2, the theoretical thermal conductivity of these mixtures were obtained and are shown in table 6.3.1.

It can be seen from these results that the theory fits the results to within 5%.

TABLE 6.3.1

THERMAL CONDUCTIVITY W $M^{-1}K^{-1}$ at 30C.

Gas Mixture	Experimental Results $x10^3$	Theoretical Results	Percentage Error
33.3% Hll 33.3% H_2O 33.3% N_2	15.9	15.1	5%
80% Hll 15% H_2O 5% N_2	9.2	9.41	2%

6.4 Discussion

As previously described Halocarbon 11 will be infilled into the collectors, to a pressure of fifteen Torr, at the production stage to mask the effect of the spurious gases. The A_{ij} terms determined from a comparison between current theories and experimental results, see table 6.1.2, can be used to predict the thermal conductivity for various relevant gas mixtures. This data when used in conjunction with the results shown in figure 4.4.1 can be used to predict the variation of thermal conductivity, and hence conductive heat loss during the life of the collector. The result of such an analysis is shown in figure 6.4.1 which shows that over a period of 10 years the conductive heat loss due to gas will only increase by 24%. This results in an increase in total heat loss from the proposed solar collectors of less than 10%; this result is discussed in more detail in section 7.3.

Figure 6.4.1

Plot of change of Thermal Conductivity of gas mixture with time in solar collectors.

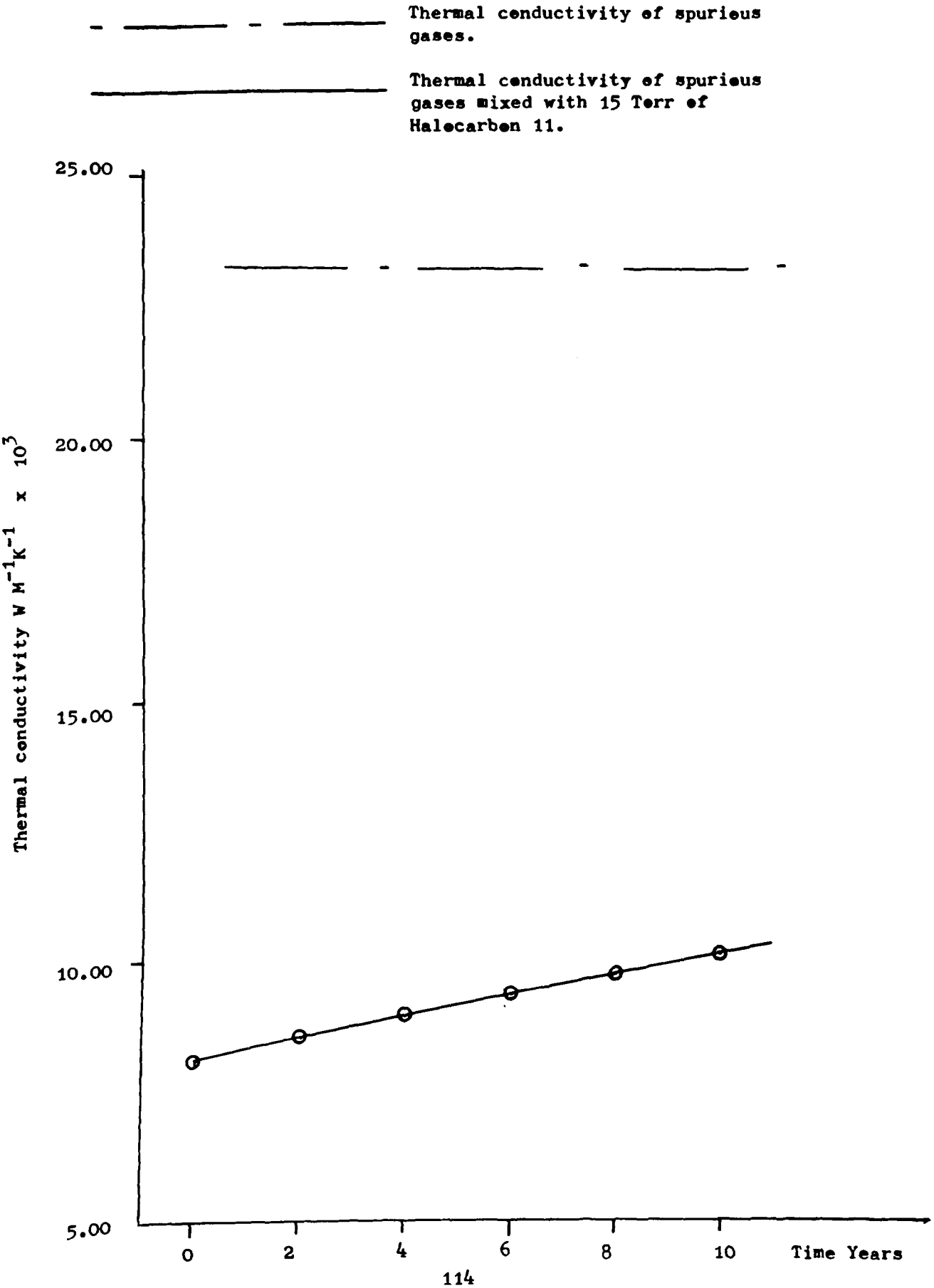

7 THE COMPLETED COLLECTOR

7.1 The design

A preliminary design of the partially filled collector is described by Roberts (1979). This initial design consisted of individual tubes all being sealed separately. This would mean that each tube has to be evacuated, baked, and infilled with the low thermal conductivity gas separately. In addition a complex tube arrangement would be required to connect the fluid carrying pipes together; this would have to include a lot of insulation to ensure that little heat loss occurred at these junctions. Because of the above problems a more elaborate design was developed; as discussed in chapter 3 and Roberts (1985).

As shown in figure 3.1.2 a number of collectors are combined together on one single manifold. This means that:

1 Vacuum tight seals are not required for the fluid carrying tube as it enters and leaves individual evacuated tubes.

2 Heat losses are reduced from the fluid carrying pipe as it leaves and enters the individual tubes, as the pipe does not leave the vacuum.

3 Evacuation of a system of tubes may be done at one point.

The manifold design and internal arrangement of the glass tubes is shown in figures 7.1.1 and 7.1.2. The internal design of each glass tube is similar to that described by Roberts (1979) and used for

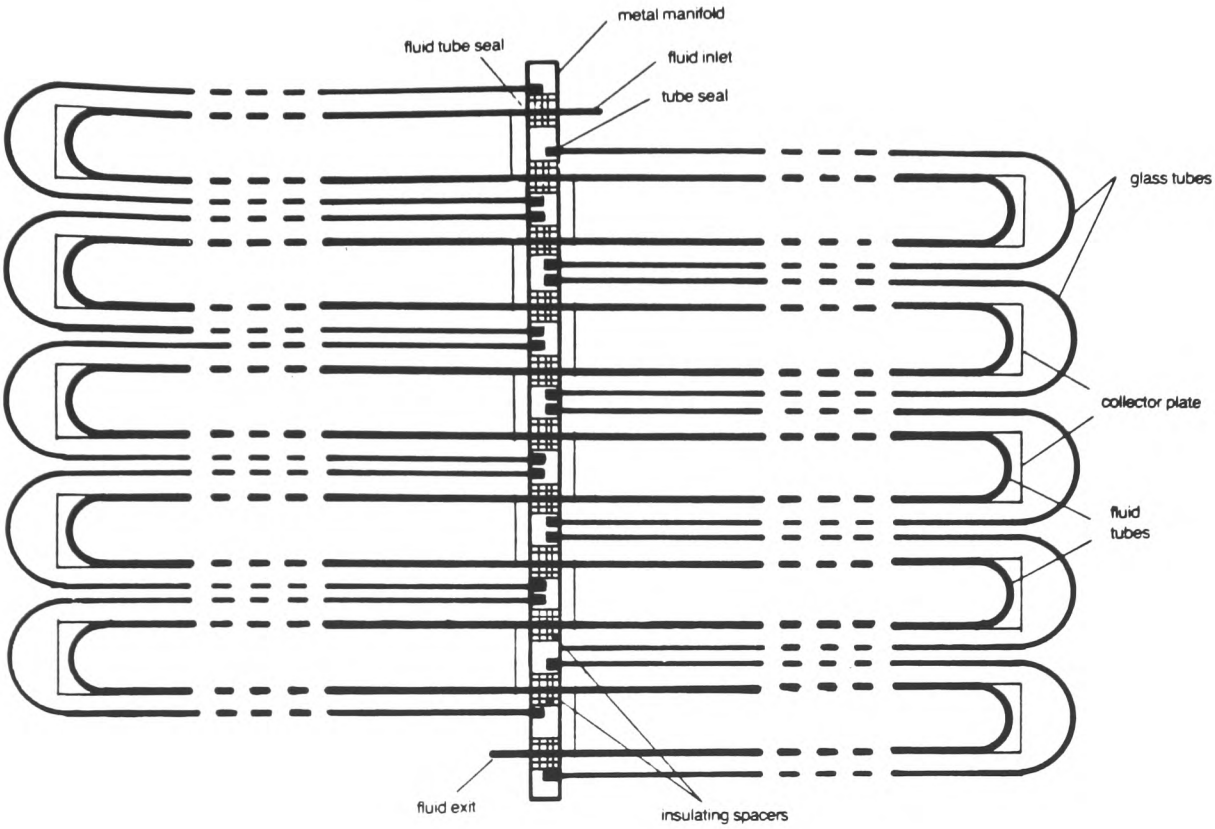
metal manifold
fluid tube seal
fluid inlet
tube seal
glass tubes
collector plate
fluid
tubes
fluid exit
insulating spacers

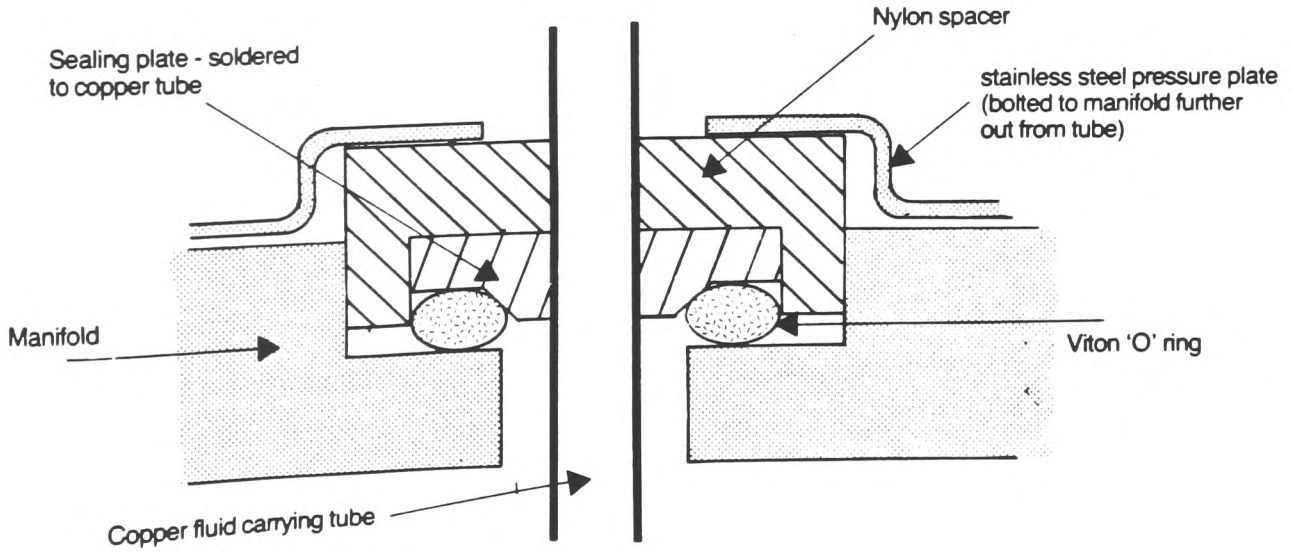
Nylon spacer
Sealing plate - soldered
to copper tube
stainless steel pressure plate
(bolted to manifold further
out from tube)
Manifold
Viton 'O' ring
Copper fluid carrying tube

Figure 7.1.1

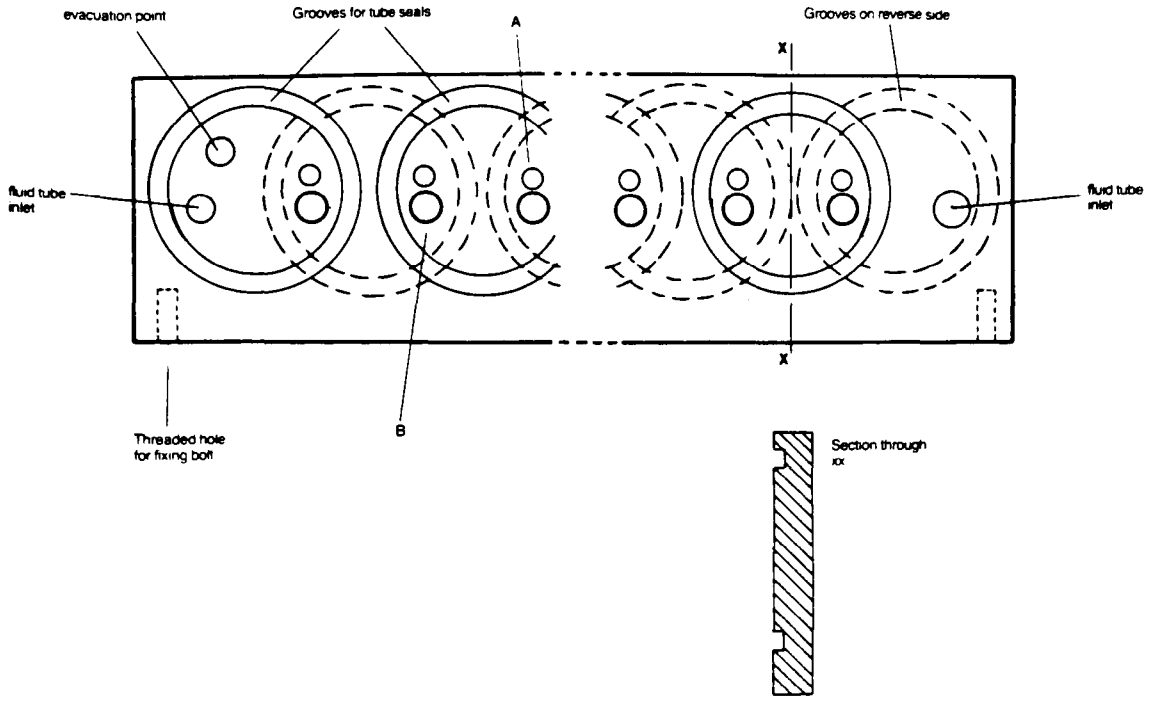
evacuation point
Grooves for tube seals
A
Grooves on reverse side
X
fluid tube inlet
fluid tube inlet
X
Threaded hole for fixing bolt
B
Section through xx

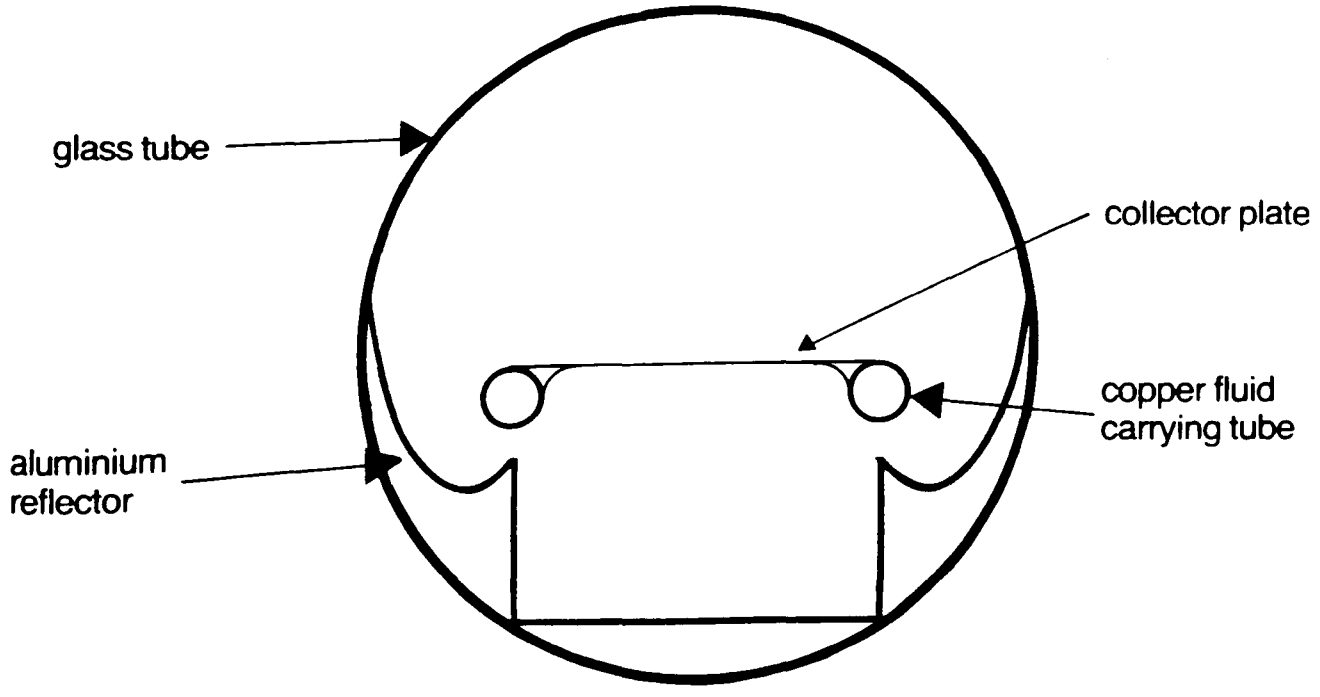
glass tube
collector plate
copper fluid carrying tube
aluminium reflector

Figure 7.1.2

example by Corning France in their evacuated collector. Figure 7.1.2 shows the internal arrangement for each glass tube. The collector plate is a copper sheet of thickness 0.2mm, fixed to the copper fluid carrying tube. The plate is coated on both sides with a selective surface, the one used was supplied by Wiggin Electrochemical Products, Birmingham, England. By ensuring that the copper sheet completely covers the copper tube both sides of the collector plate may absorb radiation.

An aluminium foil reflector is fixed to the inside of the glass tube with suitable wire supports, which also support the collector plate. The geometry of the reflector is such that almost all incoming radiation within an acceptance angle of 120 degrees will be directly incident on, or reflected onto the plates. Due to the small gap between the lower side of the plate and the reflector, the specular view factor between lower side of the plate and the reflector is approximately unity, with the result that the radiative heat loss is reduced.

A collector system as just described was constructed; The collector system was evacuated and put through a baking cycle, as described in chapter 4. After the baking cycle was completed the system was infilled with halocarbon 11 to a value of 15 torr.

7.2 Testing of completed units

A collector test system was set up at the Polytechnic of Wales; the test apparatus is shown in figure 7.2.1. The test method assumes that under steady state conditions the power balance of the collector is given by:-

$$\dot{Q} = IF'\alpha t - F'U_L(T_m - T_a) \quad \ldots\ldots\ldots 7.2.1$$

see Duffie and Beckman (1974).

$\dot{Q}$ is the output power of collector per unit effective area

I is the solar irradiance / unit area

α is the effective absorptance of collector plate

t is the effective transmittance of the glass cover

T_m is the mean fluid temperature, $(T_2 + T_3)/2$

T_a is the ambient air temperature

U_L is the heat loss coefficient between collector plate and ambient air.

U_o is the heat loss coefficient between fluid and ambient air.

F' is the collector efficiency factor, given by $F'=U_o/U_L$

The pump, as shown in figure 7.2.1, circulated the water from the constant temperature reservoir around the system at a reasonable constant flow. The constant temperature reservoir being set at approximately 12C below the required temperature of $T_m = (T_2+T_3)/2$. The heater may heat the water temperature by accurately determined electrical power so that T_m may be varied to a desired value for the test, and accurately determined flow rate is obtained by:-

$$P=C\dot{m}\,(T_2-T_1) \quad \ldots\ldots\ldots 7.2.2$$

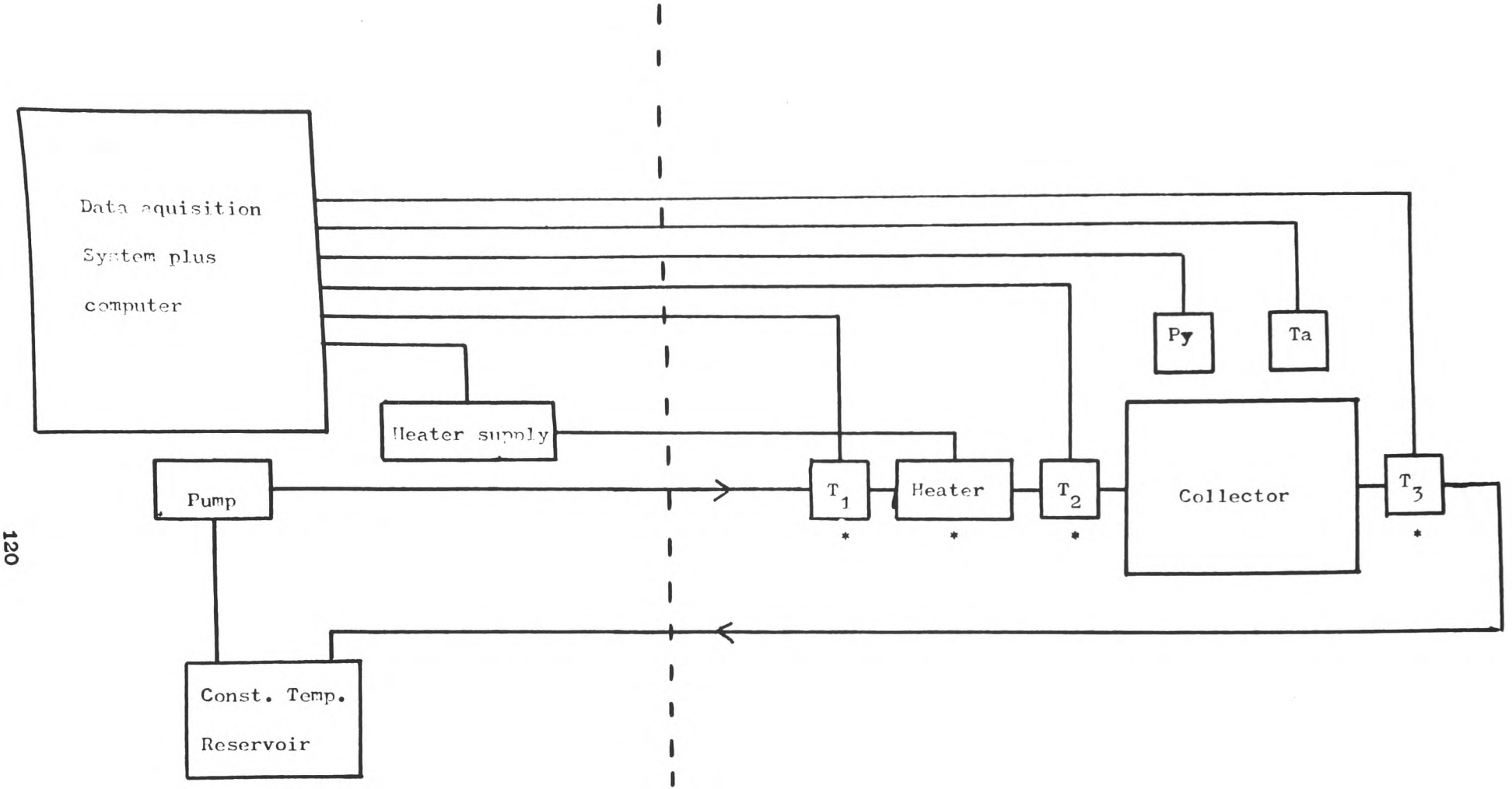

Equipment located inside building

Equipment located outside on supporting frame

T - temperature sensor
Py - pyranometer
* - well insulater items

Figure 7.2.1

P is the input electrical power

C is the specific heat capacity of water

$\dot{m}$ is the mass flow rate of water

T_1 and T_2 are water temperature determined by sensors in positions as shown in figure 7.2.1

When the water flows through the collector it is heated to a temperature of T_3, where

$$\dot{Q}A = C\dot{m}(T_3-T_2).....7.2.3$$

and A is the effective collector area.

Combining 7.2.2 and 7.2.3 then gives:-

$$\dot{Q}A = P(T_3-T_2)/(T_2-T_1)...7.2.4$$

All four temperature sensors were the platinum film type. The maximum error due to all temperature measurements being given at +/- 1.5%. The power to the heater could be evaluated to within +/-0.5%.

The pyranometer, as shown in figure 7.2.1, was an Eppley Model PSP, the calibration of which is stated to be within 2.5%. Hence the accuracy of the test system was evaluated to be within 4%.

Testing was undertaken outside, with the collector and pyranometer supported on a frame at an elevation of 45 degrees, and facing due south. The pyranometer was placed as close as possible to the center of the collector under test.

At the beginning of each test, pump speed, heater power, and the temperature of the reservoir were set to predetermined values, depending on the conditions required for the test. After these initial adjustments the test would continue over long periods of time, with the

measurements and calculations being undertaken by the computer. Results could be taken when the variations of I, the solar irradiance, was reasonably constant, as the time constant of the pyranometer was 28 minutes. The estimated error in tests taken due to variations of I, and the long time constant of the pyranometer was less than 2%. Therefore all results were correct to within 6%.

The efficiency of the collector, as mentioned before, is given by equation 7.2.1. In these test F´ was assumed to be 1. Therefore the tests were to determine αt and U_L. The results of the experiments done on the collector system described in section 7.1. are displayed in figure 7.2.2. From these results:-

$$\alpha t = 0.86 +/- 0.02$$

$$U_L = 3.3 +/- 0.2 \text{ W M}^{-2}\text{C}^{-1}.$$

Figure 7.2.2 also shows, for comparison, the efficiency plots for typical flat plate and vacuum installed collectors; Data for the typical collectors comes from BS 5918 (1980).

It can be seen from Figure 7.2.2 that when T_m-T_u is low and I is high, that the efficiencies of all the collectors are similar. However, as conditions change, the partially evacuated and 'totally' evacuated systems have much higher efficiencies than the flat plate collector. For example, under very cloudy conditions when I is approximately 150 WM^{-2}, evacuated systems could deliver energy at T_m-T_a=40C with an efficiency of approximately 25%, the efficiency of all flat plate devices would be zero.

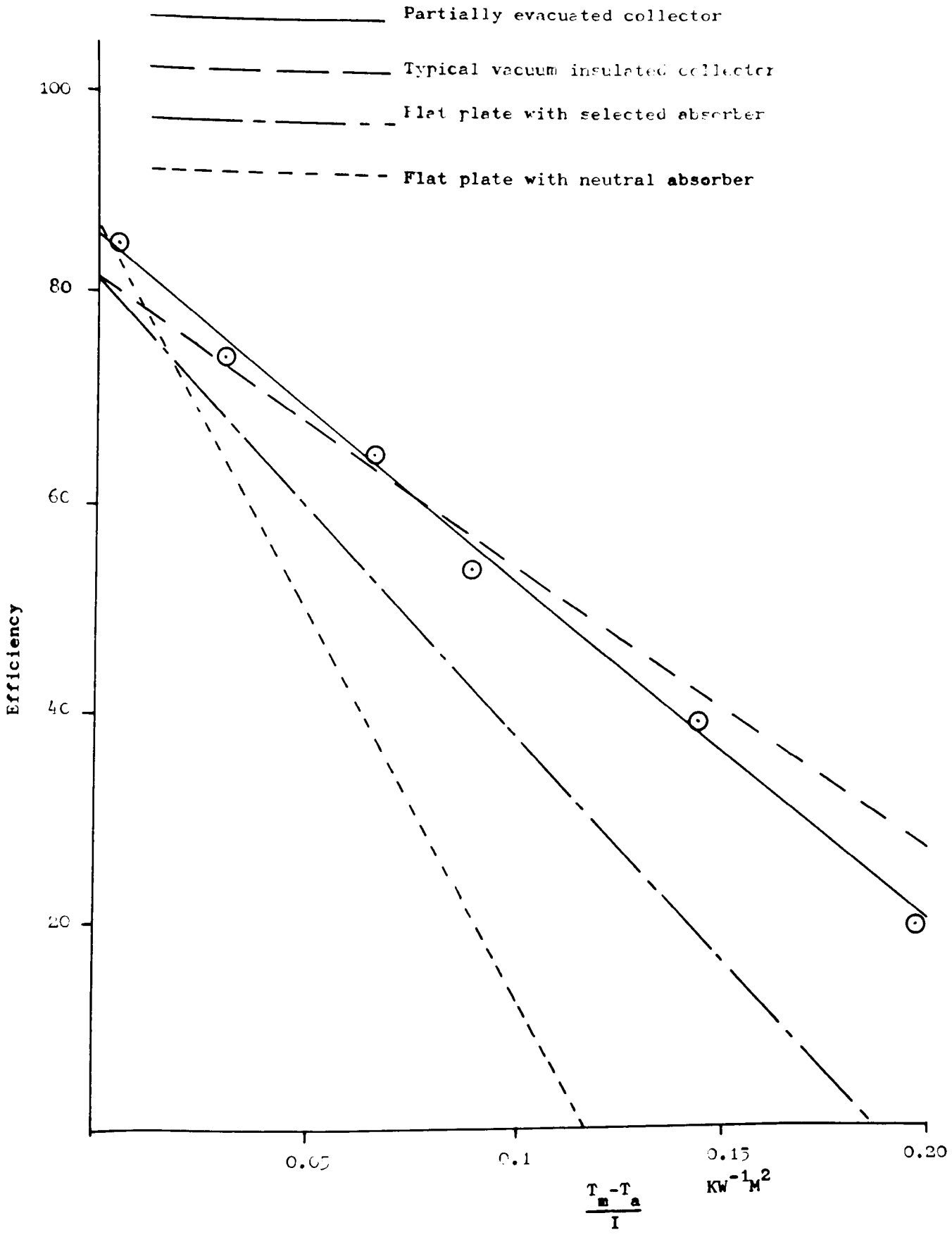

Figure 7.2.2 Plots of instantaneous efficiency versus $(T_m - T_a)/I$

7.3 Loss of efficiency of collector with time.

As shown in section 6.4 the thermal conductivity of the gases in the solar collector will rise with time, due to the permeation through the seals of spurious gases. The percentage increase in thermal conductivity is shown, in section 6.4, to be 24%. Using the results of the efficiency tests of the completed unit, given in section 7.2, in combination with the theoretical treatment for the loss of heat by conduction through the gases, given by Roberts (1979), the percentage heat loss due to conduction may be estimated.

Roberts shows that the heat loss due to conduction may be approximated to:

$$q_c = 4\ K\ L\ \Phi\ \Delta T \quad ....7.3.1.$$

Where:

q_c = Heat loss due to conduction from the absorber plate.

K = Thermal conductivity of gas.

L = length of plate.

Φ = Conductive flow expression.

Using the theoretical determined values of Φ from Roberts (1979).

$$q_c \simeq 1.34\ (T_m - T_A).$$

for the collector filled with pure halocarbon 11, per M^2. (In obtaining a value for Φ an effective width of 52 mm was taken for the absorber plate; this takes into account the reflector.) Using the experimentally found value for U_L it can be seen that the theoretical value for the heat loss due to conduction is 40% of the total heat

loss from the collector.

After ten years the thermal conductivity of the gas in the collectors is predicted to rise by 24% as stated in section 6.4. Therefore the percentage rise in heat loss from the collectors will be approximately 9.6%. so after 10 years:

$$\alpha t = 0.86$$

$$U_L = 3.6.\ W\ M^{-2}C^{-1}.$$

The predicted value for U_L, after 10 years, still being far better than for a flat plate collector, and yet achievable at a similar production cost.

It can clearly be seen that this type of collector compares well with a high vacuum type, over a period of ten years and yet has considerable advantages over it in production costs.

REFERENCES

Owen-Illinois Inc. of Tolendo, Ohio. United States Patent nos. 3,227,153 (1966).

H. Bloem, J.C. de Grigs and R.L.C. de Vaan - "An evacuated tubular solar collector incorporating a heat pipe". Philips Technical Review, 1982.

H. de Waal and F.Simonis - A report by the Institute of Applied Physics, University of Delft, the Netherlands, on "An improved version of the flat plate high performmance collector",1981.

G.T. Roberts - Solar Energy 22, 2-5, 1979.

A. Roth - Vacuum Technology, North-Holland, 1976.

R.J. Esley - Vacuum, 25, 299-306 and 347-356, 1975.

L. Ward and J.P. Bunn -"Introduction to the Theory and practise of high vacuum physics". Butterworths, London, 1967.

B.B. Dayton - Vacuum Symp. Trans. 293, 1963.

B.B. Dayton - Vacuum Symp. Trans. 42, 1962.

R.S Barton and R.P. Govier - Vacuum 2, 113-122, 1965.

Ben-hui - Int. Vacuum Cong. 3, 391-395, 1980.

B.B. Dayton - Vacuum Symp. Trans. 101, 1959.

G. Moraw - Vacuum, 24, 125, 1974.

G.T Roberts U.S. Patent Nos. 4,535,755 (1985).

F.J. Nortan - "Gas Permeation through the Vacuum envelope". 2nd. Int. Vacuum Congress. Trans.

A. Lebovits - Modern Plastics, 139, 1966.

J. Santhanam and P. Vijendran - Vacuum, 32, 487-490, 1982.

Y.S. Touloukian, P.E. Liley, S.C. Saxena - Thermophysical properties of matter. Vol 3, IFI/Plenum, New York, 1970.

H.C. Peters, J.N. Breunese and L.J.F. Hermans - International Journal of Thermophysics, 3, 27-34, 1982.

J.O. Hirschfelder, F. Curtiss, R.B. Bird - Molecular theory of gases and Liquids, Wiley and Sons, 1959.

A.L. Lindsay and L.A. Bromley - Ind. Eng. Chem. 41, 1508-1511, 1950.

E.A. Mason and S.C. Saxena Phys. Fluids 3:355, 1960.